Crossregulation of Insulin signalling and innate immunity

Dissertation

zur

Erlangung des Doktorgrades (Dr. rer. nat.)

der

Mathematisch-Naturwissenschaftlichen Fakultät

der

Rheinischen Friedrich-Wilhelms-Universität Bonn

vorgelegt von

Thomas Becker

aus

Bonn

eingereicht am 12.11.2009

Angefertigt mit Genehmigung der Mathematisch-Naturwissenschaftlichen Fakultät der Rheinischen Friedrich-Wilhelms-Universität Bonn

1. Gutachter: Prof. Dr. rer. nat. M. Hoch

2. Gutachter: Prof. Dr. rer. nat. W. Kolanus

Tag der Promotion: 17.6.2010

Bonn, 2010

Teile dieser Arbeit wurden bereits in folgenden Originalpublikationen veröffentlicht:

Fuss B, Becker T, Zinke I, Hoch M. The cytohesin Steppke is essential for insulin signalling in Drosophila. *Nature. 2006 Dec 14;444(7121):945-8.*

Becker T, Loch G, Beyer M, Zinke I, Aschenbrenner A.C, Carrera P, Inhester T, Schultze J.L, Hoch M. Foxo-dependent regulation of innate immune homeostasis. (submitted)

Einige Experimente wurden in Kooperation mit anderen Personen durchgeführt, dies ist an den entsprechenden Stellen vermerkt.

Abbreviations:

°C	degree celsius
µ	mikro-
A. bidest	aqua bidistilled
Fig.	figure
AP	alkaline phosphatase
BCIP	5-Brom-4-chlor-3-indolyl-phosphat
bp	basepaire
BSA	bovine serum albumine
c	concentration
cDNA	complementary DNA
DIG	digoxigenin
DNase	desoxyribonuclease
DNA	desoxyribonucleic adic
dNTP	desoxyribonucleosid-triphosphat
E. coli	*Escherichia coli*
EDTA	ethyldiamin-N,N-N',N'-tetraacetate
et. al.	et aliter
g	gramme
h	hour
kb	kilobases
kg	kilogramme
l	liter
LB	Luria-Bertani
m	milli-
M	molar
Min.	minute
mRNA	messenger RNA
NBT	nitrobluetetrazolinumchloride
OD	optical density
pH	pH value
RNase	ribonuclease
RNA	ribonucleic acid
RT	room temperature
sec	seconde
tRNA	transfer RNA
U	unit
o.N.	over night
rpm	rotations per minute
UV	ultraviolett
V	volt
vol.	volume
v/v	volume to volume
WT	wild type
w/v	weight to volume

Index

1 Introduction

1.1 Insulin/Insulin-like signalling in *Drosophila*

Insulin/Insulin-like signalling (IlS) is one of the major signalling pathways in *Drosophila*, which has been found to be involved in such diverse processes like regulation of organismal growth, cell size, cell proliferation, energy homeostasis, apoptosis, protein synthesis, autophagy and life-span (Hafen 2004, Grewal 2009). Although IlS is largely conserved in vertebrates and invertebrates, the architecture of this signalling cascade is more simple in the fly since most components are present as single orthologues. An exception of this model of simplicity are the *Drosophila* Insulin-like peptides (dIlps), molecules showing functional but not structural homology to the vertebrate Insulin. Seven dIlps have been identified in *Drosophila*, which show spatial and temporal dynamic expression patterns (Brogiolo et. al. 2001). It is believed that all these dIlps activate the single Insulin Receptor, thereby specifying IlS activation in individual tissues or in context of different functions, but so far this model is not proven. Some dIlps are expressed in a cluster of seven neurosecretory cells of each brain hemisphere, which project to the corpora cardiaca, a part of the endocrine gland, and the aorta, where dIlps are released into the haemolymph. Ablation of these cells, resulting in a loss of dIlp release from the neurosecretory cells, causes phenotypes found in genetic mutants of IlS (Broughton et. al. 2005). Moreover, dIlp expression is depending on nutrition and haemolymph glucose levels, suggesting that these cluster of neurosecretory cells are functionally equivalent to the ß-pancreas cells of vertebrates (Rulifson et. al. 2002).

The *Drosophila* Insulin Receptor was discovered in the 1980s (Thompson et. al. 1985) and has been shown to respond specifically to human Insulin. Mutants carrying strong *insulin receptor* alleles are embryonic lethal, whereas hypomorphic alleles showed severe growth and body size phenotypes in larvae and adult flies (Brogiolo et. al. 2001). It turned out that these phenotypes are also found in downstream components of IlS (Garofalo et. al. 2002), demonstrating a fundamental function of IlS in growth regulation. The intracellular adaptor of the Insulin Receptor is encoded by *chico* (Böhni et. al. 1999), which mediates the signal of the autophosphorylated receptor to the Phosphatidylinositol-3-Kinase (PI3K). Together with its antagonist PTEN, the phosphorylation of phosphatidylinositides (PIPs), a subclass of lipids inserted in the membrane, is regulated by PI3K. Elevated PI3K activity results in the enhanced phosphorylation of PIP2 to PIP3, which functions as a second messenger molecule by recruiting PH-domain containing proteins to the membrane (Cantley 2002, Gao et.al. 2000). One of these proteins is PKB/Akt, a protein kinase that is depending on PDK1 and functions by phosphorylating the Forkhead-box class O protein dFOXO as well as the TSC2/TSC1 protein complex (Hafen, 2004).

Downstream of PKB/Akt, IlS is devided into two branches with different tasks. One branch is responsible for transcriptional control, mediated by dFOXO. The fly genome encodes for a single *dfoxo* gene, which is conserved from worm to human and has extensively been described in context of cellular stress response and energy homeostasis (Arden 2008, Gross et. al. 2008). The dFOXO protein contains a forkhead box domain, which allows direct binding to the DNA via highly conserved recognition sequences. The PKB/Akt protein regulates dFOXO in an IlS dependent manner by phosphorylation. Increased IlS activity leads to enhanced dFOXO phosphorylation, retaining it in the cytoplasm. In contrast, dFOXO enters the nucleus when its phosphorylation status is low, subsequently followed by activation of dFOXO target gene expression (Calnan et. al. 2008). The second branch, which is defined by the TSC and TOR complexes, is mainly responsible for the regulation of translational control, autophagy and nutrient sensing (Hafen 2004b, Chang et. al. 2009). The link between IlS and TOR signalling is established via the TSC2/TSC1 protein complex, which is directly regulated by PKB/Akt via phosphorylation of TSC2. This protein complex has been described in context of tumor formation downstream of the Insulin Receptor (Pan et. al. 2004). Taken together, these two branches are responsible for all cellular processes in an IlS dependent manner (Fig. S1).

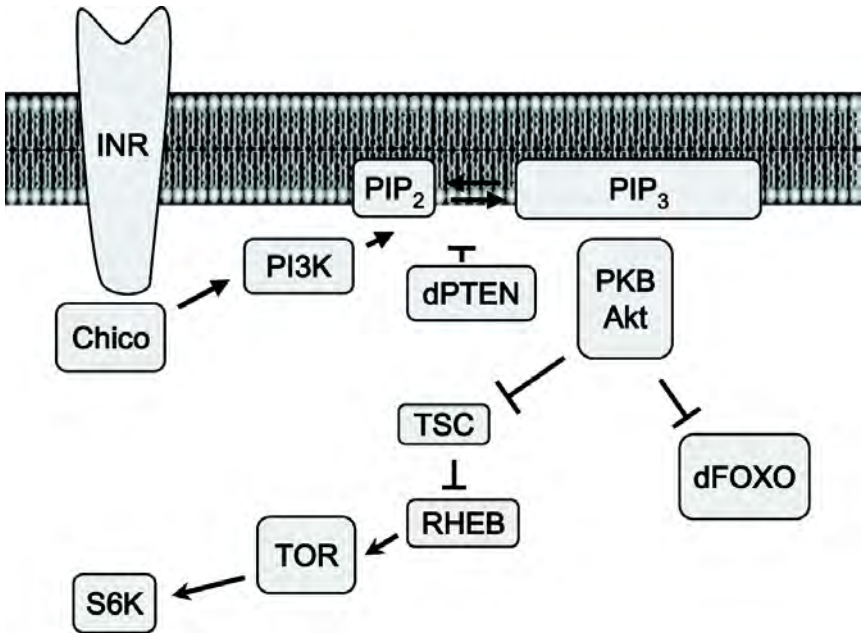

Fig. S1: The Insulin-like signalling pathway in *Drosophila.*

1.2 Main functions of IlS in *Drosophila*

Control of cell number and size

The size of an organism and its individual organs is defined by the number and the size of its cells. It has been published that mutants of the IlS cascade show body size defects, which are based on a reduction of either cell size, cell number or both (Hafen 2004). Mutants of the *insulin receptor* or its intracellular adapter *chico* are small because both cell size and cell number is reduced. The same phenotype develops when neurosecretory cells, which produce dIlps, are ablated. Conversely, loss of tumor suppressors PTEN or TSC2/TSC1 results in enhanced cell number and size. It has been shown that dFOXO is responsible for the control of cell number, but not cell size (Jünger et. al. 2003). Conversely, mutants downstream of the TOR complex are characterised by a reduction of sell size, but not cell number (Montagne et. al. 1999). These observations gave rise to a model of controlling cell size and cell number by two different branches of IlS, in which dFOXO regulates cell number and the TOR complex is responsible for cell size control. Nevertheless, it is still unclear whether IlS plays a direct role in determining the size of an animal or functions as a global modulator of other genetic programmes controlling organismal size.

Nutrient sensing and control of growth rate

IlS activity is closely connected to the availability of nutrients and couples metabolic activity and growth rates to the energetical status of the animal. Phenotypes observed in starving *Drosophila* larvae are highly comparable to those found in genetic mutants of IlS. Moreover, expression of some dILPs has been shown to be dependent on starvation, which establishes a direct link between the nutritional status and IlS (Ikeya et. al. 2002). Several lines of evidence suggest that the TOR complex is responsible for nutrient sensing and adaptation of metabolic power as well as adaptation of growth rates, which has been described in plants, yeast and metazoans (Lorberg et. al. 2004). Some important factors with central roles in the coordination of cellular and organsimal growth in a nutrient dependent manner, like 4E-BP and S6K, are directly regulated by the TOR complex (Liao et. al. 2008).

Determination of the life-span

It is known from model organisms all over the metazoan kingdom that the amount of caloric input is directly coupled to the life-span of the organism, whereas a reduction of caloric intake leads to a significant increase of life expectancy. Mutations in several components of the IlS cascade have been shown to result in longevity, including studies in *C. elegans*, the fruit fly *Drosophila* and mice (Cheng et. al. 2005). This allocates Insulin/IGF signalling a central function in context of regulating the life-span in a nutrient dependent manner. It has been shown that FOXO/DAF-16 proteins play a central role, since nutrient dependent determination of the life-span is at least partly FOXO/DAF-16 dependent. Furthermore, specific overexpression of dFOXO in *Drosophila* is sufficient to induce longevity (Hwangbo

et. al. 2004, Partridge et. al. 2008). Since dFOXO has been described in context of cellular stress response, it is obvious that activation of such stress protection programmes contribute to the dFOXO induced longevity. Nevertheless, the dFOXO target genes which are responsible for the observed effects have not been identified so far.

Tumor formation and cancer

Since IlS plays a central role in controlling cell proliferation and size, its misregulation can result in tumor formation and cancer. Two components of IlS, the protein PTEN and the TSC2/TSC1 complex, have been shown to increase both cell number and size when they are missing. Indeed, loss of PTEN activity is often found in tumor patients, highlighting the importance of its proper regulation. Moreover, TSC2 and TSC1 have been closely associated with Tuberous Sclerosis, a disease caused by tumors in the brain (Cheadle et. al. 2000). In contrast, loss-of-function mutations of several other components, including the Insulin Receptor, Chico, PKB/Akt, Rheb and TOR, show the opposite effects, meaning reduced cell number and size. These proteins therefore represent valuable targets for therapeutical interference. In fact, the natural antibiotic rapamycin, which is a potent inhibitor of TOR, has already been used in clinical trials.

Ribosome biogenesis and autophagy

Ribosome synthesis is tightly coupled to growth and the abundance of nutrients. In *Drosophila*, reduced IlS, for example by starvation, leads to a strong inhibition of ribosome synthesis and an accompanying reduction in protein synthesis capacity. This is mainly achieved by changed gene expression profiles, since starvation inhibits the transcription of many metabolic genes as well as those for ribosome biogenesis (Zinke et. al. 2002). These changes in gene expression profiles are mainly depending on dFOXO and Myc (Teleman et. al. 2008). Another starvation induced process is autophagy, which comprises degradation and recycling of the cytoplasm as well as organelles of the cell to maintain amino acid and nutrient levels. In context of autophagy, reduced IlS activity is important, which is quickly achieved in starving *Drosophila* larvae and autophagy is subsequently triggered predominantly in the fat body. One of the key players of autophagy regulation is the Atg1 protein, which is regulated by TOR. Overexpression of Atg1 is sufficient to induce autophagy also in well fed conditions (Scott et. al. 2007). Notably, the phenotypes of autophagy mutants are comparable to those of mutants for *4e-bp*, which demonstrates that autophagy and repression of translation are tightly coupled.

1.3 Conservation of IlS and diabetes disease

IlS is conserved in all metazoans, ranging from *C.elegans* to human (Hafen, 2004). Also in yeast, some components of IlS have been identified. In *C. elegans*, most components known

from IlS in *Drosophila* are highly conserved, including the Insulin Receptor homologue DAF-2, the PI3K homologue AGE-1, the PKB/Akt homologues AKT-1 and AKT-2 and the dFOXO homologue DAF-16. Moreover, most of the identified protein interactions, phenotypes and functions known from *Drosophila* are likewisely conserved in *C. elegans*. IlS in mammals consists of two independent pathways, Insulin- as well as IGF signalling. In most cases, several orthologous or homologous proteins exist in mammals for each component of the signalling cascade as compared to *Drosophila* or *C. elegans* (Hafen, 2004). The ligands for Insulin and IGF receptors are the hormones Insulin, produced by the ß-cells of the islets of Langerhans in the pancreas (ß-cells), and Insulin-like growth factors 1 and 2 (IGF-1/2), produced by the liver. Insulin is primarily responsible for maintaining blood glucose levels and is thereby closely associated with diabetes. In contrast, IGF-1 and IGF-2 regulate organismal growth. After autophosphorylation of the receptor tyrosine kinases, the internal IRS adapter proteins are recruited, linking the receptors to the PI3K/PTEN protein network. As in *Drosophila*, PKB/Akt proteins, in total three in mammals, are responsible for the phosphorylation of both TSC2 as well as several dFOXO homologs. The TSC protein complex is likewisely coupled to the TOR protein network in vertebrates. Other target genes of IlS, like *s6k* or *4e-bp*, are as well conserved. Taken together, the Insulin signalling cascade is well conserved in vertebrates and invertebrates, but the architecture of the pathway is more complex in vertebrates.

One of the most important functions of mammalian Insulin signalling is the regulation of glucose levels in the blood. In mammals, Insulin is produced in the ß-cells and secreted into the blood vessels, where it provokes enhanced permeability of the cell membranes for glucose. Patients suffering from diabetes show significantly elevated concentrations of sugar in the blood due to a disability of the cells to take up glucose. Today, diabetes is a collection of different phenomenoms and it is devided into two main branches. Type 1 diabetes, which is caused by a destruction of the ß-cells, leading to a total loss of Insulin production, is genetically fixed and heritable. In contrast, type 2 diabetes is mainly founded on mechanisms of Insulin resistance and is to a great extent age dependent. In many cases, adipositas is associated with type 2 diabetes, which is strongly increasing since some decades. As in case of cancer therapy, also treatment of diabetes is one of the big scientific challenges of the future.

1.4 *Drosophila* innate immunity

Microorganisms represent a constant threat to all animals, which forced the evolution of organismal defense mechanisms, called immunity. Thereby, precise recognition and destruction of invading pathogens, while leaving the own body cells untouched, is crucial. Innate immune response, which depends on germ-line encoded receptors and genetically fixed

defense mechanisms, is the paramount antimicrobial response of all metazoans. About five to ten million species have to deal with innate immunity alone, whereas another approximately 45000 vertebrate species use both, adaptive and innate immunity (Hoffmann et. al. 2002).

During the last 15 years, *Drosophila* has developed as a valuable model system to study innate immunity, which is roughly devided into three arms: Local immunity as well as cellular- and systemical microbial defense mechanisms (Fig. S2). The first contact to microbes is always found at epithelial barrier tissues, like the gut, trachea or the epidermis, which are in contact with the external environment. These tissues represent a physical barrier, preventing microorganisms from entering the body cavity of the fly. In addition, antimicrobial peptides (AMPs), small cationic peptides that function by damaging bacterial cell walls and membranes, are produced as a first line defense. If microbes succeed to cross these barrier tissues and enter the haemocoel, the open blood system of the fly, cellular and systemic immune response mechanisms are activated. The cellular response is mediated by the blood cell system, which includes crystal cells, plasmatocytes and lamellocytes. Most of these cellular defense mechanisms function by phagocytosis or encapsulation of microorganisms by macrophage-like cells, which are constantly circulating in the haemolymph. The systemic response is controlled by two conserved signalling cascades, which are called Toll and IMD in *Drosophila*. The function of these pathways is to detect pathogens in the haemolymph and to induce the production and release of specific effector molecules, antimicrobial peptides, to counteract the infection. The main organ of AMP production and release in the fly is the fat body (Hoffmann, 2002).

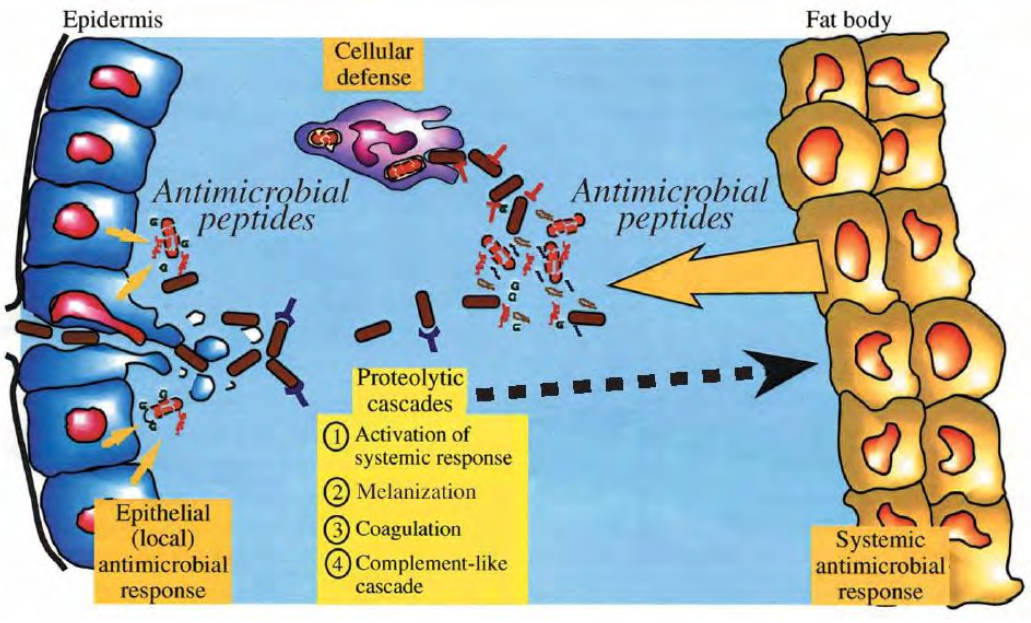

Fig. S2: Epithelial, cellular and systemic innate immunity in *Drosophila.*
Mod. after Hoffmann et. al. 2002.

1.5 Toll and IMD pathways

Since almost 20 years it is known that the *Drosophila* genome encodes for several classes of AMPs, which are active against Gram-positve as well as Gram-negative bacteria or fungi. All of the related promoter regions contain sequence motifs related to mammalian NF-κB response elements, which turned out to be crucial for AMP expression (Engström et. al. 1993). Due to this reason, the later on discovered signalling pathways, which are responsible for AMP regulation, are called NF-κB-like signalling pathways. In the mid of the 1990's, it turned out that two distinct signalling pathways are controlling AMP expression, which are the Toll and the IMD pathways.

Toll/TLR signalling in Drosophila and vertebrates

The Toll pathway (Fig. S3) is well known from dorso-ventral patterning during *Drosophila* embryogenesis (Belvin et. al 1996). In 1996, it was first described that the Toll receptor is crucial for proper organismal defense against fungi, which gave rise to a totally new function of this pathway in innate immunity (Lemaitre et. al. 1996). It turned out that the Toll pathway is also responsible for recognition and defense against Gram-positive bacteria.

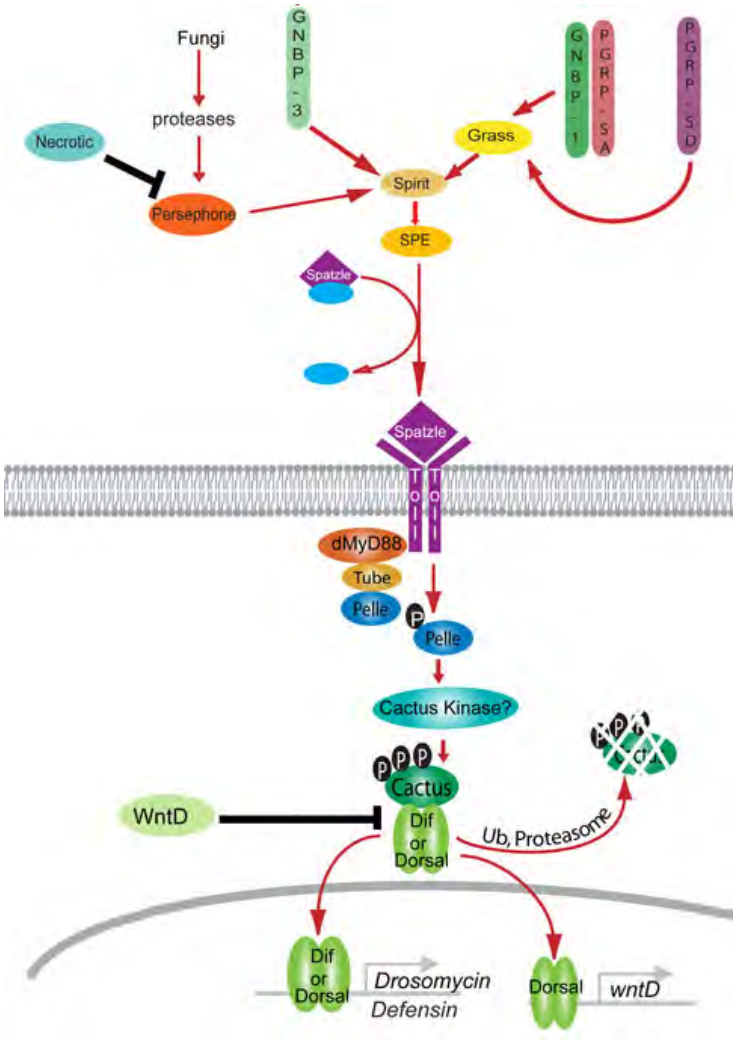

Fig. S3: The Toll pathway of *Drosophila.* Mod. after Aggarwal et. al. 2008.

The Toll receptor is a transmembrane protein, which shares sequence similarities with the vertebrate Interleukin-1 receptor (Hashimoto et. al. 1988). Toll is activated by the extracellular growth factor-like cytokine Spätzle, which is cleaved to its active form by a proteolytic cascade (LeMosy et. al. 1999). The Toll intracytoplasmic region interacts via death domains with several adapter proteins, which are MyD88 (Horng et. al. 2001), Tube (Letsou et. al. 1991) and Pelle (Shelton et. al. 1993). The Toll protein complex signals to a transcription factor of the NF-κB-Rel family, which is Dif (Ip et. al. 1993). The Dif protein is complexed by Cactus and activation of the Toll signalling cascade leads to a dissociation of the Dif-Cactus complex, following translocation of Dif into the nucleus and activation of several AMPs (De Gregorio et. al. 2001, Irving et. al. 2001). Mutants of components of the Toll signalling cascade exhibit enhanced susceptibility against infection with fungi or Gram-positive bacteria (Levashina et. al. 1998). Recognition of bacteria or fungi and activation of the Toll signalling pathway seems to be dependent on soluble pattern recognition particles, which are Semmelweis for Gram-positive bacteria (Michel et. al. 2001) and Persephone for fungi (Ligoxygakis et. al. 2002). Notably, characterisation of Toll signalling in *Drosophila* led to the identification of Toll-like-receptor proteins in mammals. In addition to this, most other components of the *Drosophila* Toll pathway are conserved in vertebrates (Fig. S4).

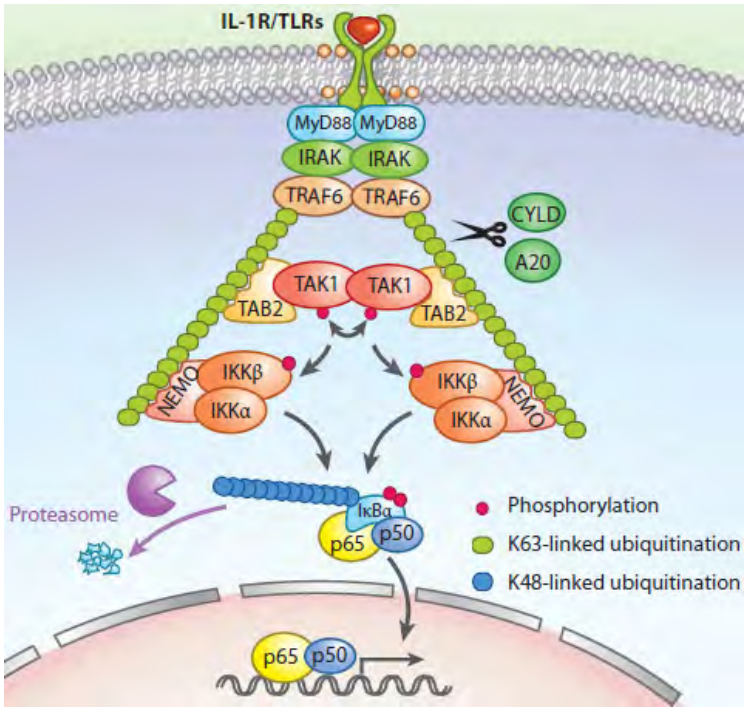

Fig. S4: TLR signalling in vertebrates. Mod. after Skaug et. al. 2009.

IMD/TNF-α signalling in Drosophila and vertebrates

The second NF-κB-like signalling pathway in *Drosophila* is the IMD pathway (Fig. S5), named by the intracytoplasmic adapter protein IMD (Lemaitre et. al. 1995a) of a long time unknown transmembrane receptor. This receptor belongs to the class of PGRP-LC proteins

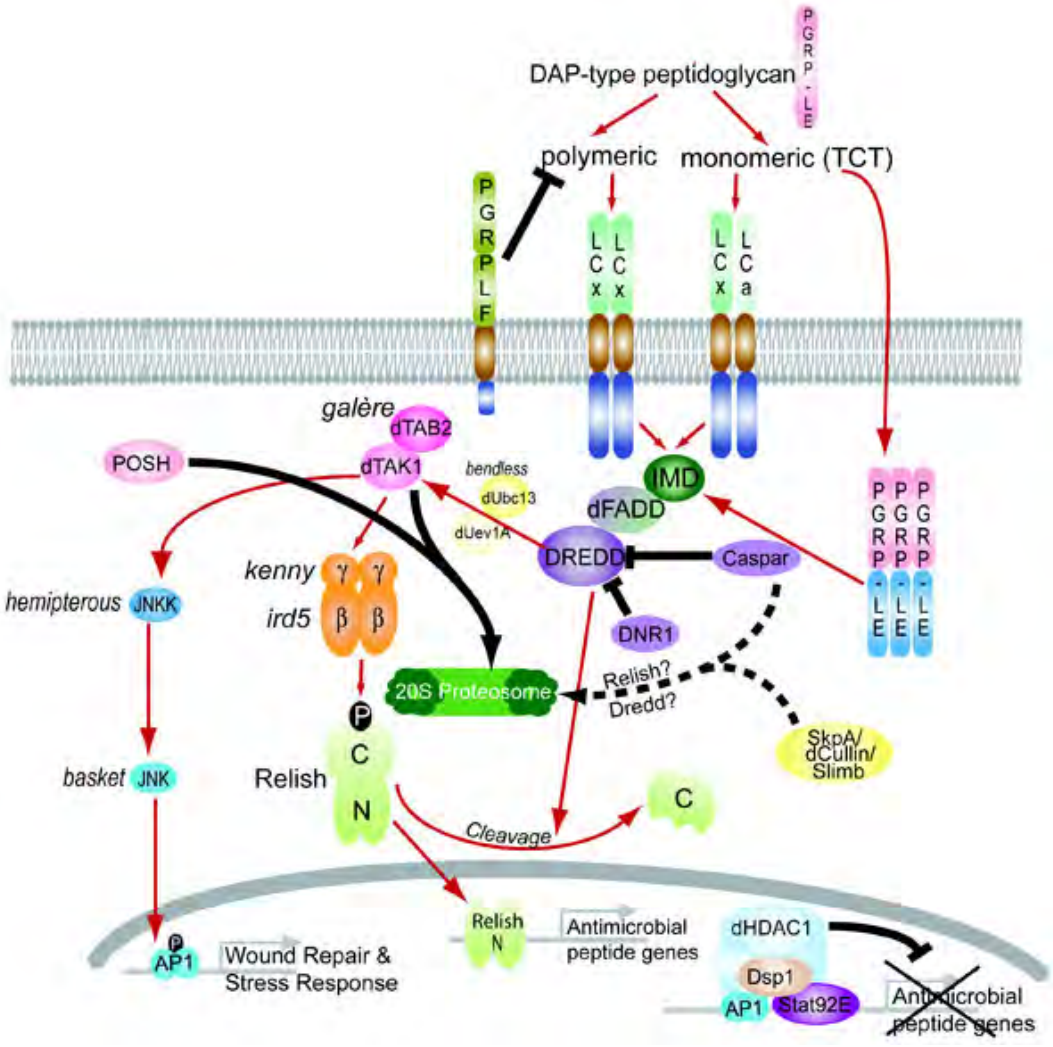

Fig. S5: The IMD pathway of *Drosophila*. Mod. after Aggarwal et. al. 2008.

and interacts with IMD via a death domain. The IMD pathway confers protection to Gram-negative bacterial infections via induction of AMPs by the NF-κB-Rel protein Relish (Hedengren et. al. 1999). Relish is inhibited by several ankyrin repeat domains and requires proteolytical cleavage before getting active. A kinase complex, containing proteins with significant similarity to the mammalian IκB kinase (IRD5) and the structural protein IKKγ (Kenny), are crucial for Relish proteolytic cleavage and activation (Silverman et. al. 2000). Some other important proteins, linking the IκB/Relish complex to the PGRP-LC/IMD transmembrane complex, are DREDD (Leulier et. al. 2000) and dTAK-1. Mutants of IMD pathway components show comparable phenotypes to Toll pathway mutants, which in general is enhanced susceptibility against Gram-negative bacteria. Moreover, as seen for Toll signalling, also the IMD pathway is conserved in vertebrates since high homology to the TNF-α pathway can be found (Fig. S6).

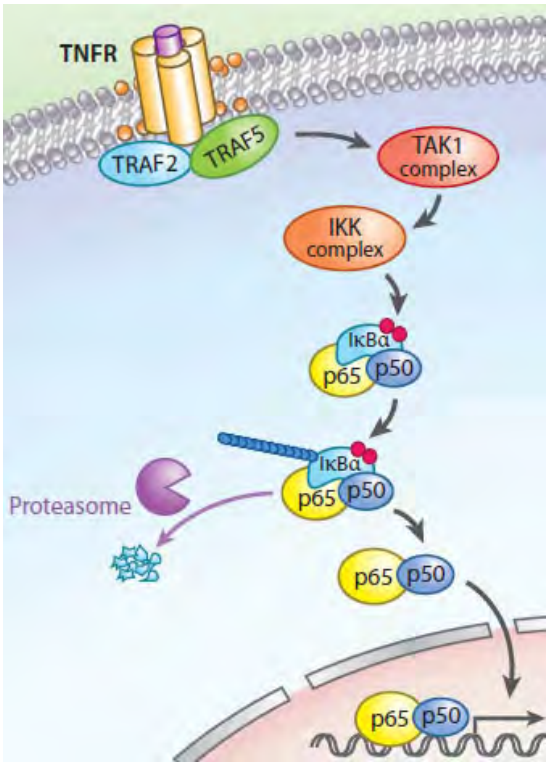

Fig. S6: The TNF-α signalling pathway in vertebrates. Mod. after Skaug et. al. 2009.

1.6 Antimicrobial peptides, systemical and local expression

AMPs are a diverse collection of host defense molecules produced by microbes, plants and animals, including human (Bulet et. al. 2004, Selstedt et. al. 2005). They have been characterised as small cationic peptides, interacting with microbial cell membranes, thereby causing stasis or lysis of the target microorganism. They have mostly a large spectrum of activity, although some have preferential targets. In mammals, AMPs include Defensins that are classified into α, β and θ categories, and Drosmycin-like-defensin, which has recently been described as a human peptide with antifungal activity and homology to *Drosophila* Drosomycin. Eight different classes of AMPs have been identified in the fly so far (Fig. S7, Hultmark et. al. 2003, Uvell et. al. 2007). The biological relevance of these peptides has been clearly demonstrated *in-vitro* and *in-vivo*, for example by overexpression of single AMPs in immune deficient flies (Tzou et. al. 2002). The major site of AMP production after infection in *Drosophila* larvae and adults is the fat body, the main organ of metabolism and innate immunity (Hetru et. al. 2003). This systemic expression is controlled by the Toll and IMD pathways, mainly on the transcriptional level via specific NF-κB binding motifs (Lemaitre et. al. 2007, Engström et. al. 1993). Some AMPs can reach µM concentrations in the haemolymph of the host organism. It has been shown that a loss of both pathways leads to a severe reduction of AMP expression after infection, resulting in quick lethality of the affected animals. In contrast, loss of either Toll or IMD signalling results in milder and pathogen

specific phenotypes (De Gregorio et. al. 2002). Beside their important role after an acute infection, AMPs can also function as a first line defense against microorganisms to prevent an infection. Most AMPs are expressed in a constitutive manner in different epithelial tissues of invertebrates and vertebrates, which are constantly exposed to bacteria and fungi of the surrounding environment (Selsted et. al. 2005, Ferrandon et. al. 2007). In *Drosophila*, these barrier tissues are mainly composed of the outer cell layer of the epidermis, digestive tract, respiratory organs and the reproductive system. They confer dual protection to the host: First, they provide a physical barrier, which cannot be passed by most microorganisms as long as this barrier is not damaged. Second, local production of AMPs and reactive oxygen species functions as a protective shield against pathogens. It has been shown that local expression of AMPs is depending on IMD signalling (Ferrandon et. al. 1998, Tzou et. al. 2000), but also other transcription factors like Caudal (Ryu et. al 2004, Ryu et. al. 2008). In contrast to systemic expression via the fat body, low concentrations of AMPs are expressed in barrier epithelia. Nevertheless, the entire network controlling local AMP expression is not well understood.

Peptides; gene name	Number of genes[a]	Antimicrobial activity	Notes on *in vivo* expression and modes of regulation[b]
Andropin; *Anp*	1	Gram-negative and Gram-positive bacteria	Constitutive in male reproductive tract; no infection-induced expression
Attacin; *Att*	4	Gram-negative bacteria	Local induction in the gastrointestinal tract; systemic induction in fat body
Cecropin; *Cec*	4	Gram-negative and Gram-positive bacteria, fungi	Constitutive in reproductive tract; local induction in the gastrointestinal tract; systemic induction in fat body
Defensin; *Def*	1	Gram-positive bacteria	Constitutive in female reproductive tract; weak induction in barrier epithelia; systemic induction in fat body
Diptericin; *Dpt*	2	Gram-negative bacteria	Local induction in the gastrointestinal tract; systemic induction in fat body
Drosocin; *Dro*	1	Gram-negative bacteria	Constitutive in female reproductive tract; local induction in the respiratory and gastrointestinal tract; systemic induction in fat body
Drosomycin; *Drs*	7	Fungi	Constitutive in salivary glands and female reproductive tract; local induction in respiratory organs (trachea); systemic infection in fat body
Metchnikowin; *Mtk*	1	Gram-positive bacteria, fungi	Constitutive and local induction in the gastrointestinal tract; systemic induction in fat body

Fig. S7: AMPs in *Drosophila* and their main expression in epithelial barrier tissues.
Mod. after Uvell et. al. 2007.

2 Material

2.1 Common material

If not mentioned separately, all chemicals used were of *pro analysi* quality and orderd from one of the following companies: Faust, La Roche, Merck, Promega, Roth, Sigma, Invitrogen, Biorad, Macherey and Nagel or Stratagene. Consumable and plastic material was from Faust, Eppendorf, Roth, VWR or Greiner.

2.1.1 Devices

Device	**Company and type**
Autoclave	H+P Varioklav steam steriliser EP-2
Bacterial incubator	Memmert 400
Binocular	Olympus S2X 12
Centrifuges	Heraeus Biofuge Pico and Eppendorf 5415R
Confocal microscope	Zeiss LSM-710
Fluorescence microscope	Olympus U-TVO.5xC-2
Fly incubator	RuMed
Gel electrophoresis	BioRad
Gel documentation	Biozym, Alpha Digi Doc
Microinjector	Eppendorf FemtoJet
Light microscope	Olympus AX 70
Luminometer	Berthold Microlumat plus LB96V
PCR cycler	MJ Research PTC-200
Photometer	BioRad SmartSpec Plus
Power supply	Bio-Rad Power Pac 3000
Real-time PCR cycler	I-Cycler with IQ5 optical unit (BioRad) Light Cycler 1.3 (Roche)
Rotator	Snjiders test-tube-rotator
Scales	Sartorius BL 150 S and Sartorius B211 D
Thermomixer	Eppendorf Thermomixer comfort
Ultra-turrax	IKA Ultra-Turrax T25 basic
Vortexer	Vortex Genie2
Waterbath	GFL 1002-1013

2.1.2 Standards, kits, buffers and enzymes

Company	Product
BioRad	SYBRGreen 2x supermix
Fermentas	DNA ladder mix DNA loading dye *Taq* polymerase
Invitrogen	SybrSafe TOPO TA cloning kit
Macherey Nagel	Nucleospin Plasmid AX-100 kit NucleoSpin Extract II kit NucleoSpin RNA II kit
Pierce (Thermo Scientific)	BCA protein assay kit
Promega	Luciferase assay system *Pfu* polymerase Go*Taq* polymerase
Qiagen	QuantiTect reverse cDNA transcription kit
Roche	PCR nucleotide mix Shrimp alkaline phosphatase and buffer T4 DNA ligase and ligation buffer Restriction endonucleases and buffers NBT/BCIP staining solution
Roth	Lysozym Ampicillin Rifampicin
Stratagene	QuikChange Lightning Mulit site-Directed mutagenesis kit

2.2 Solutions and media

If not mentioned, all solutions and media were prepared with non sterile, double deionised water (*aqua bidest*). All percent values are mass devided by volume.

2.2.1 Common solutions

Solution	Composition
AP	100 mM NaCl; 50 mM $MgCl_2$; 10 mM Tris, pH 9.5; 0.1% Tween 20
Blocking solution	5% goat serum in PBT
Buffer A	100 mM Tris-HCl (pH 7.5); 100 mM EDTA; 100 mM NaCl; 0.5% SDS
EMSA binding buffer	10 mM Tris (pH 7.5), 3.5 mM DTT, 100 mM KCl, 0.5 µg/ml poly (deoxyinosinic-deoxycytidylic acid), 0.25% Tween
EMSA tissue lysis buffer	10 mM KCl, 1 mM DTT, 0.1 mM EDTA, 10 mM HEPES (pH 7.9), 0.5 mM PMSF
EMSA nuclei lysis buffer	400 mM NaCl, 1 mM DTT, 20 mM HEPES, 1 mM EDTA, 1mM EGTA, 1 mM PMSF
Fixation solution	10% formaldehyde (ultra pure) in 1x PBS
Hybe	50% formamid ultra pure; 5x SSC (pH 5.5); 0.4 ml 10 mg/ml boiled salmon testis DNA; 0.1 ml 20 mg/ml tRNA; 20 µl 50 mg/ml heparin; ad. 20 ml aqua bidest
Hybe-B	50% formamid ultra pure; 5x SSC (pH 5.5)
Injection buffer	5 mM KCl, 0,1 mM Phosphate buffer
Nipagin solution	10% 4-hydroxybenzoeacid-methyl-ester in 70% ethanol
PBS (20x)	2.6M NaCl; 140 mM Na_2HPO_4; 60mM NaH_2PO_4; pH 7.4
PBT	0.1% Tween 20 in 1x PBS
RF-1	100 mM $RbCl_2$; 50 mM $MnCl_2$; 30 mM KOAc; 10 mM $CaCl_2$; 15% v/v glycerin; pH 5.8
RF-2	10 mM Mops, pH 7.0; 10 mM $RbCl_2$; $CaCl_2$; 15% v/v glycerin
TAE	40 mM Tris acetate (pH 8.0); 1 mM EDTA
TELT	50 mM Tris (pH 7.5); 62.5 mM EDTA; 2.5 M LiCl; 0.4% Triton X-100
XGal	2 % 5-Brom-4-chlor-3-indoxyl-ß-D-galactopyranosid stock solution

2.2.2 Bacterial culture media

Medium	Composition
LB	10 g tryptone; 5 g yeast extract; 10 g NaCl; ad. 1 l aqua bidest. Adjust pH to 7.0 and autoclave.
LB agar	10 g NaCl; 10 g tryptophan; 5 g yeast extract; 20 g agar; ad 1 l aqua bidest, adjust pH to 7.0 and autoclave, plate when cooled to 55 °C. If necessary, add antibiotics before plating.
ML	5 g peptone; 3 g meat extract; ad. 1 l aqua bidest, autoclave.

2.2.3 Cell culture media and reagents

Medium/Reagent	Source
Cellfectin, DMEM, Schneiders, RPMI	Invitrogen
Insulin	Sigma
FCS	Biowest

2.2.4 Standard fly food

Add 90 g agar to 8 l aqua bidest and boil until agar is dissolved. Add 165 g brewer's yeast, 615 g cornmeal and 1 l syrup to 3.3 l aqua dest, solubilize and add to solubilised agar. Boil for 15 minutes and stirr sporadically. Cool down to 55 °C, then add 200 ml 10% nipagin solution and aliquot.

2.2.5 Fly food with SecinH3

Add 3.75 g agar to 300 ml aqua bidest and autoclave. Dissolve 43 ml syrup, 26 g cornmeal and 7 g brewer's yeast in 100 ml aqua bidest and add to dissolved agar. Cook in a waterbath for 15 minutes and shake sporadically. Cool down to 55 °C, add 15 ml 10% nipagin solution and fill up to 450 ml with aqua bidest. Dilute appropriate amount of SecinH3 in 1.25 ml DMSO, fill up to 50 ml with aqua bidest and add to fly food while stirring.

2.2.6 Apple juice agar plates

Add 85 g agar to 4 l aqua bidest and boil until agar is dissolved, then cool down to 65 °C. Mix 1 l apple juice and 100 g sugar, heat to 65 °C and add to dissolved agar. Add 40 ml 10% nipagin solution and aliquot.

2.3 Chemical inhibitors

Inhibitor	**Source**
SecinH3	M. Famulok, Uni Bonn

2.4 Antibodies and *in-situ* probes

Antibody / probe	**Source**	**Conjugated**	**Dilution**
Anti-DIG AP	Roche	Alkaline Phosphatase	2000
Anti-GFP LGB-1 IgG1	Abcam	not conjugated	500
Control IgG1 MOPC-21	BD Bioscience	not conjugated	500
Anti-GFP	Santa Cruz	not conjugated	500
Anti-spectrin	DHB	not conjugated	500
drosomycin in-situ probe		not conjugated	20 µl / 750 µl

2.5 Vectors

Name	**Source**
pCR-II TOPO	Invitrogen, Karlsruhe
pUAST	Hoch lab
pCaSpeR4	Hoch lab
pGL3	Boutros lab
pMT	Hoch lab

2.6 Oligonucleotides

2.6.1 Oligonucleotides for EMSA, analysis and cloning

Name	Gene	Sequence
DBE1	*drosomycin*	TTATATTGTTCATAGAAATTCAACAATATAAAA GTAAAGGAAAACGCTATTAGGCCGGATG
DBE2	*drosomycin*	AAAACGCTATTAGGCCGGATCTTTATATTTTCA CGACGAAC
DBE3	*drosomycin*	TCAAATTTTTTACTTTTTCGGTCGTTTCGAATT TCCTTTACCGTTTTATCAGTCTATTATTATG
DBE4+5	*drosomycin*	TCAGTCTATTATTATGATGGGCTAGATGTTCTTT ATTAGATCTTTATTTAAGAACATTATCAATACA AAAAC
Drs_F1	*drosomycin*	CCATCAGCTTCTCCCGTG
Drs_R1	*drosomycin*	GGCTTGGGAACTTCGAGGAG
Drs_Del_F1	*drosomycin*	GCAATGAACAGAAAGCCCAAGATTTCTACATG CTGCGC
Drs_Del_R1	*drosomycin*	GCAGCATGTAGAAATCTTGGGCTTTCTGTTCA TTGCATC
Drs_287_F1	*drosomycin*	TATTTTGCAAAAGTAAATTTT
Drs_287_R1	*drosomycin*	AATTCGTATTATCACTTTCAT
Drs_287_F1M	*drosomycin*	TATTTTGCAAAAGTAAATTTTATATTGTTCATA GAAATTCAACAATATAAAATGCGCTGCAAACG CTATTAGGCCGGACAGC
Drs_287_R1M	*drosomycin*	GATTAATGCGTTACTCAATGAAGATCAAATATT ATGTTATTGAAGTTCGTCGTGAAAATTGCGCT GTCCGGCCTAATAGCGT
Drs_287_F2M	*drosomycin*	ATCTTCATTGAGTAACGCATTAATCAAATTTTT TACTTTTTCGGTCGTTTCGAATTGCAGCGCAC GTTTTATCAGTCTATTATTATGATGGGCT
Drs_287_R2M	*drosomycin*	AATTCGTATTATCACTTTCATTGATGTTTTTGTA TTGATAATGTTCTTAATGCGCTGTCTATGCGCT GCATCTAGCCCATCATAATAATAGAC
FOXO-1	*foxo*	IRD700-CAATATAAAAGTAAACAAAAACGC TAT
FOXO-1M	*foxo*	CAATATAAAATGCGCTGCAAACGCTATT
FOXO-2	*foxo*	IRD800-GTTTCGAATTTTGTTTACCGTTTTATCA

FOXO-2M	*foxo*	GTTTCGAATTGCAGCGCACGTTTTATCA
Plac1	P-Element	CACCCAAGGCTCTGCTCCCACAAT
Pry2	P-Element	CTTGCCGACGGGACCACCTTATGTTATT
step F1	*steppke*	CCCTAGTGGAGAGCTGAAAGAA
step F2	*steppke*	GCAGAAGTGCTGGGAGAAAA
step R1	*steppke*	CGTTACCAAAGCTCTTCGGACT
step R2	*steppke*	CAACAGAAGCTGCGAGCTAA

2.6.2 Oligonucleotides for SYBRgreen based real-time PCR

Name	**Gene**	**Sequence**
Att-a-Sy-F1	*attacin-a*	AGGAGGCCCATGCCAATTTA
Att-a-Sy-R1	*attacin-a*	CATTCCGCTGGAACTCGAAA
Cec-a1-Sy-F1	*cecropin-a1*	TCTTCGTTTTCGTCGCTCTCA
Cec-a1-Sy-R1	*cecropin-a1*	ATTCCCAGTCCCTGGATTGTG
Cec-c-Sy-F1	*cecropin-c*	TCATCCTGGCCATCAGCATT
Cec-c-Sy-R1	*cecropin-c*	CGCAATTCCCAGTCCTTGAAT
Dpt-RT-F1	*diptericin*	ATTGGACTGAATGGAGGATATGG
Dpt-RT-R1	*diptericin*	CGGAAATCTGTAGGTGTAGGT
DLD_F1	*drosomycin-like-defensin*	CGGCTGGACAAACAGTGC
DLD_R1	*drosomycin-like-defensin*	TGCCAACCTCATGTCCAC
Dro-Sy-F1	*drosocin*	TTTGTCCACCACTCCAAGCAC
Dro-Sy-R1	*drosocin*	ATGGCAGCTTGAGTCAGGTGA
Drs-Sy-F1	*drosomycin*	ACCAAGCTCCGTGAGAACCTT
Drs-Sy-R1	*drosomycin*	TTGTATCTTCCGGACAGGCAG
GFP-Sy-F1	*green fluorescent protein*	TGCAGTGCTTCAGCCGCTA
GFP-Sy-R1	*green fluorescent protein*	AAGATGGTGCGCTCCTGGA
InR-sy-F1	*insulin receptor*	AACAGTGGCGGATTCGGTT
InR-Sy-R1	*insulin receptor*	TACTCGGAGCATTGGAGGCAT
Lip3-Sy-F1	*lipase 3*	TGAGTACGGCAGCTACTTCCCT
Lip3-Sy-R1	*lipase 3*	TCAACTTGCGGACATCGCT
Luc-Sy-F1	*luciferase*	TGTTGTTTTGGAGCACGGAA
Luc-Sy-R1	*luciferase*	ACTCCTCCGCGCAACTTTT
Mtk-Sy-F1	*metchnikowin*	CGATTTTTCTGGCCCTGCT
Mtk-Sy-R1	*metchnikowin*	CCGGTCTTGGTTGGTTAGGAT
Rp49-Real-F1	*ribosomal protein 32L*	GCTAAGCTGTCGCACAAATG

Rp49-Real-R1	*ribosomal protein 32L*	GTTCGATCCGTAACCGATGT
Thor-Sy-F2	*4e-bp*	CATGCAGCAACTGCCAAATC
Thor-Sy-R2	*4e-bp*	CCGAGAGAACAAACAAGGTGG

2.6.3 Oligonucleotides and probes for TaqMan based real-time PCR

Name	**Gene**	**Sequence**
B2M_F	*ß2-microglobulin*	CGACATTGAAGTTGACTTACTGAAG
B2M_R	*ß2-microglobulin*	GTCTCGATCCCACTTAACTATCTTG
B2M probe	*ß2-microglobulin*	TGGTTCACACGGCAGGCATACTCAT
DEFA1_F	*defensin-α1*	TGACCCCAGCCATGAGGAC
DEFA1_R	*defensin-α1*	GCAAGGGAAACAACCACTTCTG
DEFA1 probe	*defensin-α1*	TCGCCATCCTTGCTGCCATTCTCCT
DEFB1_F	*defensin-ß1*	TCGACGAGGTTGTGCAATCC
DEFB1_R	*defensin-ß1*	GTAAGCAGAGAGTAAACAGCAGAAG
DEFB1 probe	*defensin-ß1*	CTCATGGCGACTGGCAGGCAACACC
DEFB3_F	*defensin-ß3*	CAGGTCATGGAGGAATCATAAACAC
DEFB3_R	*defensin-ß3*	TCTTTCTTCGGCAGCATTTTCG
DEFB3 probe	*defensin-ß3*	AGCACTTGCCGATCTGTTCCTCCTT

2.7 Microorganisms

Name	**Genotype**	**Source**
E. coli DH5α	fhuA2 Δ(argF-lacZ)U169 phoA glnV44 Φ80 Δ(lacZ)M15 gyrA96 recA1 relA1 endA1 thi-1 hsdR17	Stratagene, Heidelberg
E. coli XL-10 Gold	TetrÄ (mcrA)183 Ä(mcrCB-hsdSMR-mrr)173 endA1 supE44 thi-1 recA1 gyrA96 relA1 lac Hte [F' proAB lacIqZ ÄM15 Tn10 (Tetr) Amy Camr]	Stratagene, Heidelberg

Erwinia carotovora ECC-15	Wildtype isolation, Rifampicin resistance	Boutros lab
Micrococcus luteus	Wildtype isolation	Galinski lab
One-shot TOP10	F- mcrA .(mrr-hsdRMS-mcrBC) Ö80lacZ.M15 .lac×74 recA1 araD139 . (araleu) 7697 galU galK rpsL (StrR) endA1 nupG	Invitrogen, Karlsruhe

2.8 Fly strains

2.8.1 Mutants

Name	**Genotype**	**Chromosome**	**Source**
chico^{1}	*cn*^{1},P{ry11}*chico*^{1}/CyO; *ry*[506]	2	Bloomington stock center
Drs_WT	*w*;+;P[drs_wt]	3	
Drs_Δ1-5	*w*;+;P[drs_Δ1-5]	3	
foxo^{21}	*w*;*foxo*^{21}/TM6B	3	S. Cohen
foxo^{W24}	*w*;P{lacW}*foxo*^{W24}/TM6B	3	M. Tatar
rel,spz	w;*rel*^{E20},*spz*^{RM7}/TM6C	3	B. Lemaitre
steppke^{EP2195}	*y*^{1} *w*^{67c23}; P{EP}EP2195/CyO	2	Szeged stock center
steppke^{EP2531}	*y*^{1} *w*^{67c23}; P{EP}EP2531/CyO	2	Szeged stock center
steppke^{K08110}	*y*^{1} *w*^{67c23}; P{lacW}*step*^{k08110}/CyO	2	Bloomington stock center
steppke^{SH0323}	*y*^{1} *w*^{67c23}; P{lacW}*step*^{SH0323}/CyO	2	Szeged stock center
steppke^{KG09493}	*y*^{1}; P{y[+mDint2] *w*[BR.E.BR]=SUPor-P}*step*^{KG09493}/CyO; *ry*[506]	2	Bloomington stock center
white^{1118}	*y*^{1} *w*^{1118};+;+	X	Bloomington stock center

2.8.2 GAL4 strains

Name	Genotype	Chromosome	Source
gmr-GAL4	*w*; P{GMR-GAL4.w-}2/CyO	2	Bloomington stock center
hs-GAL4	*w*;P{GAL4-Hsp70.PB}89-2-1	3	Bloomington stock center
steppke^{K08110};*gmr-gal4*	y^1 w^{67c23}; P{lacW}*steppke*^{K08110},P{GMR-GAL4.w[-]}2/CyO	2	
K08110;*heatshock-gal4*	y^1 w^{67c23}; P{lacW}*steppke*^{K08110}/ SM6b, Cy ; P{GAL4-Hsp70.PB}89-2-1 / TM3B, Tb	2;3	

2.8.3 UAS strains

Name	Genotype	Chromosome	Source
UAS *dfoxo*^{TM}	*y w*; P{UAS-foxo.TM}	2	M. Tatar
UAS *dfoxo:gfp*	w; P{UAS-foxo:gfp}	2	Hoch lab
UAS *pi3k*^{CAAX}	P{w[+mC]=UAS-Pi3K92E.CAAX}1, y^1 w^{1118}	1	Bloomington stock center
steppke^{SH0323};UAS *inr*^{WT}	w;P{w[+mC]=lacW}step[sh0323],P{w[+mC]=UAS-InR.Exel}2/CyO	2	
steppke^{SH0323};UAS *pi3k*^{CAAX}	P{w[+mC]=UAS-Pi3K92E.CAAX}1, y[1] w[1118] ;P{w[+mC]=lacW}step[sh0323], L^2, Pin^1	1;2	

3. Methods

3.1 Isolation and purification of DNA and RNA

3.1.1 Isolation of plasmid DNA (mini and midi)

For analytic purpose, 3 ml of an *Escherichia coli* o/n culture was centrifuged for 2 minutes at 13000 rpm, resuspended in 200 µl TELT buffer with 10 mg/ml lysozyme, incubated at room temperature for 5 minutes and boiled for 3 minutes in a thermomixer. After cooling on ice, samples were centrifuged at 13000 rpm for 15 minutes, the supernatant was collected in a fresh tube and 200 µl isopropanol were added. Plasmid DNA was pelleted by centrifugation at 13000 rpm for 30 minutes, washed with 1 ml of 70% ethanol, air dried and resuspended in 50 µl aqua bidest.

For preparation of bigger amounts or highly pure plasmid DNA (e.g. for cell culture transfection), Nucleospin Plasmid AX-100 kit (Macherey Nagel) was used according to manufacturers instructions.

3.1.2 Electrophoresis, DNA cleanup and determination of concentration

For separation of DNA fragments, gel electrophoresis with 1% agarose gels was used. Agarose was diluted in TAE buffer and boiled until completely dissolved, then cooled to 60°C and plated. SyberSafe was mixed 1:10000 to fluid agarose before plating. Electrophoresis was done in gel chambers filled with TAE, probes were diluted 1:6 with DNA loading dye.

For cleanup of DNA fragments from enzymatic reactions or agarose gels, Nucleospin extract II kit (Macherey Nagel) was used according to manufacturers instructions.

The concentration of DNA or RNA in water was measured using SmartSpec plus photometer (BioRad). Probes were diluted in a range of 1:5 to 1:100 with water and the optical density at 260 nm was measured. An optical density of 1.0 corresponded to 50 µg/ml of DNA or 40 µg/ml of RNA.

3.1.3 Isolation of genomic DNA from flies

For isolation of genomic DNA from flies, one to six animals were homogenised with a pestle in 400 µl buffer A and incubated at 65 °C for 30 minutes. 800 µl KAc / LiCl solution (1 part of 5M KAc to 2.5 parts of 6M LiCl) were added and incubated on ice for 10 minutes. Debris

was removed by centrifugation at 13000 rpm/4°C for 10 minutes. 1 ml of the supernatant was added to 600 µl isopropanol and centrifuged at 13000 rpm/4°C for 20 minutes. The genomic DNA pellet was washed with 500 µl of 70% ethanol, air dried and resuspended in aqua bidest.

3.1.4 Isolation of total RNA from larvae, adult flies or cultured cells

For total RNA isolation from cells, tissues, larvae or adults, RNA II kit (Macherey Nagel) was used. Larvae (for 1st instar more than 100 animals, for 2nd instar more than 20 and for 3rd instar more than 5) were thoroughly washed with water, transferred to 600 µl RA1 lysis buffer (supplied with RNA II kit, ß-mercaptoethanol was added before) and homogenised with Ultra-Turrax T25 basic at full speed for 60 seconds. S2 cells and isolated tissues were directly transfered to 350 µl RA1 lysis buffer and homogenised either by using a pestle (tissues) or by pipetting up and down several times (S2 cells). Adults were shock frozen in liquid nitrogen and homogenised in 600 µl RA1 lysis buffer by using a pestle. Before RNA isolation, lysates were cleared of debris by passing through a filter column (supplied with RNA II kit). No filter column was necessary for S2 cell lysates. Total RNA was isolated according to manufacturers instructions including DNase I treatment.

3.1.5 Reverse transcription of RNA into cDNA

cDNA of *Drosophila* total RNA probes was produced by reverse transcription using QuantiTect reverse transcription kit (Qiagen) including DNaseI treatment. 500 ng of total RNA were incubated with 1 µl of DNA wipeout buffer (supplied with the kit) and aqua bidest ad. 7 µl at 42 °C for 5 minutes. Finally, 2 µl of reverse transcription buffer, 0.5 µl of primer mix and 0.5 µl of enzyme (all supplied with the kit) were added and reverse transcription was performed for 30 minutes at 42 °C, followed by an incubation at 95 °C for 3 minutes. Probes were filled up to 50 µl with aqua bidest before further use. For vertebrate RNA probes, 500 ng of total RNA were reverse transcribed using Transcriptor First Strand cDNA Synthesis Kit (Roche) according to the manufacturers protocol.

3.2 Cloning of DNA fragments

3.2.1 Enzymatic digestion, vector preparation and ligation

Enzymatic digestion of DNA was done using Roche restriction endonucleases and buffers. 1-2 µg of DNA were digested in a total volume of 20 µl, including 2 µl of the appropriate 10x buffer and 3-5 units of enzyme per µg of DNA. After 2-4 h of incubation at 37 °C, DNA

fragments were cleaned using Nucleospin extract II kit (Macherey Nagel) or separated by gel electrophoresis.

Plasmid vectors were digested as described above and dephosphorylated by adding 1 µl of shrimps alkaline phosphatase (Roche) and 2.3 µl of the appropriate buffer to the sample. Dephosphorylation was done at 37 °C for 10 minutes, followed by inactivation of the enzyme at 70 °C for 10 minutes. Linearised plasmid vectors were separated by gel electrophoresis and cleaned using Nucleospin extract II kit (Macherey Nagel).

Ligation of DNA fragments into plasmid vectors was carried out o/n at 16 °C in a total volume of 10 µl, including 1 µl 10x liagtion buffer and 1 µl T4 DNA ligase (Roche). The ratio of insert to vector was 3:1.

3.2.2 TOPO cloning

The required dATP overhang of the insert was added in a *Taq* polymerase reaction, which was performed at 72 °C for 15 minutes, followed by a cleanup using Nucleospin extract II kit (Macherey Nagel). The reaction included:

***Taq* polymerase reaction**	
Template DNA	1 µg
Taq buffer 10x	2.5 µl
dATP	1 µl
Taq polymerase	0.5 µl
Aqua bidest	ad. 25 µl

The ligation reaction was set up using TOPO TA cloning kit (Invitrogen) and incubated at room temperature for 5 minutes:

TOPO reaction	
Template DNA	0.5 µl
TOPO vector	0.5 µl
Salt solution	0.5 µl
Aqua bidest	1 µl

1 µl of this reaction was directly transformed into one-shot TOP10 competent bacteria (supplied with TOPO TA cloning kit) following manufacturers instructions and plated on LB agar plates with appropriate antibiotics and 50 µl XGal. After o/n incubation at 37 °C, positive clones were selected by blue/white screening.

3.2.3 Production and transformation of chemo-competent bacteria

To produce chemo-competent bacteria, 2 ml of an *Escherichia coli* DH5α o/n culture were diluted with 50 ml fresh LB medium and grown at 37 °C to an optical density of 0.5 (at wavelength 550 nm). Cells were harvested by centrifugation at 1000 rpm/4 °C for 15 minutes and resuspended in 17 ml ice-cold RF-1 solution. After incubation on ice for 15 minutes, cells were harvested as described and resuspended in 4.5 ml RF-2 solution, incubated on ice for another 15 minutes and frozen in liquid nitrogen (100 µl aliquots). Competent bacteria can be stored at -80 °C for several months.

For transformation of plasmid vectors into competent bacteria, cells were thawed on ice and 100 ng of plasmid DNA were added to 100 µl of bacterial suspension. After incubation on ice for 20 minutes, cells were heat-shocked at 42 °C for 60 seconds and subsequently cooled on ice. 200 µl of LB medium without antibiotics were added and samples were incubated at 37 °C in a shaking incubator for 1 h before plating to LB agar plates with appropriate antibiotics.

3.3 PCR techniques

3.3.1 Primer design for PCR and real-time PCR

Primers were designed using Primer3 software (http://frodo.wi.mit.edu/). The following conditions were used:

Primers for cloning and analytical use		
Condition	Range	Optimum
Primer length	18-25 bp	20 bp
Melting temperature	50-65 °C	60 °C
% GC (of total)	35-60	50

Quantitative real-time primers		
Condition	Range	Optimum
Primer length	18-25 bp	20 bp
Product lenght	75-150 bp	120 bp
Melting temperature	60-63 °C	61 °C
% GC (of total)	40-60	50

Primers were synthesised by Metabion (Planegg) or Invitrogen (Karlsruhe) without 5' and 3' modifications, desalted and shipped lyophilised. Before use, primers were resuspended in aqua bidest to a final concentration of 20 pmol/µl.

3.3.2 Semi-quantitative PCR for analytical purpose and cloning

For analytical purposes, *Taq* (Fermentas) or Go*Taq* (Promega) polymerases without proof-reading capability were used, whereas for cloning *Pfu* polymerase (Promega) with proof-reading activity was taken. PCR reactions were set up as follows:

***Taq*/Go*Taq* PCR assays**	
Template DNA	50 ng of pure DNA or 1 µl of genomic DNA from flies
Taq buffer	2.5 µl (Fermentas 10x) or 5 µl (Promega 5x)
Forward primer	1 µl (20 pmol/µl)
Reverse primer	1 µl (20 pmol/µl)
dNTPs	0.5 µl
Polymerase	0.5 µl (Fermentas Taq) or 0.125 µl (Promega GoTaq)
Aqua bidest	ad. 25 µl

***Pfu* PCR assays**	
Template DNA	50 ng pure DNA
Pfu buffer	2.5 µl
Forward primer	1 µl (20 pmol/µl)
Reverse primer	1 µl (20 pmol/µl)
dNTPs	0.5 µl
Polymerase	0.5 µl
Aqua bidest	ad. 25 µl

Cycling and temperature profiles			
Temperature	Time (s)	Action	Number of cycles
95 °C	120	Denaturation	1
95 °C 55-65 °C 72 °C	30 30 30-180	Denaturation Annealing Elongation	25-35
72 °C	300	Final elongation	1

Annealing temperature was primer specific, elongation time was depending on the enzyme:

Taq polymerase: 60 seconds per 1000 bp
Go*Taq* polymerase: 60 seconds per 2000 bp
Pfu polymerase: 120 seconds per 1000 bp

3.3.3 Quantitative real-time PCR

Quantitative real-time PCR experiments were done with the I-cycler and IQ5 optical system (BioRad) using SYBR-Green to detect amplification after each PCR cycle. cDNA probes of reverse transcribed total RNA were used as template. Reactions were performed as duplicates in 96-well plates in a total volume of 25 µl. Gene expression studies were analysed with IQ5 optical system software (BioRad). All expression data represent the statistical mean of at least two independent experiments, error bars show standard errors of the mean. Expression is always shown relative to a control condition and relative to an internal expression control, which was *rpl32* (*rp49*) in all experiments. Expression data were calculated according to the delta-delta-CT method.

Real-time PCR experiments for vertebrate genes were performed with a LightCycler Taqman master kit and a universal probe library assay on a Light Cycler 1.3 instrument (Roche). For each gene, three replicate reactions were performed. Analysis was done using LightCycler 4 software (Roche) using a calibrator normalised relative quantification based on the *ß-2 microglobulin* (B2M) expression.

Primers for real-time PCR assays were designed as described and testet for efficiency before use. Efficiency tests include dilution of template cDNA from 1:1 up to 1:125. Primers used for real-time PCR showed at least 80% efficiency up to a dilution of 1:25. All primers were optimised and used at an annealing temperature of 59 °C. The appearance of primer dimer was further ruled out by melt curve analysis.

SYBRgreen real-time PCR assay	
Template cDNA	1 µl
Forward primer	0.5 µl (5 pmol/µl)
Reverse primer	0.5 µl (5 pmol/µl)
2x SYBR-Green Supermix	12.5 µl
Aqua bidest	10.5 µl

Cycling and temperature profiles			
Temperature	Time (s)	Action	Number of cycles
95 °C	300	Denaturation, polymerase initiation	1
95 °C 59 °C 72 °C	30 30 30	Denaturation Annealing Elongation	40
55 °C to 95 °C (+0.5 °C per cycle)	30	Melt curve	81

3.4 Promoter studies

3.4.1 Identification of dFOXO binding motifs

A search for conserved dFOXO/Forkhead binding motifes was done within the 2 kB genomic region upstream of different antimicrobial peptides according to genomic sequences deposited in FlyBase (http://flybase.org/). Putative dFOXO/Forkhead binding motifs were identified by the following sequences:

Binding motif	Description	Sequence
dFOXO (for.d)	dFOXO binding motif on the plus strand	TTGTTTAC
dFOXO (rev.)	dFOXO binding motif on the minus strand	GTAAACAA
Forkhead (for.)	Forkhead binding motif on the plus strand	T(X)TTTA
Forkhead (rev.)	Forkhead binding motif on the minus strand	TAAA(X)A
IRE (for.)	Insulin responding element on the plus strand	TT(Y)TTT(T/G)(G/T)
IRE (rev.)	Insulin responding element on the minus strand	(A/C)(A/C)AAA(C/T)AA

X: Any nucleotide and **Y**: purine A or G

3.4.2 Luciferase assays in cell culture

luciferase pGL3 constructs or empty pGL3 vector were cotransfected with pMT-GAL4 and UAS dFOXO-GFP into S2 cells. 16 h after transfection, dFOXO overexpression was induced by adding $CuSO_4$ to a final concentration of 0.5 mM into the medium. Cells were incubated for 24 h, followed by lysis in 350 µl RA1 buffer (Macherey Nagel) and RNA isolation. *luciferase* expression was measured by real-time PCR (using primers Luc-Sy-F1 and Luc-Sy-R1) and normalised to GFP expression (with primers GFP-Sy-F1 and GFP-Sy-R1).

3.4.3 Luciferase assays in transgenic larvae

Luciferase activity in transgenic larvae (aged 70-74 h after egg laying at 25 °C) was triggered either by starvation on PBS for 6 h or by overexpression of dFOXO^{TM} under control of a *heatshock* GAL4 driver line. Larvae were shock frozen in liquid nitrogen, homogenised in buffer RLB (Promega) with a tightly fitting pestle and subjected to three freeze-thaw cycles, each two minutes in liquid nitrogen and a 37 °C waterbath. Debris were removed by centrifugation (5 minutes at 5000 rpm/4 °C) and the supernatant was collected in a fresh tube. Total protein was determined using protein assay kit (Pierce) and Luciferase activity was subsequently measured using Luciferase assay system (Promega) and Microlumat plus LB96V luminometer system (Berthold). Luciferase activity was normalised to total protein.

3.4.4 Electromobility shift assay (EMSA)

Flies carrying *heatshock*-GAL4 were crossed with UAS *foxo:gfp* flies and progeny were grown on apple-juice agar plates with yeast paste for 72 h. Heatshocks were done after 24, 48 and 72 hours for 30 minutes at 37 °C to induce dFOXO:GFP protein production. After 72 hours, larvae were starved on PBS (see chapter 3.5.4) for 6 h to allow dFOXO:GFP translocation into the nucleus. Animals were shock frozen in liquid nitrogen and tissues were homogenised with a pestle in EMSA lysis buffer, followed by addition of Nonidet P-40 to a 1% final concentration. Nuclei were pelleted by a brief centrifugation and washed once with the buffer mentioned above. Nuclei were lysed in 100 µl EMSA nuclei lysis buffer, nuclear debris was removed by centrifugation at 4°C and the supernatant was stored in a fresh tube at -80°C. The protein concentration was determined with protein assay kit (Pierce) following manufacturers instructions. Binding reactions of oligonucleotides (MWG Biotech) and protein extracts were conducted at room temperature for 20 minutes with 5 µg of nuclear extract and 50 nM of oligonucleotide probe in EMSA binding buffer. Competing oligonucleotides were added in at least 10-fold excess. Mouse anti-GFP (Abcam) or control antibodys (BD Biosciences) were added for 40 minutes after incubation of the probe.

3.5 Work with *Drosophila*

3.5.1 Cultivation, crossing and recombination experiments

Drosophila stocks were kept on standard fly food at 18 °C and amplified at 25 °C. For amplification, adult flies were put to fresh food vials every three days. Stocks were kept homozygous or balanced, using chromosome specific balancers, to avoid changes in genotypes due to recombination. For crossing experiments, virgin female flies were crossed with male flies at 25 °C. A proportion of 2:1 (females to males) was used for crossing, genotypes were followed by genetic markers. Virginity was assured by isolating freshly hatched females in time, which was 5 h at 25 °C and 16 h at 18 °C. For recombination of chromosomes, virgin female progeny carrying two chromosomes in a transheterozygous combination were crossed with males carrying appropriate balancer chromosomes. Offspring being candidates for recombined chromosomes were selected, amplified and analysed.

3.5.2 Germline transformation

To generate transgenic flies, two P element transformation vectors were used. One vector (transformation plasmid) carried the transgene of interest and the *white* gene within a P element lacking the *transposase* gene. The second vector (helper plasmid) encodes the *transposase* gene, but lacked inverse terminal repeat regions. 6 µg of the purified transformation plasmid were mixed with 2 µg of the helper plasmid. 2 µl of a 3 M sodium acetate solution, aqua bidest up to a volume of 20 µl and finally 50 µl ethanol were added. Probes were frozen at -20 °C for at least one hour, then centrifuged at 13000 rpm for 20 minutes. The DNA pellet was washed once with 70% ethanol, air dried and resuspended in 50 µl sterile injection buffer. Embryos were taken 30 minutes after deposition, aligned on a piece of agar gel and transfered to double sided tape on top of a glass slide. The glass slide was transfered to a dish with silica gel and embryos were dried for 10 minutes before they were covered by halocarbon oil (Sigma). The injection buffer containing both vectors was injected into the posterior region of the embryos using a FemtoJet micro injector device (Eppendorf). Larvae were allowed to hatch at 18 °C and subsequently transfered to vials with standard fly food. Hatched adult flies were individually crossed with *white*^{1118} flies and progeny were screened for yellow or red eyes, which indicates the integration of the transformation plasmid into the genome. Finally, homozygous stocks of transgenic flies were established by eye color selection.

3.5.3 GAL4-UAS experiments and heatshock

Overexpression of specific proteins was done by using the GAL4/UAS system from yeast in *Drosophila*. To generate offspring that contain both, promoter dependent GAL4 expression and UAS dependent target gene sequences, flies carrying GAL4 elements were crossed with flies containing UAS sequences followed by a specific gene of interest. If not further mentioned, all GAL4/UAS experiments were done at 25 °C. GMR-GAL4 dependent overexpression in the eye was done at 28 °C. Overexpression in larvae or adult flies using the *heatshock* GAL4 system was achieved by incubation at 37 °C for 45 minutes, followed by incubation at 25 °C for 4-6 h if not further mentioned.

3.5.4 Starvation experiments and SecinH3 feeding

Starvation experiments in larvae were done by incubation on cellulose filters soaked with PBS. Larvae were grown at 25 °C on apple juice agar plates with yeast paste until desired age, then collected in a mesh and rinsed with water to wash away residual food. The animals were subsequently transfered to 9 cm petri dishes which were equipped with a cellulose filter soaked with PBS. Control experiments did additionally contain yeast paste on the filter surface. If not mentioned separately, starvation was done for 4-6 h at 25 °C.

Treatment of adult flies with SecinH3 was done by mixing the small compound into the food as describes in chapter 2.2.5. Control food did also contain DMSO, but no SecinH3. The food was stored at 4 °C up to two weeks. Flies were put to prewarmed food vials and flipped every two days.

3.5.5 Analysis of body length and weight

For body size measurements, flies were allowed to lay eggs within a time window of 2 h on apple juice agar plates. Eggs were put on fresh plates with yeast paste and incubated at 25 °C for 96 h. To avoid crowding and food stress, no more than 30 larvae were incubated per plate. Before measuring, larvae were collected in a mesh and rinsed with water, put into an Eppendorf cap with 100 µl of water and incubated in a water bath at 65 °C for 5 minutes. Animals were transfered to fresh plates and body length was measured using U-TVO.5xC-2 microscope and camara system (Olympus). Body weight of adult flies was measured 1-2 days after hatching, larvae were constantly grown on standard fly food at 25 °C. Flies were anaesthetised in diethyl ether for 3-5 minutes and measured on a precise scale (Sartorius).

3.5.6 *In-situ* hybridisation

For *in-situ* hybridisation, larvae were roughly dissected in PBS, fixed in fixation solution for 1 h at room temperature and washed in PBT (4x 15 minutes) on a rotator. Tissues were stepwise transfered to Hybe buffer by incubation in PBT + Hybe-B (1:1, room temperature), Hybe-B (65 °C) and Hybe-B + Hybe (1:1, 65 °C), each for 10 minutes. Pre-hybridisation was done in Hybe buffer at 65 °C (waterbath) for at least 1 h. RNA probes were diluted in Hybe buffer, boiled at 95 °C for 3 minutes and cooled on ice. Pre-hybridisation solution was removed from larval tissues, probes were added and incubated o/n at 65 °C. Probes were then removed completely and tissues were stepwise transfered to PBT by incubation in Hybe-B + Hybe (1:1, 65 °C), Hybe-B (65 °C) and PBT + Hybe-B (1:1, room temperature), each for 10 minutes, followed by washing in PBT (4x 15 minutes). Before additon of the primary antibody, blocking in PBT + 5% goat serum was done for at least 30 minutes. Anti-DIG AP antibody was added in blocking solution in a dilution of 1:2000 for 1 h at room temperature, followed by washing in PBT (4x 15 minutes) and AP buffer (2x 5 minutes). Staining was done in 500 µl AP buffer with 10 µl NBT/BCIP (Roche) and stopped by addition of 1,5 ml PBT.

3.5.7 Clonal analysis

The Flp/Gal4 technique was used to overexpress dFOXO-GFP in a mosain pattern of cells in the fat body. Females of the genotype hs-Flp;Sp/CyO; Act>CD2>Gal4, UAS-GFP/TM6B, Tb were crossed to homozygous UAS-dfoxogfp males and allowed to lay eggs for 4 h. Early third instar Tb+ larvae were screened for clusters of cells expressing GFP and quickly dissected in PBS. In-situ hybridisation for drosomycin was done as described, followed by alkaline phosphatase chemical staining and incubation with anti-GFP (Santa Cruz) and anti-spectrin (DHB) antibodies overnight at 4C. The anti-GFP and anti-spectrin antibodies were overlaid with Alexa488 and Cy3, respectively. Pictures were taken at a Zeiss LSM-710 confocal microscope for both transmission and laser light.

3.5.8 Tissue dissection

For tissue dissection, about 10 larvae were transfered to a glass dish with PBS and carefully dissected from the ventral side. Pieces of fat body, gut, epidermis and trachea were subsequently transfered to RA1 lysis buffer (Macherey Nagel) containing ß-mercaptoethanol.

3.5.9 Infection and survival assays in adult flies

Bacterial cultures of *Erwinia carotovora* ECC-15 and *Micrococcus luteus* were grown o/n at 30 °C in appropriate culture medium, which is LB for *Erwinia carotovora* (supplied with 50 µg/ml Rifampicin) and ML for *Micrococcus luteus* (without antibiotics). A volume of 2 ml was taken from both o/n cultures, bacteria were harvested by centrifugation (1 minute at 5000 rpm), pooled and resuspended in 1 ml sterile PBS. Flies were anaesthetised with carbon dioxid and a sharp tungsten needle was pricked into the lateral thorax after dipping into the bacterial suspension or sterile PBS. Flies were transferred to fresh food vials for recovery.

3.6 Cell culture work

3.6.1 Cultivation and starvation

Drosophila Schneider cells as well as human cell lines were cultivated in plastic flasks with appropriate culture medium, which is Schneiders medium (Invitrogen) for *Drosophila* cells and RPMI or DMEM (both from Invitrogen) for human cells, each containing 10 % FCS. For starvation experiments, $1x10^5$ cells were seeded to 6-well or 24-well plates. Starvation was done by incubating cells in appropriate medium without FCS for 24 h or in PBS for 4 h.

3.6.2 Transient transfection and induction

$1x10^5$ cells were seeded to 6-well or 24-well plates with fresh medium containing 10 % FCS. For each well, 10 µl Cellfectin (Invitrogen), 100 µl cell culture medium and 1.5 µg of each plasmid were mixed in a 1.5 ml Eppendorf cap and incubated for 30 minutes at room temperature before addition to the cells. The transfection solution was incubated for 5 h and plates were gently shaken every hour. After this time, the medium was removed completely, cells were washed twice and incubated with fresh medium containing 10 % FCS.

3.6.3 SecinH3 application and insulin stimulation

$0,5 \times 10^6$ S2 cells were grown in 6-well plates and starved in serum free medium for 24 h, followed by 10 µg/ml Insulin stimulation for 4 h in the presence of 10 µM SecinH3 or vehicle (0.2% final concentration of DMSO). For human cells, $1x10^5$ HEK293T, HL60, HCT116, CaCo2, or HaCaT cells were seeded in 24-well plates and cultured for 24 h in RPMI or DMEM containing 10% FCS. Cells were then serum starved in RPMI or DMEM for 24 h and stimulated for 12 h with 10 nM Insulin in the presence of the inhibitor SecinH3 or vehicle.

4 Results

4.1 Former work on *Drosophila* Steppke

Former work (Fuss et. al. 2006) characterised *Drosophila* Steppke, as the only fly homologue of the vertebrate cytohesin family of proteins. Steppke is strongly conserved and shows about 70 % of identity compared to human and murine Cytohesins within its functional domains. The mRNA of *steppke* is ubiquitiously expressed and isolated *steppke* mutants show increased lethality during embryogenesis and early larval stages as well as larvae of abnormal size. The function of Steppke in the fly has not been characterised so far and is part of this work.

4.2 Characterization of *steppke* mutant growth phenotypes

4.2.1 Larval mutant phenotypes

Previous work (Fuss et. al. 2006) suggested that *steppke* mutants show growth defects. In *Drosophila*, organismal growth is completely accomplished during larval development, which also defines the size of the adult fly (Hafen 2004). To see whether *steppke* plays a role during larval development, the size of wild type and *steppke* mutant larvae was compared. A good time point for this analysis is the mid of the third larval instar, which is about 96 h after egg laying under optimal conditions. Wild type larvae reach their maximal size at that time before shifting into the wandering phase. To fulfill this optimal conditons for the desired growth analysis, larvae were incubated constantly at 25 °C on apple juice agar plates supplemented with yeast paste, which is a sufficient food source for optimal growth rates. Egg collections of small time windows (2 h) were used and the number of larvae per plate was restricted to 30 animals to avoid crowding and food stress. Under these conditions, wild type larvae reached a body size of 4.1 mm (Figs. 1a,b). To uncover the impact of Steppke on larval growth, three different *steppke* mutant alleles were analysed in parallel and all of the associated animals showed reduced body size (Figs. 1a,b). Both $steppke^{K08110}$ and $steppke^{SH0323}$ were derived from P element screens. It turned out that $steppke^{K08110}$ is a very strong allele causing a severe phenotype, whereas $steppke^{SH0323}$ showed milder effects. To avoid effects which could be related to second hits on both *steppke* mutant alleles, a transheterozygous $steppke^{K08110}/steppke^{SH0323}$ allelic combination was analysed, which also elicited a clear growth defect. This analysis demonstrates that Steppke plays a pivotal role during larval growth and determines the size of the animal.

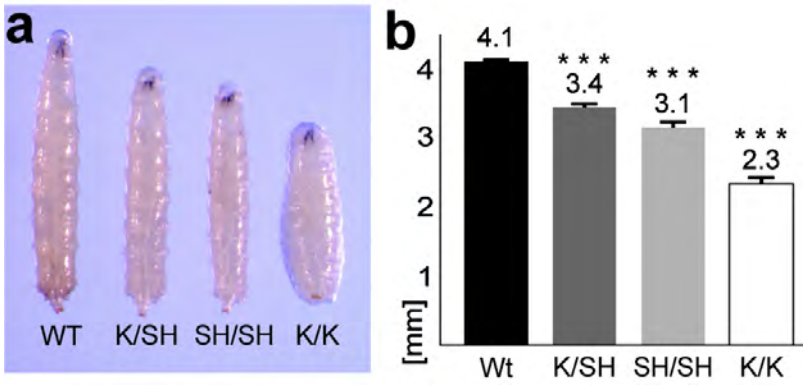

Fig. 1: *steppke* mutants show larval growth phenotype. **a)** Wild type (WT) and *steppke* mutant (K/SH, SH/SH, K/K) larvae 96 h after egg laying. **b)** Body length of wild type and *steppke* mutant larvae. K=*steppke*^{K08110}, SH=*steppke*^{SH0323}. Asterisks indicate statistical significance (P-value < 0.001).

4.2.2 Adult mutant phenotypes

The size of adult flies is determined during larval development (Hafen 2004). As *steppke* mutants showed impaired larval growth, the impact on adult fly size was analysed. Both *steppke*^{K08110} and *steppke*^{SH0323} homozygous mutant animals were lethal before the reaching the adult stage, but flies could be isolated from transheterozygous *steppke*^{K08110}/*steppke*^{SH0323} alleles. This allelic combination showed a milder, but significant growth phenotype in larvae and is accessible for experiments in the adult stage. To quantify the impact of mutant *steppke* on adult flies, larvae were raised at 25 °C on standard fly food and the weight of single female and male flies was determined on a precise scale two days after hatching. As already seen in larvae, *steppke* mutant animals showed impaired body size also in the adult stage (Fig. 2a), indicated by a loss of body weight of approximately 20 % in females and males (Fig. 2b).

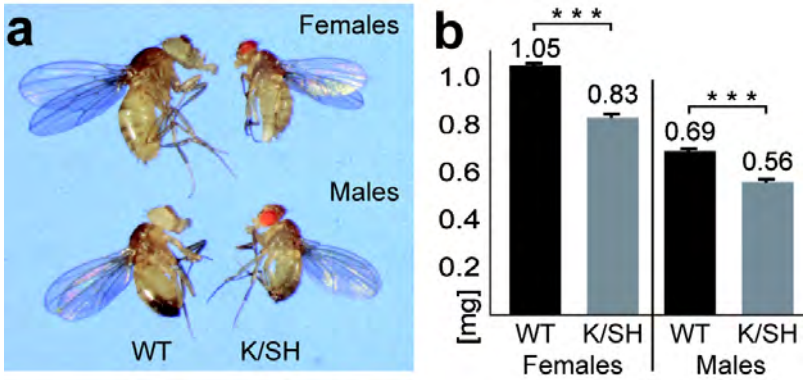

Fig. 2: *steppke* mutant flies exhibit reduced in body size. **a)** Wild type and transheterozygous *steppke* mutant male and female flies. **b)** Body weight of wild type and *steppke* mutant flies. WT= wild type, K=*steppke*^{K08110}, SH=*steppke*^{SH0323}. Asterisks indicate statistical significance (P-value < 0.001).

4.2.3 *steppke* mRNA expression in *steppke* mutants

(done in cooperation with I. Zinke)

While analysing the phenotypes of *steppke* mutant larvae and adult flies, two *steppke* alleles turned out to be of high interest for further analysis. First, the *steppke*^{K08110} allele which showed strong growth defects in homozygous animals during larval development, but no penetration into adult stages. Second, the transheterozygous allelic combination *steppke*^{K08110}/*steppke*^{SH0323} which showed a weaker phenotype in larvae but a clear body size defect in adult flies. As mentioned, both alleles were derived from P element screens and the respective transposons inserted into the *steppke* ORF. To further analyse the impact of the transposon insertions of *steppke*^{K08110} and *steppke*^{SH0323} on gene transcription, quantitative real-time RT-PCR experiments were carried out. Expression of *steppke* in wild type larvae, pupae and adult flies was compared to animals of both *steppke* mutant alleles. All *steppke* allelic combinations showed reduced expression of *steppke* transcript in the appropriate animals at all stages (Figs. 3a,b,c). Moreover, as already indicated by the strength of the associated phenotypes, homozygous *steppke*^{K08110} animals showed a stronger reduction of *steppke* gene expression compared to transheterozygous animals in both larvae and pupae. Notably, *steppke* expression in transheterozygous *steppke*^{K08110}/*steppke*^{SH0323} adult flies was almost completely diminished, whereas in first instar larvae and pupae, about 58 % and 34 % of residual *steppke* transcript could be detected. This points to either a strong maternal *steppke* contribution, which is retained in larvae, or to high transcription levels during larval development, which is reduced later on in pupae and adults.

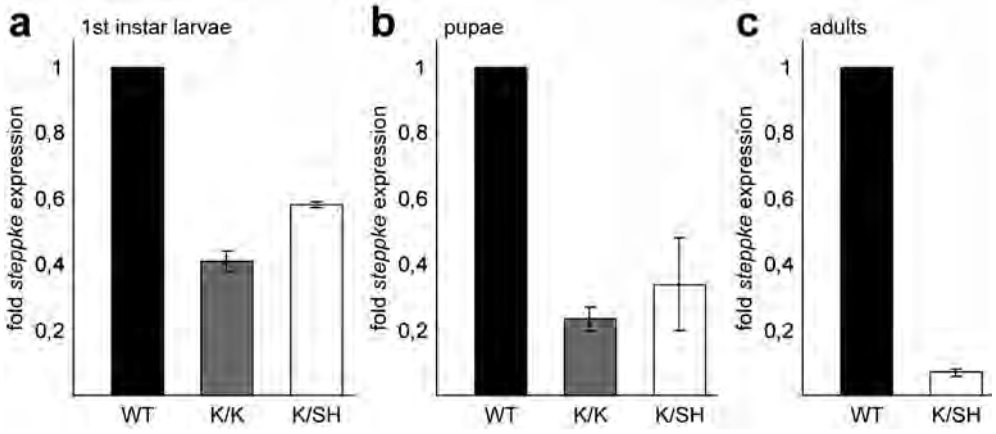

Fig. 3: *steppke* mRNA is reduced in *steppke* mutants. **a)** *steppke* mRNA in wild type and *steppke* mutant first instar larvae. **b)** *steppke* mRNA in wild type and *steppke* mutant pupae. **c)** *steppke* mRNA in wild type and transheterozygous *steppke* mutant adult flies. WT= wild type, K=*steppke*^{K08110}, SH=*steppke*^{SH0323}.

4.2.4 Complementation analysis of *steppke* mutant alleles

To further verify steppke mutant alleles *steppke*^{K08110} and *steppke*^{SH0323} concerning specificity, complementation analysis of three other *steppke* mutant alleles as well as a *steppke* deficient

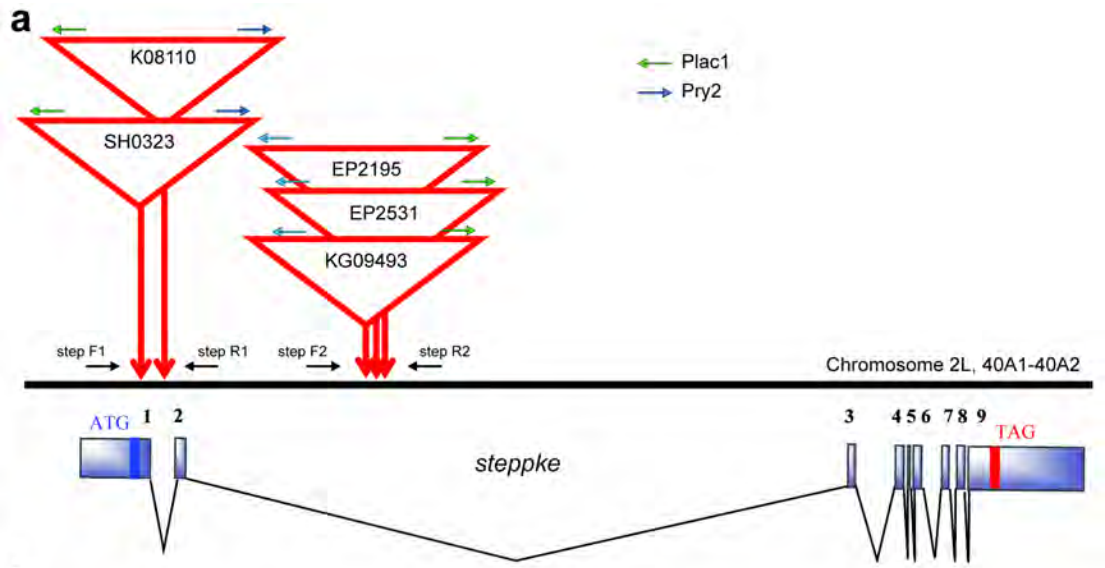

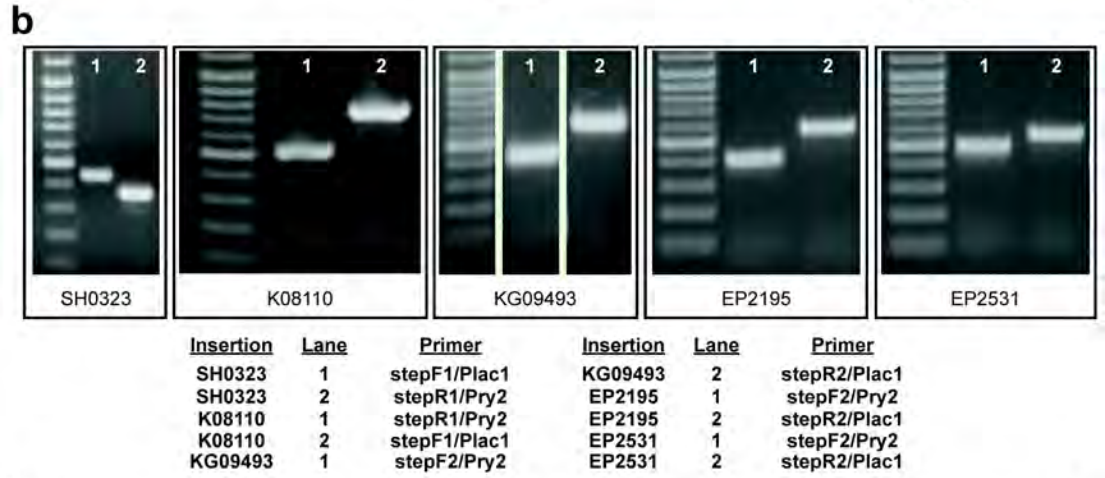

Insertion	Lane	Primer	Insertion	Lane	Primer
SH0323	1	stepF1/Plac1	KG09493	2	stepR2/Plac1
SH0323	2	stepR1/Pry2	EP2195	1	stepF2/Pry2
K08110	1	stepR1/Pry2	EP2195	2	stepR2/Plac1
K08110	2	stepF1/Plac1	EP2531	1	stepF2/Pry2
KG09493	1	stepF2/Pry2	EP2531	2	stepR2/Plac1

c

Allelic combination	Viability	Allelic combination	Viability
$steppke^{SH0323}/steppke^{K08110}$	viable	$steppke^{KG09493}/steppke^{EP2195}$	lethal
$steppke^{SH0323}/steppke^{SH0323}$	lethal	$steppke^{KG09493}/steppke^{EP2531}$	lethal
$steppke^{SH0323}/steppke^{KG09493}$	lethal	$steppke^{EP2195}/steppke^{EP2195}$	lethal
$steppke^{SH0323}/steppke^{EP2195}$	viable	$steppke^{EP2195}/steppke^{EP2531}$	lethal
$steppke^{SH0323}/steppke^{EP2531}$	viable	$steppke^{EP2531}/steppke^{EP2531}$	lethal
$steppke^{K08110}/steppke^{K08110}$	lethal	$steppke^{SH0323}/steppke^{Df\ ED1473}$	lethal
$steppke^{K08110}/steppke^{KG09493}$	lethal	$steppke^{K08110}/steppke^{Df\ ED1473}$	lethal
$steppke^{K08110}/steppke^{EP2195}$	viable	$steppke^{KG09493}/steppke^{Df\ ED1473}$	lethal
$steppke^{K08110}/steppke^{EP2531}$	lethal	$steppke^{EP2195}/steppke^{Df\ ED1473}$	lethal
$steppke^{KG09493}/steppke^{KG09493}$	lethal	$steppke^{EP2531}/steppke^{Df\ ED1473}$	lethal

Fig. 4: Complementation analysis of different *steppke* mutant alleles. **a)** Shematic overview of the *steppke* gene locus, the identified P-Element insertions and the primers used for verification. **b)** PCR verification of the insertion position of all five P-Element alleles. The DNA ladder is a 100 bp ladder, the 500 bp position is marked by an asterisk. **c)** Viability analysis of adult progeny for all steppke allelic combinations and the deficiency DF(2L)ED1473.

allele were performed. The *steppke* mutant alleles $steppke^{KG09493}$, $steppke^{EP2195}$ and $steppke^{EP2531}$ were likewise derived from P element screens and are inserted into the second intron of the *steppke* gene locus (Fig. 4a). In contrast, $steppke^{SH0323}$ and $steppke^{K08110}$ are inserted into the first exon and the first intron, respectively (Fig. 4a). In case of these two alleles, which are

located nearby, the possibility existed that regulatory elements of other genes except *steppke* were affected by these insertions. The intermediate genomic sequence of 3 kb to the three new alleles in the second intron strongly reduces the possibility that this is also the case for transheterozygous combinations of *steppke*^{K08110} or *steppke*^{SH0323} with one of these alleles. Moreover, transheterozygous animals of one *steppke* mutant allel and the deficiency Df(2L)ED1473 could be used to demonstrate specificity of the P element insertion for the *steppke* gene locus. To make sure that all indicated positions of the related P elements were correct, the insertion positions were determined by PCR. In each case, a primer located upstream or downstream of the P element position in the genomic locus of the *steppke* gene was combined with a second primer located within the P element sequence, either at the 5' or 3' end of the transposon (Fig. 4a). By this method, the indicated insertion positions of all five P elements could be confirmed (Fig. 4b). Next, transheterozygous animals of all allelic combinations as well as the deficiency were established by crossing experiments and screened for viability of adult progeny (Fig. 4c). Beside *steppke*^{K08110}/*steppke*^{SH0323} transheterozygous animals, three other allelic combinations could be isolated that produced adult progeny. In contrast, all other allelic combinations, including transheterozygous animals of *steppke* P-Elementdeficiency Df(2L)ED1473, were lethal. The latter point demonstrates that all five *steppke* mutant alleles are specific for the *steppke* gene. In addition, the high rate of lethal transheterozygous animals composed of two *steppke* P element alleles suggests that other genes, which could also be included in the deficiency, are not affected by the transposons.

4.3 Characterization of gene expression in *steppke* mutants

4.3.1 Gene expression in *steppke* mutant animals

A prominent pathway controlling organismal growth is Insulin/Insulin-like signalling (IlS), which is conserved in vertebrates and invertebrates (Hafen 2004). Transcriptional regulation of growth control by IlS in *Drosophila* is dependent on dFOXO and occurs at the level of the translational repressor *4e-bp* and the *insulin/insulin-like receptor* (*inr*) via an autoregulatory negative feedback loop (Puig et. al. 2003). To test whether *steppke* mutants show transcriptional regulation of these known dFOXO target genes, gene expression of *steppke*

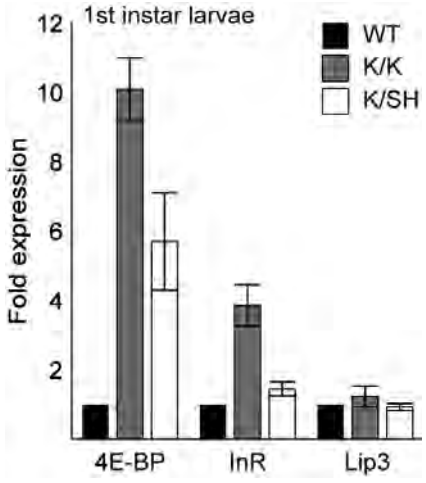

Fig. 5: Expression of *4e-bp, inr* and *lip3* in first instar *steppke* mutant larvae compared to wild type. WT=wild type, K=*steppke*^{K08110}, SH=*steppke*^{SH0323}, Lip3=*lipase3*, 4E-BP=*4e binding protein*, InR=*insulin receptor.*

mutants was compared to equally aged wild type animals by quantitative real-time RT-PCR. Experiments were done for homozygous *steppke*^{K08110} and transheterozygous *steppke*^{K08110}/*steppke*^{SH0323} first instar larvae. For both alleles, a robust increase of *4e-bp* and *inr* expression was detected (Fig. 5), pointing to impaired Insulin signalling and elevated dFOXO activity in the mutants. In line with the observed growth phenotypes, upregulation of dFOXO target genes was more severe in homozygous *steppke*^{K08110} mutants than in transheterozygous animals. As a control for lipid metabolism, *lipase3* (*lip3*) expression was analysed in *steppke* mutants in parallel. Upregulation of *lip3* is independent of dFOXO and indicates the usage of endogenous lipid stores when larvae are suffering from food. In case of *steppke* mutants, no enhanced *lip3* expression was detected (Fig. 5). This dedicates that lipid stores are not affected and the mutant animals are able to take up food. Overall, these results point to a specific misregulation of IlS in *steppke* mutants.

4.3.2 Gene expression in *chico* mutant larvae

Chico is a well established component of IlS in *Drosophila*, which directly interacts with the Insulin Receptor (Böhni et. al. 1999). To examine whether *chico* mutants show the same gene expression profiles as observed for *steppke* mutants, expression of *4e-bp*, *inr* and *lip3* was likewise quantified in homozygous *chico*^{1} mutant larvae, which is a null allele of *chico*. The expression profile resembled that of *steppke* mutants, strengthening a direct role of *steppke* in IlS (Fig. 6). Also *chico* mutants did not suffer from extensive usage of endogenous lipid stores, which would have been indicated by enhanced *lip3* expression, although larval growth is strongly affected in these animals. Interestingly, *chico* mutants showed enhanced expression of *steppke*, which points to a putative *steppke* regulation by dFOXO, as seen before for *4e-bp* and *inr*.

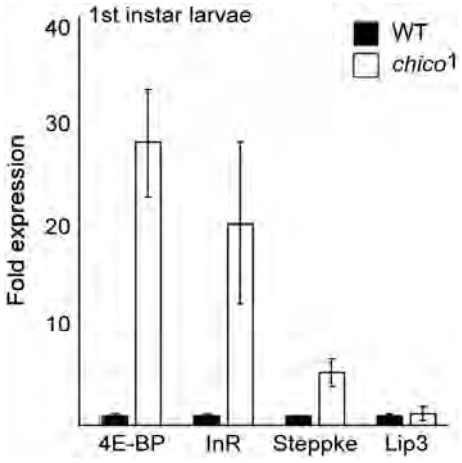

Fig. 6: Expression of IlS target genes *e4-bp* and *inr* as well as *steppke* and the starvation marker *lip3* in homozygous *chico*^{1} mutant larvae compared to wild type. Lip3=*lipase3*, 4E-BP=*4e binding protein*, InR=*insulin receptor*.

4.3.3 Starvation regulates transcription of IlS target genes

In *Drosophila*, IlS is known to be tightly coupled to the abundance of food when larvae are growing (Zinke et. al. 2002). As a direct result, IlS activity is quickly reduced when food is

scare and dFOXO is activated. In consequence, dFOXO dependent gene expression is comparable between starving wild type animals and IlS mutants (Kramer et. al. 2003), which means that starvation should phenocopy genetic IlS pathway mutants. To show that this is also true for *steppke* mutants, wild type larvae were raised on yeast paste and then starved on PBS for 6 h. As seen in *steppke* and *chico* mutants, dFOXO target genes *4e-bp* and *inr* showed enhanced expression in starved wild type animals (Fig. 7a). In contrast to genetic IlS mutants, where IlS is specifically inhibited, starvation led to extensive usage of lipid stores in the animal, as indicated by a strong upregulation of *lipase3* under these conditions (Zinke et. al. 2002). Notably, as already observed for *chico* mutants before, *steppke* expression was also elevated in starved wild type larvae. This hints to the possibility that *steppke* transcription itself is regulated by dFOXO in an autoregulatory feedback loop, as described for *4e-bp* and *inr*. To test this hypothesis, starvation of $dfoxo^{21}/dfoxo^{W24}$ null mutant larvae (Min et. al. 2008) of the same age was done and analysed for *steppke* expression. In these animals, upregulation of *steppke* after starvation was abolished (Fig. 7b), indicating that *steppke* expression is at least partly controlled by dFOXO.

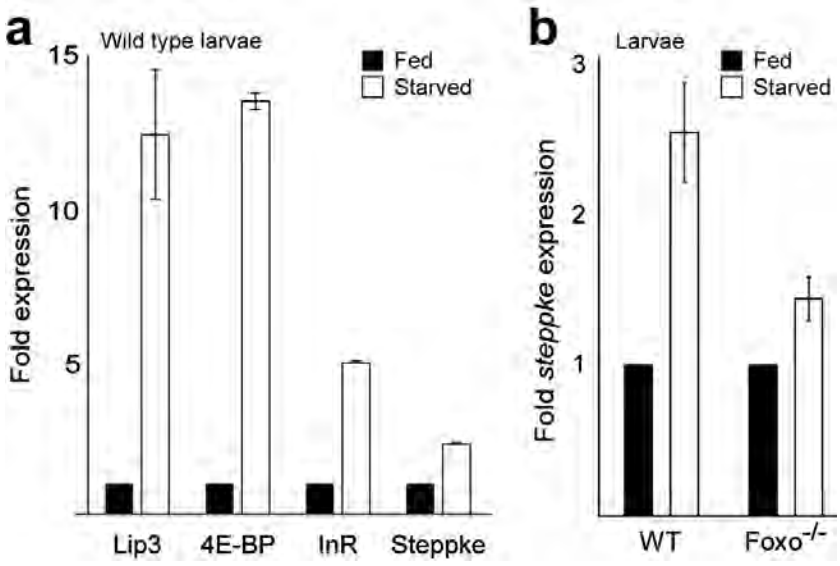

Fig. 7: dFOXO target genes are upregulated after starvation. **a)** Expression of IlS target genes *e4-bp* and *inr* as well as *steppke* and the starvation marker *lip3* in starved wild type second instar larvae. **b)** *steppke* expression in starved wild type and *dfoxo* mutant second instar larvae. WT=wild type, Foxo $^{-/-}$=$dfoxo^{21}/dfoxo^{W24}$, Lip3=*lipase3*, 4E-BP=*4e binding protein*, InR=*insulin receptor.*

4.4 Positioning of Steppke in the Insulin signalling cascade

4.4.1 Overexpression of PI3K in *steppke* mutants

(done in cooperation with I. Zinke)

Former results indicated that Steppke is a new component of IlS. Due to gene expression studies, Steppke function could be positioned upstream of dFOXO, which is regulated by PKB/Akt and PI3K in *Drosophila* (Hafen 2004). Activation of PI3K leads to high activity of PKB/Akt and to a downstream activation of IlS. To test whether Steppke might be acting upstream of PI3K, a genetic rescue experiment was performed by activating PI3K activity in *steppke* mutant animals. In consequence, a rescue of *steppke* dependent mutant growth phenotypes should have been possible only in case of a Steppke function upstream of PI3K, but not in the contrary. For activation of PI3K, the GAL4/UAS system was used to overexpress a constitutively active PI3K protein ($PI3K^{CAAX}$, see Leevers et. al. 1996) under control of an inducible *heatshock* promoter. First, two transgenic fly stocks were generated that combined $steppke^{K08110}$ and the *heatshock*-GAL4 driver as well as $steppke^{SH0323}$ and the UAS $pi3k^{CAAX}$ target gene. By crossing UAS $pi3k^{CAAX}$;$steppke^{SH0323}$ females with $steppke^{K08110}$;*heatshock-gal4* males, 12,5 % of the F1 female flies overexpressed $PI3K^{CAAX}$ in a $steppke^{K08110}$/$steppke^{SH0323}$ mutant background under control of the *heatshock*-GAL4 driver (Fig. 8a). As a control, *heatshock*-GAL4 dependent overexpression of $PI3K^{CAAX}$ was also activated in a heterozygous $steppke^{K08110}$/+ background. These flies contained one functional copy of the *steppke* gene, which is sufficient to suppress the body weight phenotype obtained in $steppke^{K08110}$/$steppke^{SH0323}$ mutants. Further controls were wild type as well as transheterozygous *steppke* mutant flies that did not overexpress PI3K. As the UAS $pi3k^{CAAX}$ insertion is located at the X chromosome, rescue experiments were only possible in female progeny. Measuring the weight of single flies of the appropriate genotypes revealed that activation of $PI3K^{CAAX}$ lead to increased body weight compared to normal wild type flies, which was equal in heterozygous and transheterozygous mutant flies (Fig. 8b). In consequence, a full rescue of the *steppke* mutant body weight phenotype was possible, pointing to a Steppke function upstream of PI3K.

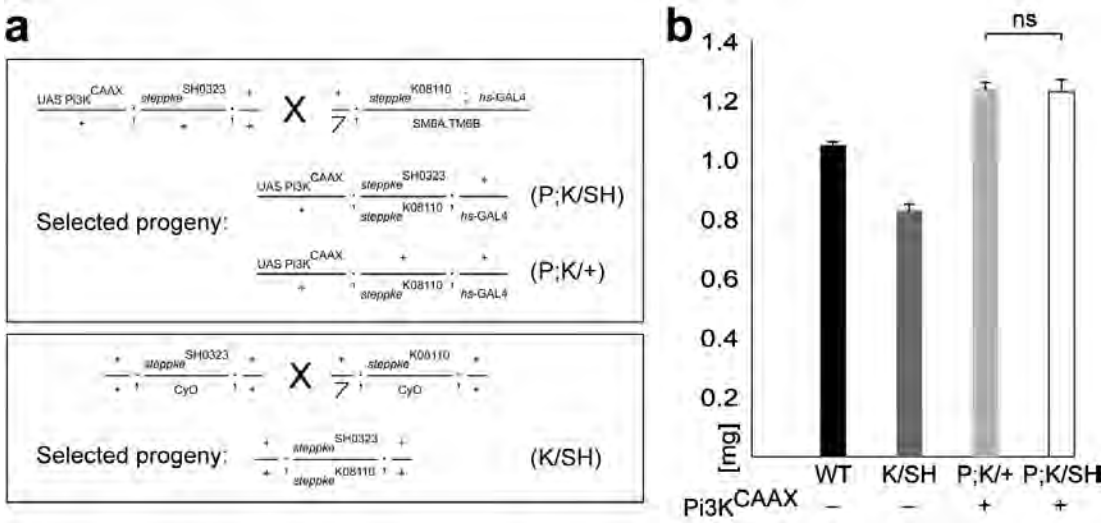

Fig. 8: Steppke functions upstream of PI3K. **a)** Crossing sheme to obtain the desired progeny overexpressing $Pi3K^{CAAX}$ in a *steppke* mutant or wildtypic heterozygous genetic background. **b)** Body weight of single flies of different genotypes. WT=wild type, K=$steppke^{K08110}$, SH=$steppke^{SH0323}$, P=overexpression of $Pi3K^{CAAX}$ under control of the *heatshock*-GAL4 driver.

4.4.2 Overexpression of the Insulin Receptor in the eye

Analogous to the genetic rescue experiment presented before, another overexpression study was performed to test whether Steppke acts upstream or downstream of the Insulin Receptor. It is known that overexpression of the INR in the adult eye results in a rough eye phenotype (Brogiolo et. al. 2001), caused by overproliferation of the cells due to hyperactivated IlS. This rough eye phenotype should be attenuated by a mutation in *steppke* in case of a Steppke function downstream of the INR, whereas an upstream function should have no influence on IlS activity when overexpressing the INR. To drive expression of a wild type INR protein (INR^{WT})in the eye, the GAL4/UAS System was used under control of the eye specific driver line *gmr*-GAL4. By crossing $steppke^{K08110}$ mutants to *gmr-gal4* flies as well as $steppke^{SH0323}$ mutants to UAS inr^{WT} flies, the two transgenic fly stocks $steppke^{K08110}$;*gmr-gal4* and $steppke^{SH0323}$;UAS inr^{WT} were established and balanced with the SM6A,TM6B balancer chromosome, which allowed selection of progeny with appropriate genotype by genetic markers. By using these fly stocks, one third of the resulting F1 progeny overexpressed INR^{WT}

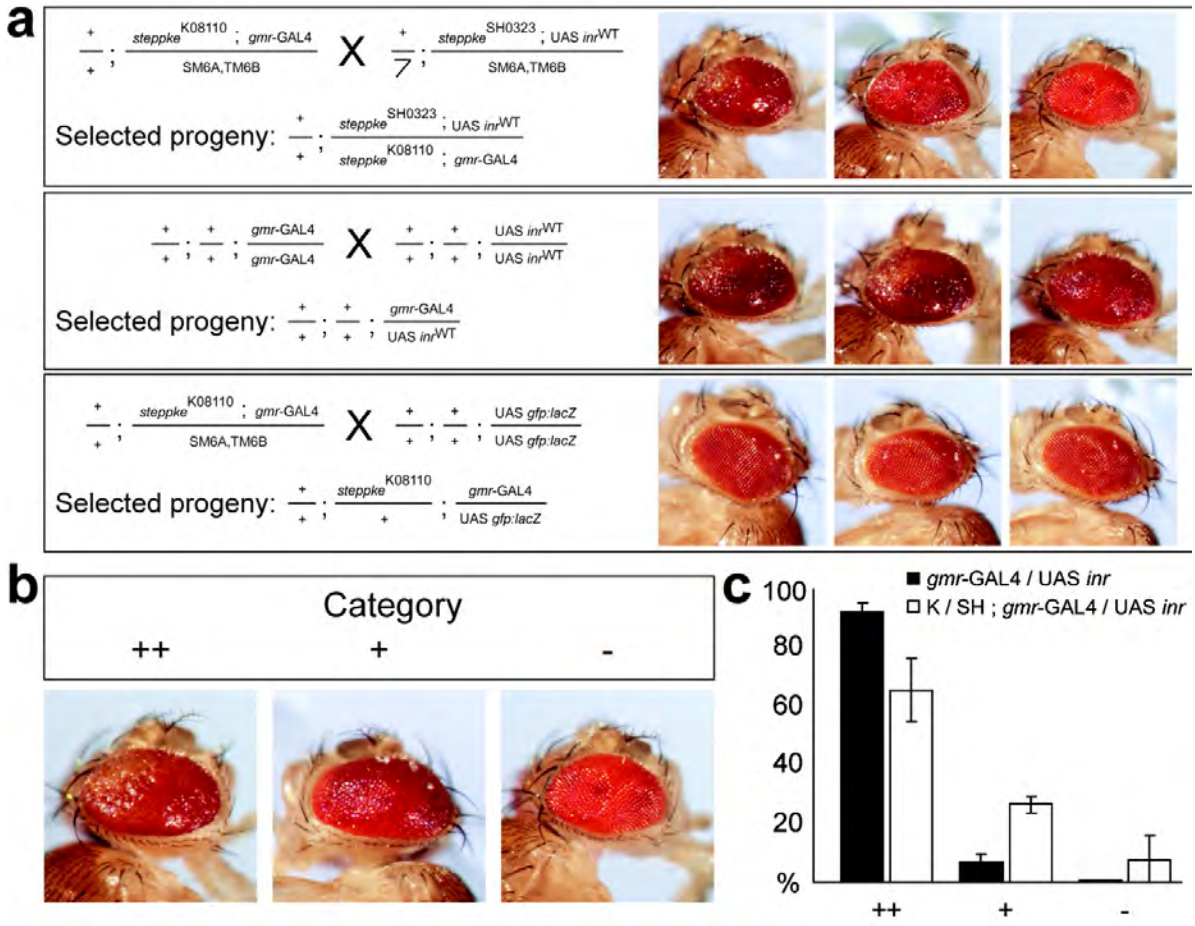

Fig. 9: Steppke functions downstream or at the INR. **a)** Crossing sheme to obtain the desired progeny overexpressing INR^{WT} in the eye in a *steppke* mutant or wild type genetic background. The pictures show the variability of resulting eye phenotypes. **b)** Categorization of eye phenotypes by their strenght: (++) strong increase in eye size and roughness, (+) mild increase in eye size and roughness, (-) no phenotype. **c)** Percentage of phenotypes occuring in each category after overexpression of INR^{WT} in either a *steppke* mutant or a wild typ background. K=$steppke^{K08110}$, SH=$steppke^{SH0323}$.

in the eye. Beside overexpression in a *steppke* transheterozygous mutant background, overexpression of INR^{WT} (positive control) as well as GFP:LACZ (negative control) was also performed in a wild type genetic background. The GFP:LACZ transgene did not generate any phenotype, whereas overexpression of INR^{WT} in a wild type background lead to a severe rough eye surface (Fig. 9a). Nevertheless, the rough eye phenotype was of different strength, even at constant temperature and culture conditions. This was especially the case when INR^{WT} was overexpressed in a *steppke* mutant background (Fig. 9a). To evaluate the experiment, progeny were devided into three categories, depending on the strength of the phenotype (Fig 9b). In summary, the penetrance and strength of rough eye phenotypes were much lower in a *steppke* mutant compared to a wild type background (Fig. 9c). This points to an attenuation of IlS downstream of the INR and in consequence to a Steppke function downstream or at the level of the Insulin Receptor.

4.5 Characterization of AMP expression in Insulin signalling mutants

4.5.1 AMP expression in *steppke* and *chico* mutants

The vertebrate homologs of Steppke, the Cytohesin proteins, have been discovered in the context of immune regulation (Kolanus 2007). While analysing *steppke* mutant phenotypes and gene expression profiles, regulation of antimicrobial peptides (AMPs) was noticed. These cationic peptides exhibit one of the most important defense mechanisms against microorganisms in *Drosophila*, but also other species (Lemaitre 2007). In homozygous $steppke^{K08110}$ mutants, AMP expression in non-infected larvae was upregulated compared to wild type animals (Fig. 10a). Since this could either be a *steppke* specific mutant phenotype or a consequence of misregulated IlS in these animals, *chico* mutants (Böhni et. al. 1999) were analysed for AMP expression as well. As seen for IlS dependent target genes *4e-bp* and *inr*, AMP expression was comparable in both IlS mutants since an upregulation could also be observed in homozygous $chico^{1}$ mutants (Fig. 10b). Remarkably, expression of *drosomycin*, a peptide with anti-fungal activity, was most strongly affected in both mutants.

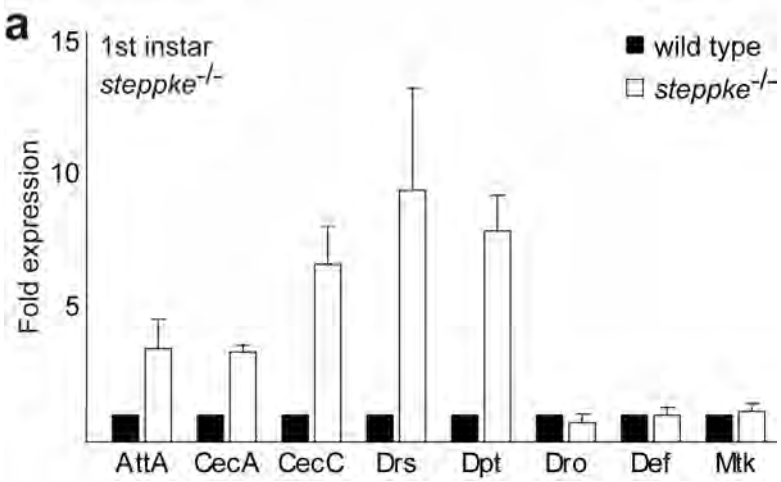

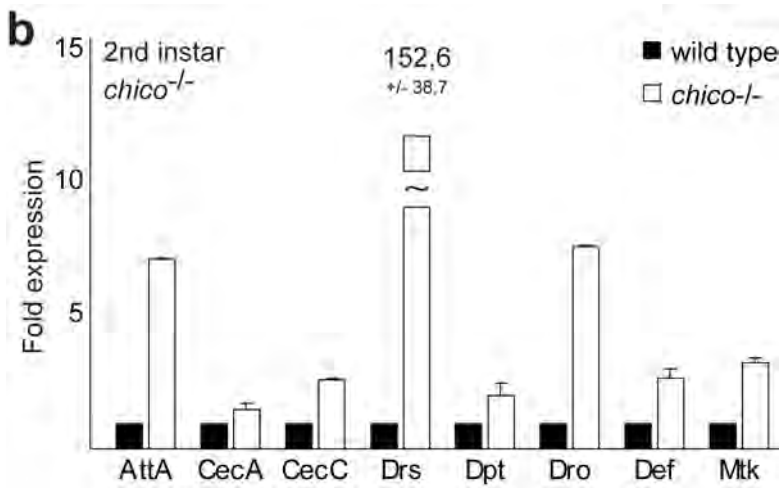

Fig. 10: Expression of antimicrobial peptides (AMPs) in *steppke* and *chico* mutants. **a)** Expression of AMPs in non-infected *steppke*^{K08110}/*steppke*^{SH0323} first instar larvae compared to wild type (control). **b)** Expression of AMPs in non-infected *chico*^{1}/*chico*^{1} second instar larvae compared to wild type (control). Att=*attacin A*, CecA=*cecropin A1*, CecC=*cecropin C*, Def=*defensin*, Dpt=*diptericin*, Dro=*drosocin*, Drs=*drosomycin*, Mtk=*metchnikowin*.

4.5.2 *drosomycin* expression in different *steppke* and *chico* alleles

It is known that AMP regulation is highly depending on the developmental stage and on hormone levels like ecdysone (Flatt et. al. 2008b). As many genetic IlS mutants show a developmental delay during larval stages (Hafen 2004), it was important to rule out that the observed effects in *steppke* and *chico* mutants were based on such an effect. To deal with this problem, two different strategies were used. First, different allelic combinations were used for both mutants, especially those alleles which showed comparatively mild growth effects and which were not significantly delayed during larval development. These alleles were transheterozygous *steppke*^{K08110}/*steppke*^{SH0323} in case of *steppke* and *chico*^{1}/*chico*^{flp147E} in case of *chico* mutants. The analysis was restricted to *drosomycin*, which was likewise upregulated also in both weaker alleles (Fig. 11). Second, *drosomycin* expression in all allelic combinations was compared to wild type controls of different age. Beside equally aged larvae, AMP expression was also compared to wild type animals of younger age, which mimicked a putative developmental delay of the mutants. *steppke* mutants were aged for 44 h (late first instar) after egg laying and compared to wild type larvae aged for 44 h (late first instar) and 32 h (mid of first instar) after egg laying. *chico* mutants were aged for 65 h (late second instar) and compared to wild type larvae aged for 65 h (late second instar), 44 h (late first instar) and 32 h (mid of first instar) after egg laying. In all cases, a robust increase in *drosomycin* expression was detected in both IlS mutants (Fig. 11), which did not found in a developmental delay. Taken together, data from *steppke* and *chico* mutants suggest that IlS mutants show an upregulation of AMP genes, which is not depending on developmental delay.

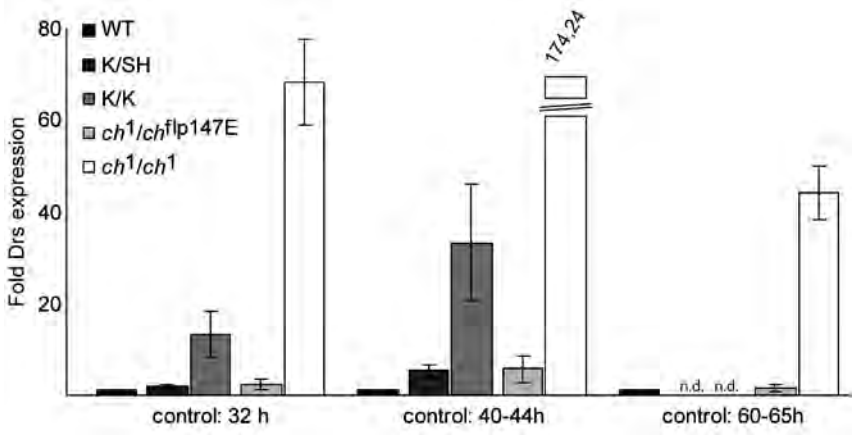

Fig. 11: *drosomycin* expression in *steppke* and *chico* mutants compared to wild type controls of different age. *steppke* mutants (40-44h after egg laying) and *chico* mutants (60-65h after egg laying) were compared to wild type controls of identical as well as earlier time points (indicated by the control age). WT=wild type, K=*steppke*^{K08110}, SH=*steppke*^{SH0323}, ch^{flp147E}=*chico*^{flp147E}, ch^{1}=*chico*^{1}, n.d. = not determined.

4.6 Impact of dFOXO on AMP expression

4.6.1 Sequence analysis of AMP gene promoters

As mentioned before, dFOXO is the main signal transducer of IlS on the level of transcriptional regulation in *Drosophila* (Puig et. al. 2003). Regulation of *4e-bp* and *inr* turned out to be dFOXO dependent in *steppke* mutants, so regulation of AMP genes could rest upon the same mechanisms. Binding of FOXO to DNA molecules is in general restricted to specific binding motifs, which are conserved in metazoans (Furuyama et. al. 2000) and located in the regulatory region of a gene. Three types of FOXO binding motifs with different strength exist: FOXO binding motifs (TTGTTTAC), Forkhead binding motifs (TXTTTAY) and Insulin responding elements (TT[G/A]TTT[T/G][G/T]), whereas X represents any nucleotide and Y any pyrimidine. FOXO binding motifs are of highest strength, followed by Forkhead binding motifs, which allow a more general binding of proteins with Forkhead domains. Insulin responding elements have not been clearly characterised, but described as motifs that are important for an Insulin dependent response at the transcriptional level. In case of AMP genes, a database search was performed to identify FOXO binding motifs in the regulatory region of these genes. As the entire promoter is not known for all AMPs, the 2 kb upstream sequence (taken from http://flybase.org/) of each AMP transcript was analysed. Several putative binding motifs of all three types were identified in all AMP gene promoters (Fig. 12), reinforcing the possibility that dFOXO has a direct role in controlling immunoresponsive genes.

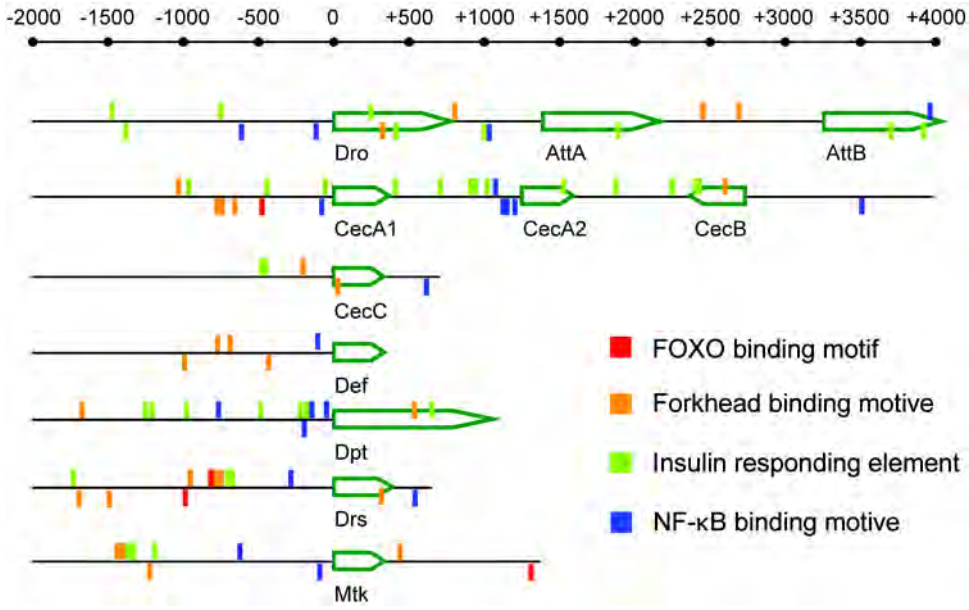

Fig. 12: Shematic overview of the 2 kb upstream region of several AMPs. Binding motifs for FOXO, Forkhead, insulin responding elements and NF-κB are shown. An upward bar indicates orientation of the binding motif in forward direction, a downward bar indicated reverse orientation. AttA=*attacin A*, AttB=*attacin B*, CecA1=*cecropin A1*, CecA2=*cecropin A2,* CecB=*cecropin B,* CecC=*cecropin C,* Def=*defensin*, Dpt=*diptericin*, Dro=*drosocin*, Drs=*drosomycin*, Mtk=*metchnikowin*.

4.6.2 AMP induction in starved wild type larvae

To further characterise the role of dFOXO concerning AMP regulation, a series of starvation experiments in wild type larvae was done. Under these conditions, dFOXO translocates into the nucleus and activates transcription of its target genes, among them *4e-bp*, *inr* and *steppke* (Puig et. al. 2003, Fuss et. al. 2006). Two larval stages, second and third instar, were choosen for this experiment to rule out that effects were stage specific. In both cases, starvation on PBS for 6 h was sufficient to upregulate a broad spectrum of AMP genes, with *drosomycin* being most strongly regulated (Figs. 13a,b). This correlated well with triggered dFOXO activity in those larvae, but to show that this upregulation was really dFOXO dependent, second instar $dfoxo^{21}/dfowo^{W24}$ null mutant larvae (Min et. al. 2008) were starved in parallel. In contrast to the wild type situation, no induction of AMP expression was detectable in *dfoxo* mutants (Fig. 14), demonstrating that dFOXO is essential for upregulation of AMPs when IlS is reduced. To validate that starvation conditions were adequate and that *dfoxo* mutants were able to respond to this treatment in general, *lipase3* expression was analysed (Zinke et. al. 2002). As seen in wild type animals before, *lipase3* induction after starvation was not affected in *dfoxo* mutants, showing that a dFOXO independent response to starvation is still possible.

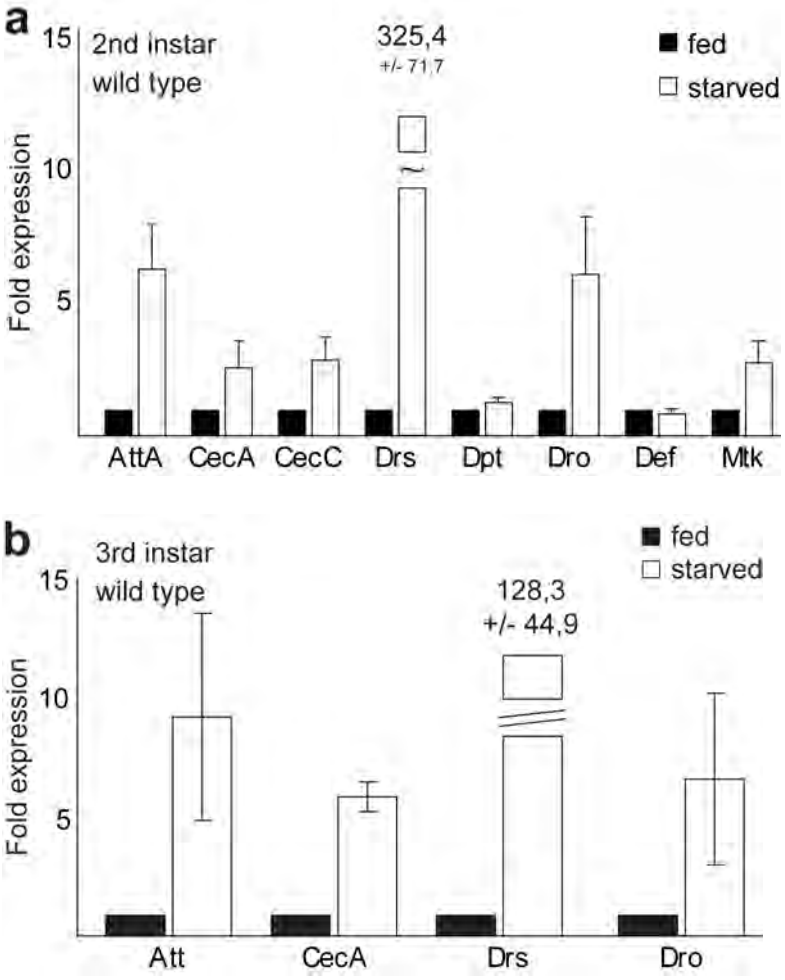

Fig. 13: Expression of AMPs is nutrient dependent. **a)** Expression of AMPs in non-infected second instar wild type larvae and **b)** in non-infected third instar wild type larvae, both after starvation on PBS compared to full nutrition (fed). Att=*attacin A*, CecA=*cecropin A1*, CecC=*cecropin C*, Def=*defensin*, Dpt=*diptericin*, Dro=*drosocin*, Drs=*drosomycin*, Mtk=*metchnikowin*.

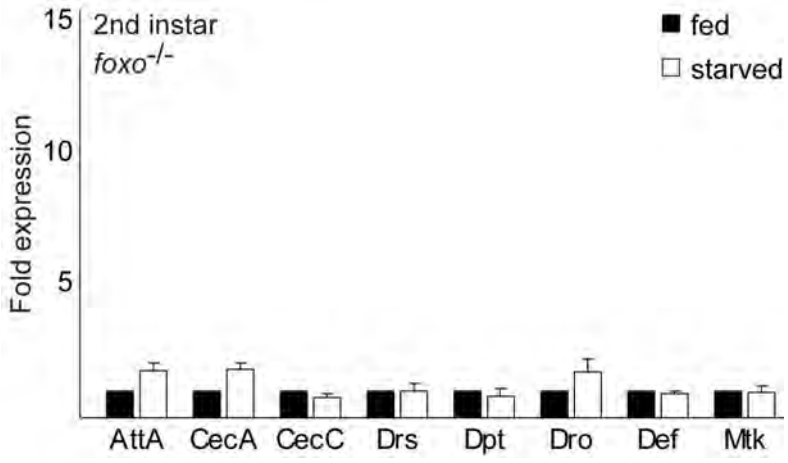

Fig. 14: Expression of AMPs in non-infected second instar *dfoxo* mutant larvae after starvation on PBS compared to full nutrition (fed). foxo$^{-/-}$=*dfoxo*^{21}/*dfoxo*^{W24}, Att=*attacin A*, CecA=*cecropin A1*, CecC=*cecropin C*, Def=*defensin*, Dpt=*diptericin*, Dro=*drosocin*, Drs=*drosomycin*, Mtk=*metchnikowin*.

4.6.3 AMP expression after SecinH3 feeding to adult flies

An alternative approach to inhibit IlS in *Drosophila* is feeding the small molecule compound SecinH3 (Fuss et. al. 2006). This chemical inhibitor is specific for Steppke in *Drosophila* as well as Cytohesins in vertebrates and targets the Sec7 domain of the protein, which is essential for the guanine nucleotide exchange reaction (Hafner et. al. 2006). Since adult flies are discontinuous feeders, application of SecinH3 targets IlS more specifically and more constantly than starvation. For this purpose, a feeding assay was established for adult flies, offering SecinH3 in normal fly food. Feeding this Steppke specific inhibitor for only eight days caused a significant upregulation of different AMPs in wild type adult females (Fig. 15a). Again, this regulation was dFOXO dependent, as already observed for starvation of larvae. Feeding SecinH3 to *dfoxo*^{21}/*dfoxo*^{W24} null mutant adult females had no impact on AMP transcription (Fig. 15b).

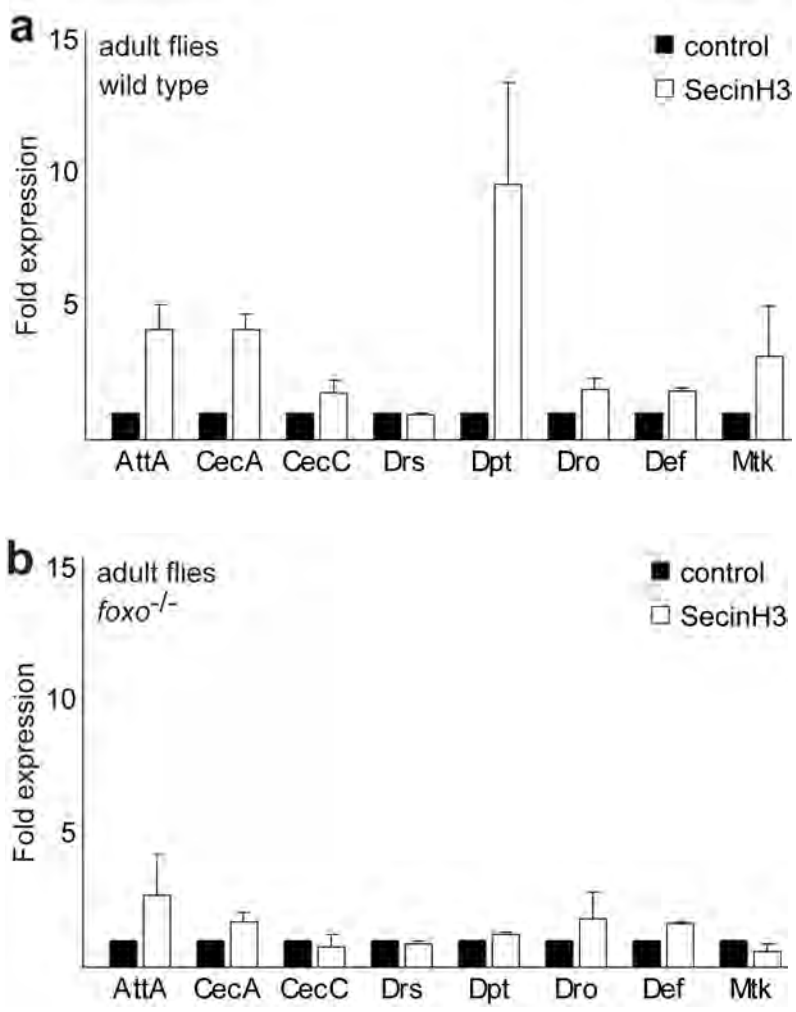

Fig. 15: Expression of AMPs can be triggered in adults by feeding of SecinH3. **a)** AMP expression in non-infected wild type adult female flies after feeding of SecinH3 for 8 days compared to control food. **b)** AMP expression in non-infected *dfoxo* mutant adult female flies after feeding of SecinH3 for 8 days compared to control food. foxo$^{-/-}$=*dfoxo*^{21}/*dfoxo*^{W24}, Att=*attacin A*, CecA=*cecropin A1*, CecC=*cecropin C*, Def=*defensin*, Dpt=*diptericin*, Dro=*drosocin*, Drs=*drosomycin*, Mtk=*metchnikowin*.

4.6.4 AMP expression in S2 cells

Drosophila S2 cell culture represents a system that allows quick manipulation of conditions without triggering the humoral response of the whole animal. To validate the *in-vivo* results of starvation as well as SecinH3 feeding, both assays were repeated in cell culture. Starvation of S2 cells can be achieved by two ways, either depletion of growth factors or incubation in PBS. Growth factor starvation represents the milder way to target IlS and can be performed for several days, whereas starvation in PBS is restricted to several hours to avoid apoptosis. As seen *in-vivo*, expression of AMPs was nutrient dependent also in S2 cells. Both growth factor starvation for 24 h as well as full starvation in PBS for 4 h caused increased AMP transcription (Figs. 16a,b).

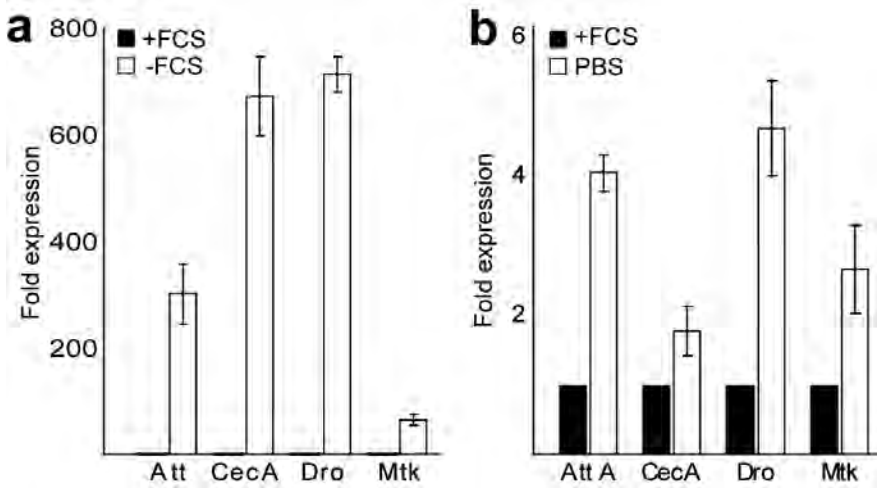

Fig. 16: Nutrient dependent expression of AMPs in *Drosophila* S2 cells. **a)** AMP expression in S2 cells after growth factor starvation (-FCS) for 24 h compared to full medium (+FCS). **b)** AMP expression in S2 cells after full starvation in PBS for 4 h compared to full medium (+FCS). Att=*attacinA*, CecA= *cecropinA1,* Dro=*drosocin,* Mtk= *metchnikowin.*

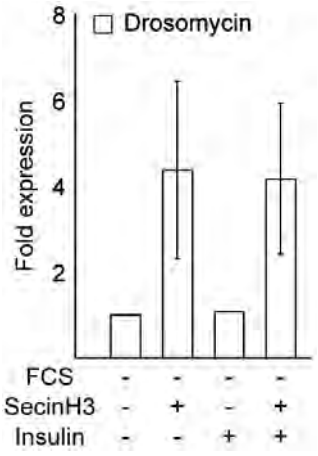

Fig. 17: Expression of *drosomycin* in S2 cells after insulin stimulation and treatment with 10 µM SecinH3.

To analyse whether also SecinH3 causes an identical effect in S2 cells, SecinH3 treatment combined with Insulin stimulation was performed. Cells were starved for growth factors and SecinH3 was applied with and without stimulation by Insulin. In both cases, an upregulation of *drosomycin* was detected, which was even stronger than seen for growth factor starvation alone (Fig. 17). Insulin stimulation was not able to silence this SecinH3 dependent regulation.

4.6.5 AMP expression after dFOXO overexpression

To demonstrate that dFOXO activity alone is sufficient to trigger AMP transcription, a series of overexpression experiments using the GAL4/UAS system were realized, both in larvae and adult flies. A modified dFOXO protein was used for overexpression, which is constitutively active in the nucleus due to changed phosphorylation sites (dFOXO^{TM}, see Jünger et. al. 2003). To tightly control dFOXO^{TM} expression in the transgenic animals, the *heatshock*-GAL4 driver line was choosen, which is ubiquitiously induced in all tissues following heat stress. Activation of the GAL4 driver was achieved by shifting the temperature from 25 °C to 37 °C for 45 min. either in second instar larvae or in adult flies, followed by re-incubation at 25 °C. AMP expression was analysed 6 h after heatshock and was found to be strongly increased in both cases (Figs. 18a,b). Together with results obtained from *dfoxo* mutants, these data give strong evidence for a dFOXO dependent regulation of AMP genes in *Drosophila* larvae and adults.

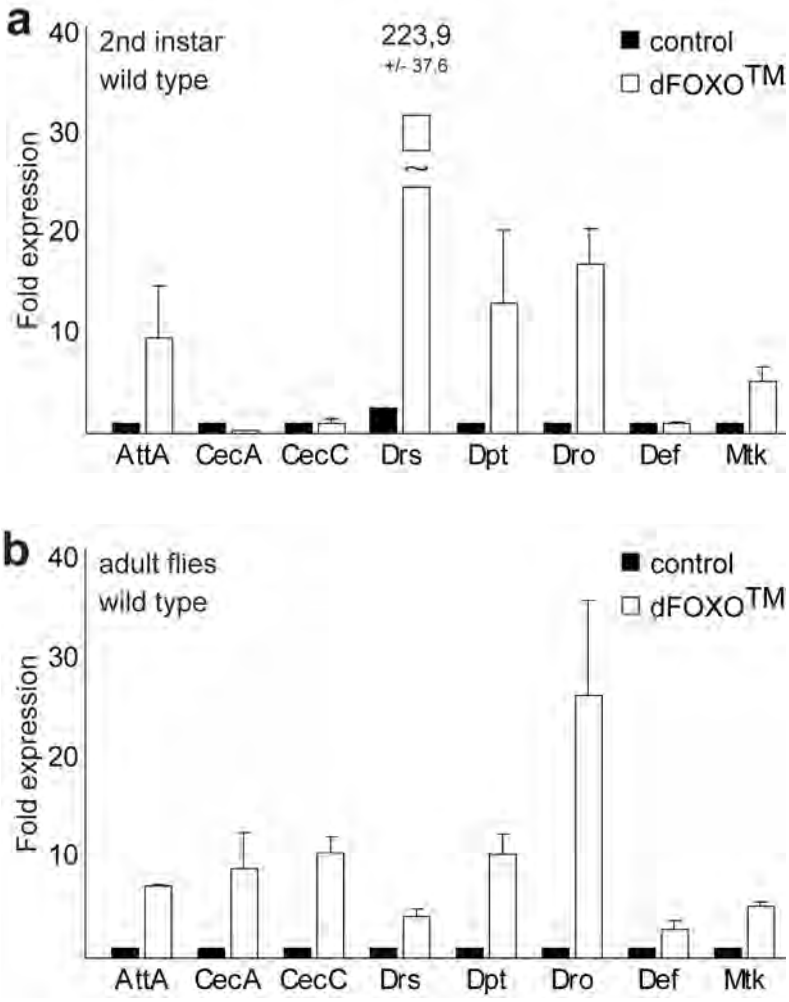

Fig. 18: Upregulation of AMPs after overexpression of constitutively active dFOXO^{TM}. **a)** AMP expression in non-infected second instar wild type larvae and **b)** wild type adult flies after *heatshock*-GAL4 dependent overexpression of dFOXO^{TM}. Att=*attacin A*, CecA=*cecropin A1*, CecC=*cecropin C*, Def=*defensin*, Dpt=*diptericin*, Dro=*drosocin*, Drs=*drosomycin*, Mtk=*metchnikowin*.

4.7 Molecular analysis of dFOXO dependent *drosomycin* regulation

Further analysis concerning molecular interaction of dFOXO with AMP promoters were restricted to *drosomycin*, which turned out to be the most strongly dFOXO dependent regulated AMP gene in IlS mutants, after starvation and after dFOXO^{TM} overexpression. *in-silico* analysis revealed that within the 2 kb regulatory region, which has also been characterised before to reproduce the endogenous *drosomycin* expression pattern, a cluster of five putative dFOXO/Forkhead binding motifs exists (Fig. 19). This cluster is located in a region covering nucleotides -805 to -990 upstream of the *drosomycin* transcript and contains two dFOXO as well as three Forkhead binding motifs. In addition, a binding site for NF-κB like proteins, which include DIF, Dorsal and Relish in *Drosophila*, exists at upstream position -319 bp.

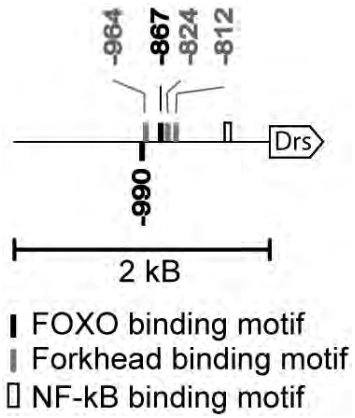

Fig. 19: 2 kb drosomycin promoter with dFOXO/ Forkhead binding motifs.

4.7.1 *In-situ* hybridisation in wild type and *dfoxo* mutant larvae

(done in cooperation with P. Carrera)

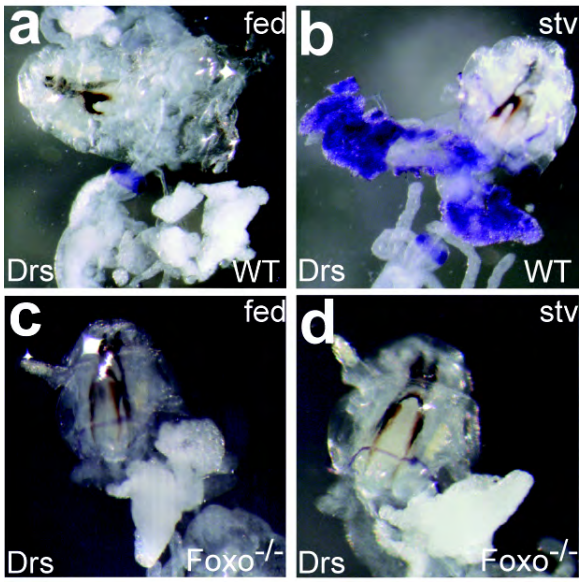

Fig. 20: In-situ hybridisation for *drosomycin* in larval fat body tissues. **a-b)** *drosomycin* expression in wild type larval fatbodys after starvation and full nutrition (fed). **c-d)** *drosomycin* expression in larval fatbodys of *dfoxo* mutants after starvation and full nutrition (fed). Foxo$^{-/-}$=*dfoxo*^{21}/*dfoxo*^{W24}, WT=wild type, Drs=*drosomycin*.

To show that *drosomycin* regulation *in-vivo* depends on dFOXO, *in-situ* hybridisation experiments in larval fat body tissues were done. The fat body is the main responsive organ of both metabolism and innate immunity in *Drosophila* (Hafen 2004, Lemaitre et. al. 2007). IlS is known to be highly active in this tissue and also *drosomycin* is strongly regulated and expressed. Wild type as well as *dfoxo*^{21}/*dfoxo*^{W24} null mutant larvae were grown on yeast paste until early third instar and then starved on PBS for 6 h to trigger

dFOXO activity. Using a *drosomycin* RNA antisense probe, a strong fat body response was visible in wild type larvae after starvation, whereas in fed control animals, this *drosomycin* response was missing (Figs. 20a,b). In contrast, any fat body derived drosomycin regulation was absent in *dfoxo* mutant larvae, both in fed as well as starved animals (Figs. 20c,d). As indicated before by RT-PCR experiments, this demonstrates that *drosomycin* expression in the fat body is specifically regulated by dFOXO in a nutrient dependent manner.

4.7.2 Electromobility shift assay for dFOXO binding sites

(done in cooperation with M. Beyer)

Direct binding of dFOXO to specific binding motifs in the regulatory region of its target genes is essential for dFOXO dependent transcriptional regulation (Furuyama et. al. 2000). A cluster of five putative binding motifs was identified in the *drosomycin* promoter and direct dFOXO targeting of this cluster should be demonstrated by electromobility shift assays (EMSA). To do this, four different DNA oligos were synthesised and fluorescently labeled. Two of these oligos were designed to match dFOXO binding sites at positions -867 and -990, respectively. The oligos covered the core sequence of the dFOXO binding motif and aditionally about eight bases of flanking genomic region at each site. Two other oligos did also cover binding motifs at -867 and -990, but contained changes in the core binding sequence, whereas the flanking region was left untouched. As a source of dFOXO protein, third instar larvae overexpressing dFOXO-GFP were used to isolate nuclear protein extracts. Larvae were starved prior to lysis to allow dFOXO-GFP localization into the nucleus. In case of the binding motif at position -990, direct binding of a protein from the nuclear lysate to the appropriate oligo was visible, indicated by a band shift after electrophoresis (Fig. 21). Incubation with a ten-fold excess of the mutated oligos did not show any binding competition, in contrast to the oligo matching the exact binding site at position -867. This demonstrates that the core consensus sequence is

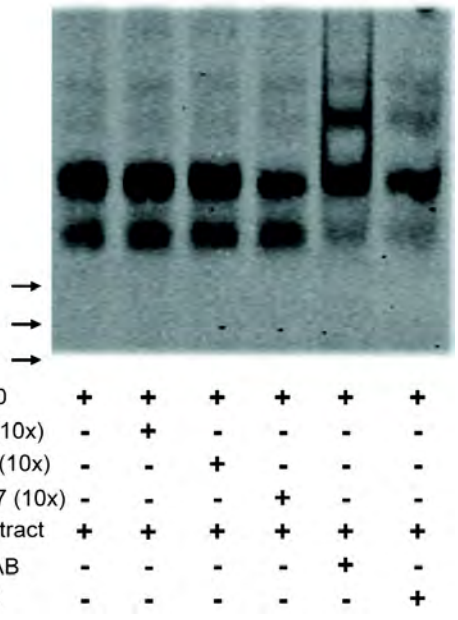

Fig. 21: EMSA for dFOXO binding motif at position -990 in the *drosomycin* promoter with nuclear extract of third instar larvae overexpressing dFOXO-GFP. Oligos FOXO -990 and -867 match the appropriate binding motifs with wildtypic sequence, whereas Mutated I and II cover the same region, but sequences of the core binding motifs are changed. AB=antibody.

essential for binding and not the flanking genomic region. The bound protein was identified as dFOXO-GFP by a supershift, caused by incubation with an anti-GFP antibody. This supershift was not detected after incubation with a control antibody. Taken together, this EMSA demonstrated direct binding of a nuclear protein to the core binding motif at position -990 in the *drosomycin* promoter, which could be identified as dFOXO.

4.7.3 Cloning of *drosomycin* promoter *luciferase* constructs

(done in cooperation with I. Zinke, G. Loch and A.C. Aschenbrenner)

To study the usage of these clustered dFOXO binding sites in cell culture and *in-vivo*, several *luciferase* constructs covering the *drosomycin* promoter were cloned (Fig. 22). All cell culture constructs used the pGL3 *luciferase* vector (Promega), whereas *in-vivo* constructs for usage in transgenic flies were based on pCaSpeR4 vector. The *drosomycin* promoter sequence was derived from *white*^{1118} genomic DNA. Construct Drs_WT was amplified in a single reaction using primers Drs_F1 / Drs_R1 and covered the whole wildtypic 2 kb promoter region. Construct Drs_Δ1-5 lacked the complete dFOXO binding cluster and was made in two steps. First, the regions upstream and downstream of the deletion, covered by primer pairs Drs_F1 / Drs_Del_R1 and Drs_Del_F1 / Drs_R1, were amplified. An overlap PCR, using the former products and primers Drs_F1 / Drs_R1, amplified the final construct (Figs. 22a,b).

To get a more precise insight into the usage of single binding motifs, four constructs carrying point mutations in each binding motif (Furuyama et. al. 2000) or combinations of them were made (Figs. 22a,b). Based on construct Drs_WT, point mutations in the core dFOXO binding motif were inserted using QuikChange Lightning Multi site-directed mutagenesis kit (Stratagene). dFOXO binding motifs were mutated by changing the core consensus sequence TTGTTTAC to TCCTTTAC (primers DBE1 for motif at position -990 and DBE3 for motif at position -867), which is sufficient to prevent dFOXO binding. Accordingly, Forkhead binding sequences were changed from TGTTTAT to TCTTTAT (primers DBE2 for motif at position -964 and DBE4+5 for motifs at position -824 and -812).

Finally, a short 287 bp genomic region covering the dFOXO binding cluster was isolated and cloned into pGL3 vector (Figs. 22a,b). Construct Drs_287_WT was amplified with primers Drs_287_F1 / Drs_287_R1 and contained wildtypic promoter sequence. In contrast, construct Drs_287_ Δ1,2,3,4,5 was amplified in two steps, containing mutated core consensus sequences for all five binding motifs. First, two short fragments were amplified with primers Drs_287_F1M / Drs_287_R1M and Drs_287_F2M / Drs_287_R2M, whereas the primers covered all five mutated binding motifs. In the second step, both products were used as template in an overlap PCR reaction with primers Drs_287_F1M / Drs_287_R2M, resulting in the final construct.

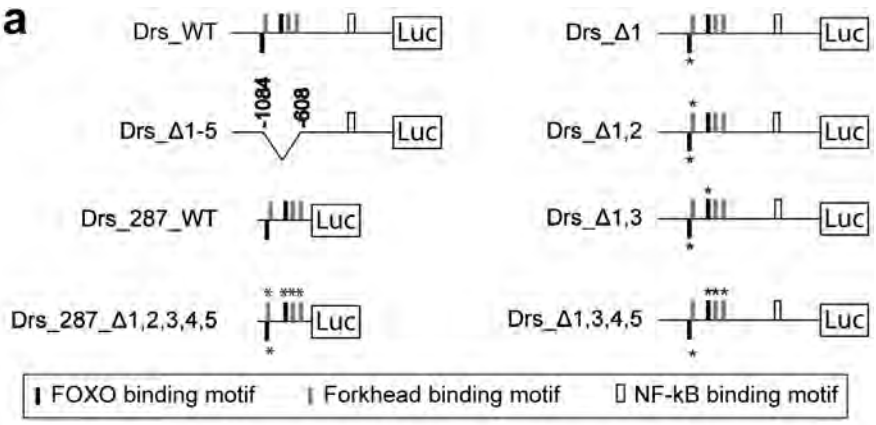

b

Construct	Length	Binding motif at position: -990	-964	-867	-824	-812
Drs_WT	2000 bp	GTAAACAA	TGTTTAT	TTGTTTAC	TTGTTTAT	TGTTTAT
Drs_Δ1-5	1524 bp	Deleted				
Drs_Δ1	2000 bp	GT—AGGA	TGTTTAT	TTGTTTAC	TTGTTTAT	TGTTTAT
Drs_Δ1,2	2000 bp	GT—AGGA	TCTTTAT	TTGTTTAC	TTGTTTAT	TGTTTAT
Drs_Δ1,3	2000 bp	GT—AGGA	TGTTTAT	TCCTTTAC	TTGTTTAT	TGTTTAT
Drs_Δ1,3,4,5	2000 bp	GT—AGGA	TGTTTAT	TCCTTTAC	TTCTTTAT	TCTTTAT
Drs_287_WT	287 bp	GTAAACAA	TGTTTAT	TTGTTTAC	TTGTTTAT	TGTTTAT
Drs_287_Δ1,2,3,4,5	287 bp	TGCGCTGC	CAGCGCA	GCAGCGCA	CAGCGCA	CAGCGCA

Fig. 22: Overview of the different *luciferase* constructs covering the *drosomycin* promoter. **a)** Summary of eight *luciferase* constructs, changes in the promoter region are shown shematically. **b)** Detailed description of the changes in dFOXO/Forkhead binding motif and the resulting lenght of each construct.

4.7.4 Luciferase assay in S2 cells

(done in cooperation with G. Loch)

Constructs Drs_WT and Drs_Δ1-5 were used in S2 tissue culture cells to verify that the cluster of five dFOXO binding motifs, located at position -805 to -990 upstream of the drosomycin transcript, is essential for dFOXO dependent regulation. Either contructs Drs_WT or Drs_Δ1-5 were co-transfected with plasmids pMT-GAL4 and UAS-*dfoxo-gfp* into S2 cells. The two latter plasmids allowed GAL4/UAS dependent overexpression of dFOXO-GFP (Fuss et. al. 2006) in transfected cells under control of a metallothionein promoter, which is inducible by addition of $CuSO_4$. Induction of dFOXO-GFP overexpression was done 16 h after transfection, followed by a 24 h incubation before cells were harvested and subjected to RNA preparation. The assay was analysed by quantitative real-time RT-PCR, which allowed normalization of *luciferase* transcription according to dFOXO-GFP activity only in transfected cells. This point was of high importance since transfection efficiency in S2 cells was just between 5 % and 10 %. Normalization to a co-transfected renilla *luciferase* construct, which is constitutively active and typically used for these assays, would just have allowed

normalization to general transfection efficiency, but not dFOXO activity. Induction tests comparing construct Drs_WT to the empty pGL3 vector showed that dFOXO-GFP dependent *luciferase* expression in the wild type construct worked properly (Fig. 23a). However, comparison of constructs Drs_WT and Drs_Δ1-5 revealed that the identified cluster of dFOXO binding sites was essential for *drosomycin* regulation, as construct Drs_Δ1-5 failed to induce *luciferase* expression after dFOXO-GFP overexpression in S2 cells (Fig. 23b).

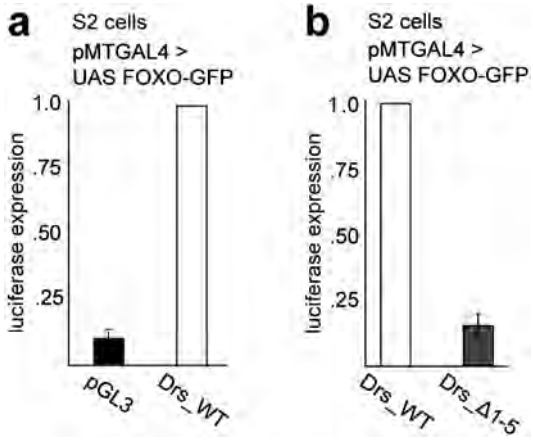

Fig. 23: Luciferase assay in S2 cells after dFOXO-GFP overexpression. **a)** Induction of *luciferase* expression in construct Drs_WT compared to empty pGL3 control vector. **b)** Induction of *luciferase* expression in constructs Drs_WT and Drs_Δ1-5.

4.7.5 Luciferase assay in transgenic larvae

Transgenic flies were made carrying constructs Drs_WT or Drs_Δ1-5 to show that the dFOXO dependent regulation, which was observed in S2 cells, is also essential *in-vivo*. Both constructs were shuttled from pGL3 vector to pCaSpeR4 vector, which was used for germline mediated transformation into wild type *white*^{1118} embryos. Beside the *drosomycin* promoter region, the *luciferase* ORF contained in the pGL3 vector was also transfered to allow Luciferase expression in

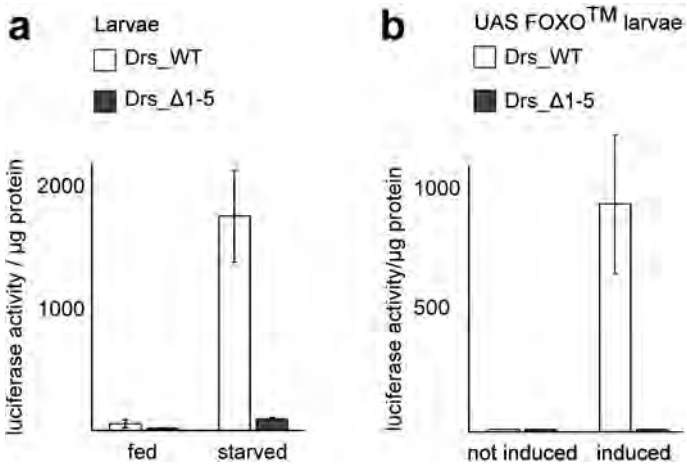

Fig. 24: Luciferase assay in transgenic third instar larvae carrying constructs Drs_WT or Drs_Δ1-5. **a)** Induction of luminescence by constructs Drs_WT or Drs_Δ1-5 after starvation on PBS compared to full nutrition (fed). **b)** Induction of luminescence by constructs Drs_WT or Drs_Δ1-5 after overexpression of dFOXO^{TM} (induced) compared to control animals (not induced).

larvae. Luciferase activity in transgenic third instar larvae was quantified using Luciferase assay system (Promega) and normalized to total protein of the animals. Instead of dFOXO-GFP, the constitutively active dFOXO^{TM} protein was overexpressed in larvae carrying either Drs_WT or Drs_Δ1-5 constructs using the GAL4/UAS system. Overexpression was controlled by the *heatshock*-GAL4 driver line and induced in early third instar larvae. As seen in S2 cells, construct Drs_WT responded strongly to enhanced dFOXO^{TM} activity also in larvae, whereas construct Drs_Δ1-5 failed to induce Luciferase activity. In a control experiment, both constructs showed comparable basal expression without dFOXO^{TM} overexpression (Fig. 24a). To further test the *in-vivo* significance of dFOXO binding motifs in a more physiological way, endogenous dFOXO activity was triggered by starvation instead of overexpressing a constitutively active protein. For this purpose, transgenic larvae carrying constructs Drs_WT or Drs_Δ1-5 were raised on yeast paste until early third instar stage and then either yeast fed or starved on PBS for 6 h. As seen before, Luciferase activity was equally depending on endogenous dFOXO activity and the presence of dFOXO binding motifs (Fig. 24b). To this end, experiments in cell culture and *in-vivo* revealed an essential role for the identified cluster of dFOXO/Forkhead binding motifs in IlS dependent *drosomycin* regulation.

4.7.6 Luciferase assay in S2 cells with mutated constructs

(done in cooperation with G. Loch)

As demonstrated in experiments using either the wild type or the deletion construct, a dFOXO dependent *drosomycin* induction failed when the whole cluster of dFOXO/Forkhead binding motifs was deleted. To unravel this in more detail, several constructs based on the wildtypic Drs_WT were made carrying point mutations in each dFOXO binding motif or combinations of them (see Fig. 22). Furthermore, using these constructs allowed to rule out that other *cis* regulatory elements, being important for *drosomycin* regulation in a non-dFOXO dependent manner, were as well deleted in the Drs_Δ1-5 construct. Again, *luciferase* expression was analysed in S2 cells as depicted before. It turned out that mutating the dFOXO binding motif at position -990 already reduced a dFOXO-GFP dependent *luciferase* expression by more than two third. Taking out four of the five binding motifs totally abolished *luciferase*

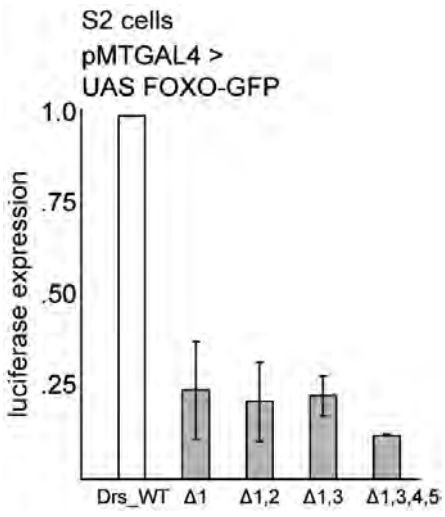

Fig. 25: Luciferase assay in S2 cells after dFOXO-GFP overexpression comparing construct Drs_WT and different constructs with mutated dFOXO/Forkhead binding sites.

expression (Fig. 25). This further strengthened the EMSA results, which also allocated the dFOXO binding motif at position -990 a special importance.

The other way around, the 287 bp region covering the cluster of dFOXO/Forkhead binding motifs was separated and ligated into pGL3 vector (see Fig. 22). Isolating this region allowed to analyse dFOXO dependent *luciferase* expression without the influence of other *cis* regulatory elements, for example the proximally located NF-κB motif. The construct containing wildtypic promoter sequence showed dFOXO-GFP dependent *luciferase* induction, as already seen for the full length region (Fig. 26). Notably, *luciferase* induction compared to empty pGL3 vector as a control was weaker in the short construct than in the full length construct, suggesting that other regulatory elements outside the isolated region might be targeted as well. Nevertheless, mutating all five dFOXO/Forkhead binding motifs in the short 287 bp construct lead to a complete loss of dFOXO-GFP dependent *luciferase* expression (Fig. 26). Taken together, experiments using *drosomycin* promoter constructs with point mutations in dFOXO/Forkhead binding motifs revealed that the isolated cluster is essential and sufficient to drive dFOXO dependent *drosomycin* expression.

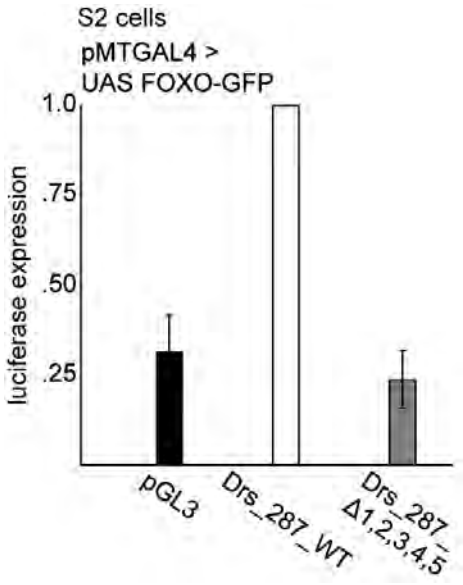

Fig. 26: Luciferase assay in S2 cells after dFOXO-GFP overexpression comparing construct Drs_287_WT and construct Drs_287_Δ1,2,3,4,5 with mutated dFOXO/Forkhead binding sites.

4.8 Uncoupling of dFOXO and NF-κB dependent AMP expression

4.8.1 dFOXO dependent AMP expression in immune deficient animals

Former results showed that dFOXO is able to directly regulate the expression of AMP genes. Moreover, direct binding to the *drosomycin* promoter has been shown. This raises the question whether dFOXO can regulate AMP expression independently of the NF-κB innate immune pathways. Regulation of the short 287 bp *drosomycin* promoter construct, which did not contain any NF-κB binding motif, suggested that this could be indeed the case. Nevertheless, *in-vivo* experiments were done to verify this assumption. For this purpose, starvation as well as SecinH3 feeding experiments were done in *relish*^{E20},*spätzle*^{RM7} homozygous double mutant larvae and adults. In these mutants, both the IMD and the Toll pathway are defective, resulting in immune deficient animals that have been shown to be unable to respond to bacterial

challenge and AMP upregulation (De Gregorio et. al. 2002). Surprisingly, triggered *drosomycin* expression was detected in starved *relish,spätze* mutant second instar larvae (Fig. 27a). Moreover, also feeding of SecinH3 to these double mutant adult flies resulted in enhanced AMP expression (Fig. 27b), as shown for wild type flies before. Due to complete lack of NF-κB dependent AMP regulation in these mutants, upregulation of those peptides following starvation and SecinH3 feeding can only be explained by a dFOXO dependent mechanism which is totally independent of the innate immune pathways.

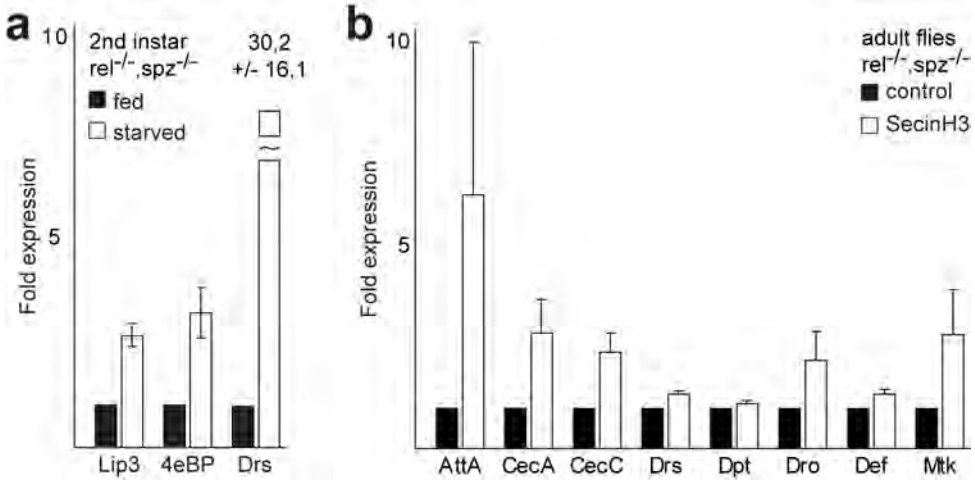

Fig. 27: IIS dependent AMP induction in immune mutants of Toll and IMD pathways. **a)** Induction of *drosomycin* in homozygous *relish,spätzle* mutant second instar larvae after starvation on PBS compared to full nutrition (fed). **b)** Induction of *drosomycin* in homozygous *relish,spätzle* mutant adult females after feeding of SecinH3 for 8 days compared to control food. rel,spz$^{-/-}$ =*relish*^{E20}/*relish*^{E20}, *spätzle*^{RM7}/*spätzle*^{RM7}, *Att=attacin A, CecA=cecropin A1, CecC=cecropin C, Def=defensin, Dpt=diptericin, Dro=drosocin, Drs=drosomycin, Mtk=metchnikowin,* Lip3=*lipase3,* 4eBP=*4e binding protein*.

4.8.2 NF-κB dependent AMP expression in *dfoxo* mutants

Since dFOXO acts independently of NF-κB innate immune pathways, the question came up whether vice versa NF-κB dependent AMP expression is still possible in animals lacking dFOXO. To adress this issue, infection experiments were performed in *dfoxo*^{21}/*dfoxo*^{W24} null mutants (Min et. al. 2008). A systemic infection was achieved by pricking a mixture of gram positive *Micrococcus luteus* as well as gram negative *Erwinia carotovora* into the lateral thorax of adult flies. It has been shown that this type of infection specifically triggers a fat body derived innate immune response, which is NF-κB dependent (De Gregorio et. al. 2002). In case of *dfoxo* mutants, both survival and AMP expression levels after infection were compared to wild type flies. Survival experiments clearly demonstrated that *dfoxo* mutant flies were not hypersensitive to infection, in contrast to severel IMD and Toll pathway mutants. In fact, survival of *dfoxo* mutants was identical to wild type flies, showing that these animals were able to deal with a strong bacterial infection without dFOXO activity (Fig. 28a). To

analyse this in more detail, AMP expression levels in *dfoxo* mutant and wild type flies were quantified after infection by quantitative real-time RT-PCR. Consistent with results of the survival experiments before, AMP expression in *dfoxo* mutants was comparable to wild type flies (Fig. 28b). A several thousand fold induction of different AMPs clearly demonstrated that NF-κB dependent AMP regulation is still possible in animals lacking dFOXO activity. Taken together, experiments in NF-κB as well as in *dfoxo* mutants indicate that AMP regulation by both mechanisms occurs independently.

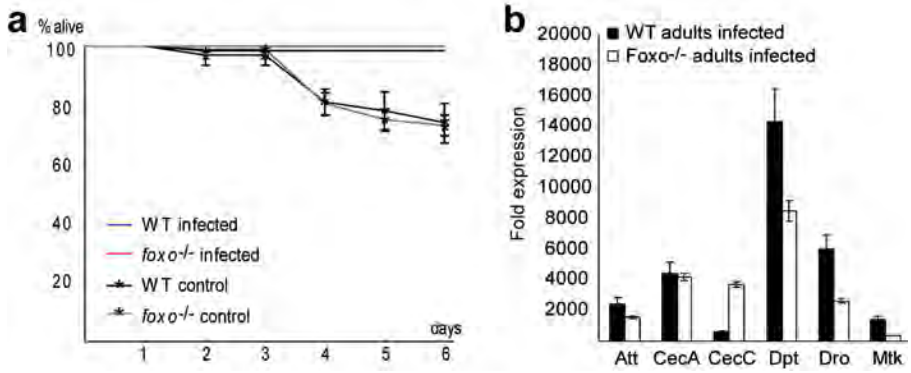

Fig. 28: Survival and AMP expression of *dfoxo* mutants after bacterial infection with *Erwinia carotovora* and *Micrococcus luteus*. **a)** Survival of *dfoxo* mutant adult females after bacterial infection (infected) and control treatment with sterile PBS (control) compared to wild type adult females. **b)** AMP expression of *dfoxo* mutant adult females 24 h after infection compared to wild type adult females. Foxo$^{-/-}$=*dfoxo*^{21}/*dfoxo*^{W24}, WT=wild type, Att=*attacinA*, CecA= *cecropinA1*, CecC= *cecropinC,* Dro=*drosocin,* Dpt=*diptericin,* Mtk=*metchnikowin*.

4.9 Analysis of tissue dependent AMP expression by dFOXO

For NF-κB dependent regulation of AMPs it has been shown that innate immunity triggers expression of these peptides either locally in barrier epithelia or systemically in the fat body (Lemaitre et. al. 2007). The tissue of choice is thereby only dependent on the type of infection. In contrast, dFOXO dependent AMP regulation occurs in non-infected animals and is depending on the energy status of the cell, which uncouples AMP expression by dFOXO and by NF-κB. So far, it is unclear in which tissues a dFOXO dependent AMP regulation is taking place. *In-situ* hybridisation experiments revealed that the fat body is targeted by this new mechanism, but the question remained whether also barrier epithelia show a nutrient dependent regulation of AMPs. To analyse this, real-time RT-PCR experiments were done in isolated larval tissues, including fat body, epithelia, gut and trachea. Early third instar wild type larvae grown on yeast paste were either yeast fed or starved on PBS for 6 h to trigger dFOXO activity. Selected tissues were carefully dissected in PBS and subsequently transfered to lysis buffer, followed by RNA preparation. For each tissue, expression of different AMPs was analysed from either control (fed) or starved animals and AMP upregulation in starved tissues was calculated relative to the appropriate control tissue. In summary, fat body as well

as barrier tissues showed dFOXO dependent AMP expression (Fig. 29), whereas barrier epithelia expressed a broader spectrum of AMPs, as nearly all analysed genes were induced in these tissues. In contrast, AMP expression in the fat body seemed to be restricted to selected AMPs, respectively.

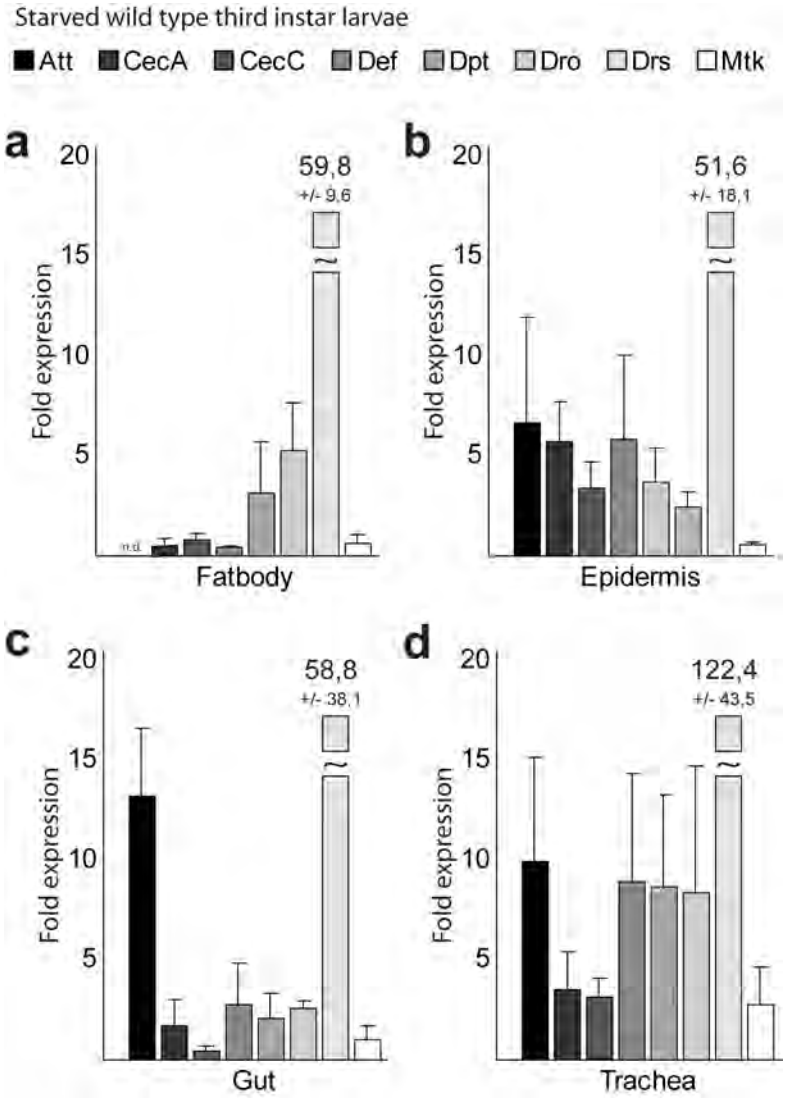

Fig. 29: AMP Expression in isolated tissues of wild type third instar larvae after starvation on PBS. **a)** Fat body **b)** Epidermis **c)** Gut **d)** Trachea. Induction of AMPs in tissues from starved larvae is shown relative to the appropriate control tissue from normal fed animals. WT=wild type, Att=*attacin A*, CecA=*cecropin A1*, CecC=*cecropin C*, Def=*defensin*, Dpt=*diptericin*, Dro=*drosocin*, Drs=*drosomycin*, Mtk=*metchnikowin*.

4.10 dFOXO dependent *drosomycin* expression is cell autonomous

(done in cooperation with P. Carrera)

To check whether AMP expression by dFOXO occurs in a cell autonomous manner, dFOXO-GFP was overexpressed in a mosaic pattern of cells in the fat body using the FLP/GAL4 technique. Cells overexpressing dFOXO-GFP were identified by GFP expression and turned

out to be slightly smaller than surrounding cells which did not overexpress dFOXO-GFP. Furthermore, it was found that dFOXO-GFP expression correlated with an upregulation of *drosomycin* transcription, as visualised by *in-situ* hybridisation. In contrast, no *drosomycin* expression was found in adjacent control cells (Fig. 30).

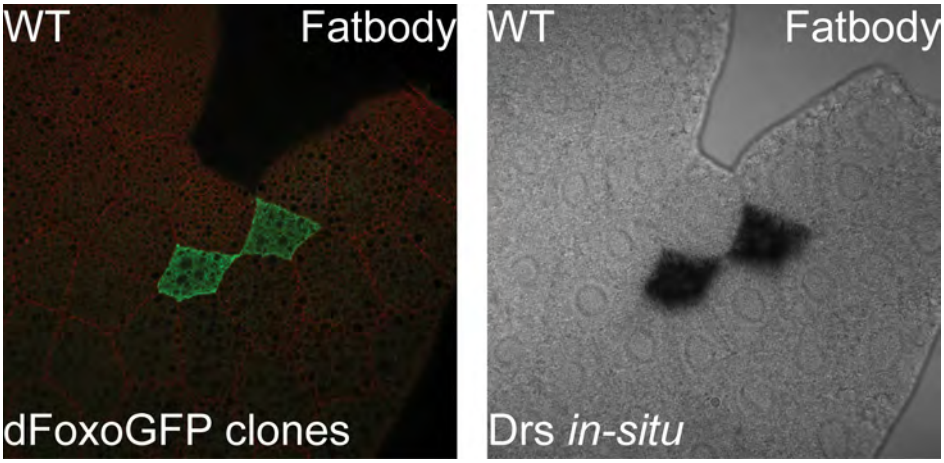

Fig. 30: Overexpression of dFOXO-GFP in a mosaic pattern of cells in the fat body using the FLP/GAL4 technique. dFOXO-GFP expression was visualised with an anti-GFP antibody (left panel), whereas *drosomycin* expression was detected by *in-situ* hybridisation (right panel). WT=wild type, Drs=*drosomycin*.

4.11 Conservation of FOXO dependent AMP expression in human cells

(done in cooperation with A.C. Aschenbrenner and M. Beyer)

IlS dependent regulation of AMPs by the transcription factor dFOXO turned out to be a ubiquitiously acting mechanism in *Drosophila*. Since FOXO is conserved from worm to human, it was of great interest to see whether regulation of AMPs was as well conserved in vertebrates. For this purpose, several human cell lines, derived from different tissues, were analysed for IlS dependent expression of defensins and *drosomycin-like-defensin*, which was recently discovered as a new peptide with anti-fungal activity related to *Drosophila* Drosomycin (Simon et. al. 2008). Tested cell lines included HEK293 (kidney cells), HaCaT (skin cells), CaCo2 (colorectal adenocarcinoma cells), HCT116 (colorectum cells), A549 (lung cells) and HL60 (blood cells). In case of A549 cells,

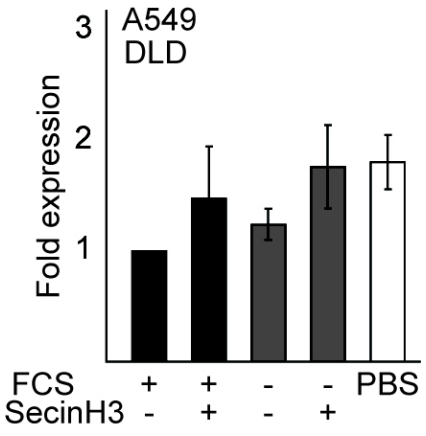

Fig. 31: Expression of *drosomycin-like-defensin* (DLD) in human A549 lung cells after growth factor starvation for 24 h (-FCS) with and without treatment with 10 µM SecinH3 as well as full starvation in PBS for 4 h, both compared to full medium (+FCS).

starvation experiments combined with SecinH3 treatment were performed. As already seen for *Drosophila* Schneider cells, expression of *drosomycin-like-defensin* in A549 cells was nutrient dependent and triggered by SecinH3 (Fig. 31). Moreover, Insulin stimulation assays combined with SecinH3 treatment of several other cell lines revealed that expression of *ß-defensin-1*, *ß-defensin-3*, α-*defensin-1* and *drosomycin-like defensin* was IlS dependent (Fig. 32), indicating that a FOXO derived mechanism of AMP regulation is conserved in human.

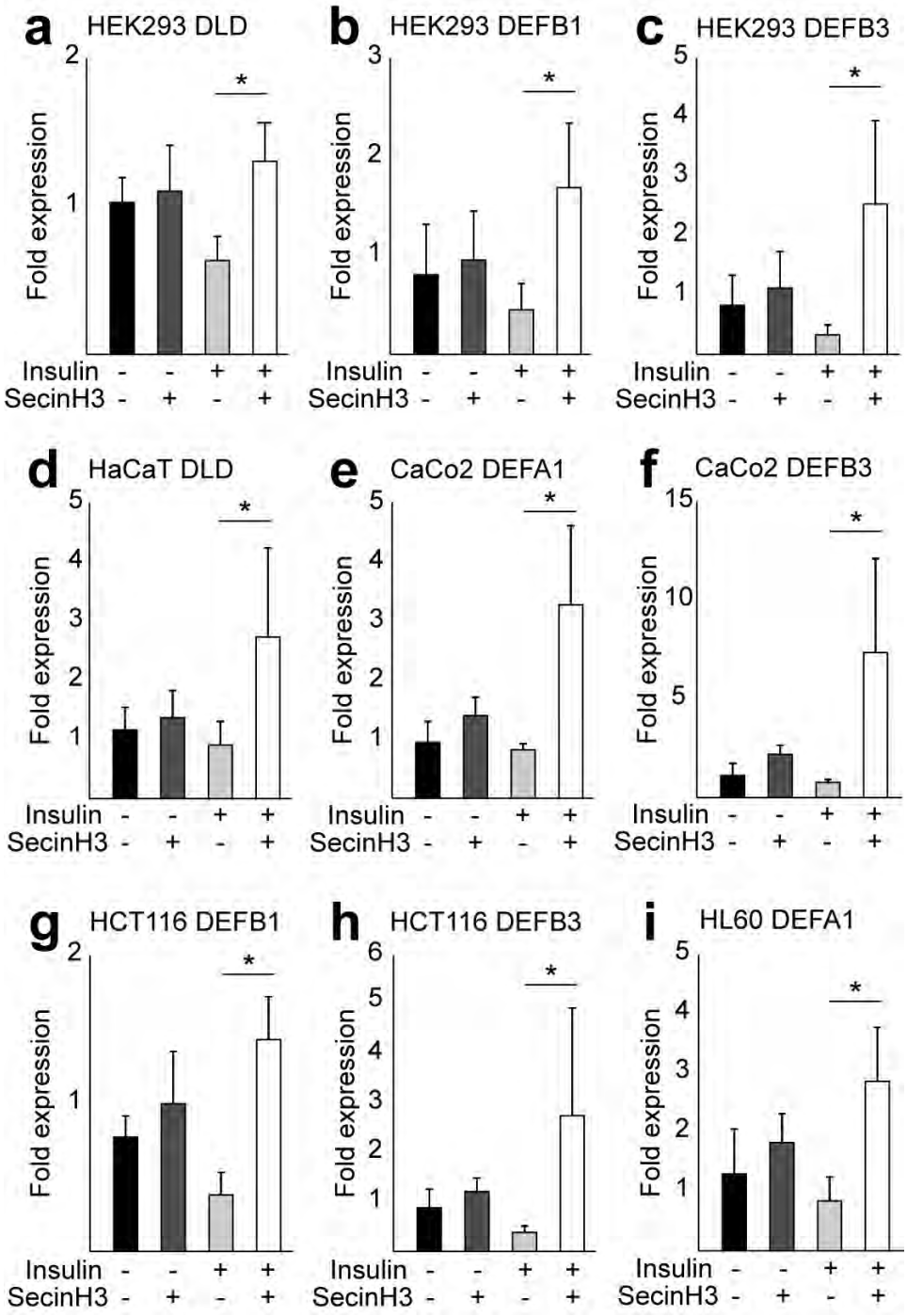

Fig. 32 a-i: Expression of *drosomycin-like-defensin, ß-defensin-1, ß-defensin-3 and α-defensin-1* in human HEK293, HaCaT, CaCo2, HCT116 and HL60 cells after insulin stimulation and treatment with 10 µM SecinH3. DLD=*drosomycin-like-defensin,* DEFB1=*ß-defensin-1,* DEFB3=*ß-defensin-3 and* DEFA1=*α-defensin-1.* An asterisks indicates statistical significance (P-value < 0.05).

5 Discussion

The results of this work can be devided into two parts. In the first section, the *steppke* gene was characterised as a novel and essential component of IlS, showing phenotypes comparable to other components of this pathway. In the second part, based on the phenotypic characterisation of *steppke*, a new crossregulation of IlS and innate immunity was described, which couples energy homeostasis and growth to organismal defense against microorganisms.

5.1 Characterisation of *steppke* mutant phenotypes

In a screen for new components affecting regulation of larval growth, the *steppke* mutant alleles *steppke*^{K08110} and *steppke*^{SH0323} were isolated, showing severe body size phenotypes during larval development. In addition, an allelic combination of *steppke* was isolated which produced adult progeny. These *steppke* mutant adult flies showed a likewise reduction of general body size, as seen for the larvae before. Body size defects of *steppke* mutants in both larvae and adults are consistent with previously described phenotypes of other IlS mutants, for example the *insulin receptor* (Chen et. al. 1996, Brogiolo et. al. 2001), *chico* (Böhni et. al. 1999), *pi3k* (Weinkove et. al. 1999) and *akt* (Verdu et. al. 1999, Scanga et. al. 2000). The growth defects observed in *steppke* mutants were based on P element insertions in the gene locus, causing a reduction of *steppke* mRNA transcription in larvae, pupae and adult flies. By using other *steppke* mutant alleles as well as a deficiency covering the *steppke* gene locus, it was shown that the isolated alleles K08110 and SH0323 are *steppke* specific and that the observed phenotypes were not caused by secondary hits. Further analysis revealed that the body size defects of *steppke* mutants were derived from a reduction in cell size and cell number (Fuss et. al. 2006). It has been shown before that this is also the case for other IlS mutants upstream of PKB/Akt, for example *chico* (Böhni et. al. 1999) or *insulin receptor* mutants (Brogiolo et. al. 2001). Furthermore, it has been shown that in *dfoxo* mutants only cell number is affected (Jünger et. al. 2003, Puig et. al. 2003), whereas in mutants of the TSC/TOR branch of IlS, only cell size is affected, as demonstrated for S6K (Montagne et. al. 1999). These observations have established a model of regulation of both cell size and cell number by IlS, which is separated downstream of PBK/Akt, so that dFOXO regulates cell number and the TSC/TOR pathway is responsible for cell size regulation (Hafen, 2004). Based on this hypothesis, Steppke function should be located upstream of PKB/Akt, as both cell number and cell size were reduced in the mutants.

5.2 Gene expression profiles of *steppke* mutants

It is known that the Forkhead transcription factor dFOXO is the main signal transducer of IlS and some components of the signalling cascade are regulated themselves in a dFOXO dependant manner by an autoregulatory negative feedback loop (Puig et. al 2005). In this context, dFOXO plays a pivotal role in adapting metabolism to nutrient conditions (Jünger et. al. 2003, Kramer et. al. 2008). When food is plentiful, Insulin Receptor activation and signalling via PI3K and the serine-threonine protein kinase PKB/Akt results in the phosphorylation of dFOXO, causing its cytoplasmic retention. Upon starvation, IlS is down-regulated and dFOXO phosphorylation is reduced, allowing the transcription factor to enter the nucleus (Calnan et. al. 2008) and induce transcription of dFOXO target genes like *4e-bp*, a translational repressor or the *insulin receptor* (Puig et. al. 2003). By analysing the expression of dFOXO target genes in *steppke* mutants, it was shown that IlS is impaired in these animals, resulting in enhanced dFOXO activity and increased *4e-bp* and *inr* expression. The same was detected for *chico* mutants, demonstrating that *steppke* mutant phenotypes are comparable to mutants of other well established components of IlS, which is not restricted to body size and cell number/cell size reduction. In addition, experiments in wild type animals showed that starvation phenocopies the gene expression profiles of both *steppke* and *chico* mutants, indicating that reduced IlS in general results in an activation of dFOXO target genes. This is further strengthened by phenotypical analysis of dFOXO overexpression *in-vivo*, which likewise resulted in a phenocopy of starvation (Kramer et. al. 2003). Importantly, *lipase3* expression was neither induced in *steppke* nor in *chico* mutants, indicating that the observed phenotypes were not based on a general impairment of food intake, resulting in prolonged starvation (Zinke et. al. 2002). In contrast, starvation of wild type animals resulted in *lipase3* upregulation, indicating enhanced lipolysis under these conditions. Although IlS and lipid metabolism are tightly coupled (Baker et. al. 2007), lipolysis does not occur in genetic IlS mutants, which separates the phenotypes observed in genetic IlS mutants and wild type animals after starvation. Moreover, it was shown that the Steppke specific inhibitor SecinH3 is able to reproduce the gene expression pattern of genetic IlS mutants in *Drosophila* Schneider cells, larvae and adult flies, as well without affecting lipolysis (Fuss et. al. 2006). SecinH3 is a small molecule compound that targets the Sec7 domain of the Steppke protein, a structure which is essential for the guanine nucleotide exchange reaction of the protein. As Steppke is highly conserved, addition of SecinH3 reproduced the gene expression patterns found in *Drosophila* also in human cell lines and murine *in-vivo* models (Hafner et. al. 2006). Taken together, gene expression studies in *Drosophila*, mice and human cell lines revealed that both *Drosophila* Steppke and vertebrate Cytohesin proteins are involved in IlS upstream of FOXO. In addition, analysis of *chico* mutants as well as starvation experiments in wild type larvae suggested that *steppke* transcription itself is controlled by dFOXO in an autoregulatory feedback loop, as demonstrated before for the *insulin receptor* (Puig et. al.

2005). Starvation experiments in *dfoxo* null mutants strengthened this point, indicating that also *steppke* is a direct dFOXO target gene.

5.3 Steppke functions at the level of the Insulin Receptor

Some additional experiments were done to clarify the position of Steppke in the IlS cascade. Biochemical analysis showed that reduced Steppke activity in S2 Schneider cells by incubation of SecinH3 lead to impaired PKB/Akt phosphorylation (Fuss et. al. 2006), which points to a Steppke function upstream of PKB/Akt. Again, this function seems to be conserved in vertebrates, since PKB/Akt phosphorylation after SecinH3 treatment was also impaired in HepG2 cells (Hafner et. al. 2006). Moreover, this is in line with former results of *steppke* mutants concerning the reduction of cell number and cell size. Regulation of these two parameters is separated downstream of PKB/Akt, whereas upstream components of the IlS cascade, like the Insulin Receptor or Chico, show a reduction of both (Hafen, 2004). Since both cell size and cell number was reduced in steppke mutants, this indicates a Steppke function upstream of PKB/Akt. The activity of PKB/Akt itself is depending on the phosphorylation status of phosphatidylinositides PIP2 and PIP3 in the membrane (Stocker et. al. 2002), which is regulated by the conserved PI3K/PTEN protein complex (Cantley 2002, Gao et.al. 2000). Both PKB/Akt and Steppke proteins contain a conserved PH domain, which is responsible for membrane recruitment of these proteins depending on the concentration of phosphorylated PIP3 (Martin 1998, Lemmon et. al. 2000, Lietzke et. al. 2000). Although regulation of Steppke subcellular localisation clearly depends on PIP3 levels and thereby PI3K activity (Britton et. al 2002), an upstream function cannot be ruled out. To test this hypothesis, a genetical rescue experiment was done using the GAL4/UAS System to activate IlS at the level of PI3K by overexpressing a constitutively active form of the protein named $PI3K^{CAAX}$, which was shown to increase organ size in the eye and the wing in a wild type genetic background (Leevers et. al. 1996). For the desired rescue experiment, overexpression of $PI3K^{CAAX}$ was done in a *steppke* transheterozygous mutant background in adult flies, which were characterised by a body weight phenotype. In case of a Steppke function upstream of PI3K, the mutant body weight phenotype should be suppressed, whereas a downstream function should prevent any rescue of the phenotype. As shown, overexpression of $PI3K^{CAAX}$ lead to increased body weight in a wild type as well as a *steppke* mutant background, which demonstrates that the overexpression system worked properly. Since the body weight of *steppke* mutant flies overexpressing $PI3K^{CAAX}$ was identical to that of appropriate wild type flies, the body weight phenotype was fully suppressed, indicating a Steppke function upstream of PI3K. Moreover, Steppke function seems to be located at the level of the Insulin Receptor, as indicated by another genetical rescue experiment. Overexpression of a wild type Insulin Receptor (INR^{WT}) protein in the eye by using the *gmr*-GAL4 driver system has been shown to generate severe rough-eye phenotypes due to overproliferation of the cells (Brogiolo

et. al. 2001). This system was used to test whether Steppke functions upstream or downstream of the Insulin Receptor. Since rough-eye phenotypes by overexpressing INR^{WT} were significantly reduced in a *steppke* transheterozygous mutant background as compared to wild type, but not completely abolished, speculation about a Steppke function downstream or at the level of the Insulin Receptor can be done (Fig. S8).

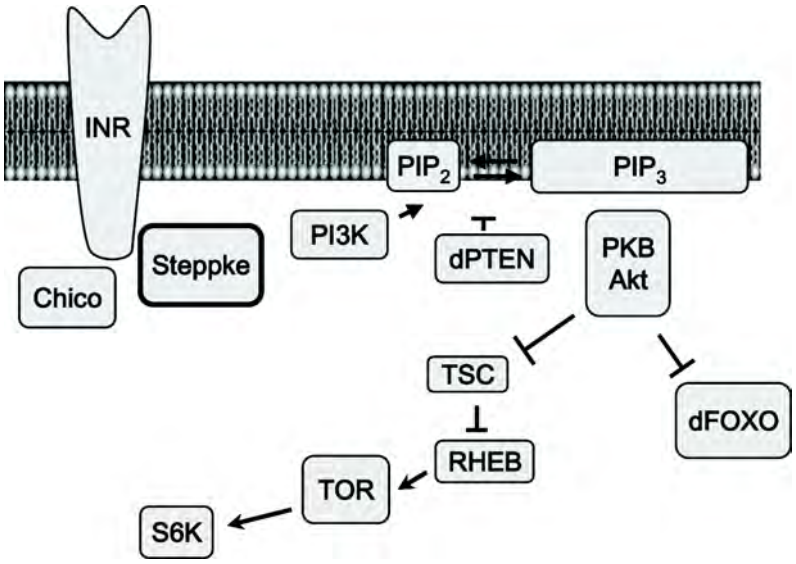

Fig. S8: Sheme of IIS in *Drosophila* including the discovered Steppke protein located at the Insulin Receptor.

5.4 IIS mutants *steppke* and *chico* show induced AMP expression

Beside their function in Insulin signalling, Cytohesins have been described earlier in context of ß2-Integrin regulation, mitogen-associated protein kinase signalling and T-cell anergy (Kolanus 2007). Crossregulation of Insulin/PI3K signalling and immunity has been discovered for some aspects (Koyasu 2003) and also FOXO proteins have been described in context of immune cell homeostasis (Birkenkamp et. al. 2003, Coffer et. al. 2004, Peng 2008). Nevertheless, this crossregulation seemed to be largely restricted to the branch of adaptive immune response, which lacks completely in invertebrates like *Drosophila*. The immune system of the fly is genetically fixed and combines aspects of epithelial barrier functions (Uvell et. al. 2007), cellular defense (Lemaitre et. al. 2007) and systemical production of effector molecules (Engström 1999). These defense patterns are non-adaptive and only to a minor degree pathogen specific (Lemaitre et. al. 1997), but the underlying signalling pathways are conserved from invertebrates to vertebrates (Hoffmann et. al. 2002). Some previous studies in *Drosophila* and *C. elegans* suggest that also crossregulation of innate immunity and IIS could exist (Bernal et. al. 2000, Garsin et. al. 2003), which would represent a totally new mechanism of interaction between metabolism and organismal defense. Based

on the characterisation of *steppke* mutans, systemic expression of antimicrobial peptides was analysed in mutants affecting IlS in *Drosophila*. It was shown that AMP expression was induced under non-infected conditions in *steppke* and *chico* mutants, which was not founded in a developmental delay of the mutants. This observation is highly interesting with regard to previously reported enhanced survival of *chico* mutants after bacterial infection (Libert et. al. 2008). Induced AMP levels in these mutants could indeed explain the observed effects of enhanced survival. This is also strengthened by data from *C. elegans*, reporting enhanced survival after pathogen infection of the Insulin Receptor homologue DAF-2 and the PI3K homologue AGE-1 (Garsin et. al. 2003, Evans et. al. 2008). Furthermore, it was reported that the dFOXO homologue DAF-16 is important for this enhanced survival (Kenyon et. al. 1993, Murphy et. al. 2003, Lin et. al. 1997, Miyata et. al. 2008). Since dFOXO/DAF-16 is the main signal transducer of IlS, the possibility exists that IlS and organismal defense are directly coupled at the level of AMP transcription because dFOXO/DAF-16 activity is triggered in IlS mutants, resulting in enhanced AMP expression as shown for *steppke* and *chico* mutants.

5.5 dFOXO directly regulates AMP expression

FOXO proteins bind to the DNA by their forkhead box domain, using conserved binding motifs of approximately eight bases as recognition sites (Kaufmann et. al. 1996, Furuyama et. al. 2000, Xuan et. al. 2005). In parallel to an AMP induction found in IlS mutants, dFOXO/Forkhead binding motifs were identified in the promoter region of most AMP genes, hinting at a direct dFOXO dependent regulation. Based on this observation, some more approaches to reduce IlS and thereby triggering dFOXO activity were performed and analysed for AMP expression. A physiological way to reduce IlS is nutrient depletion, which is very effective especially in larvae since they are continuous feeders and signalling activity is strongly coupled to the abundance of nutrients. It was shown that starvation had an impact on AMP transcription identical to that seen in IlS mutants, strengthening a theory of direct dFOXO dependent regulation of these genes. Moreover, starvation represents a normal physiological situation for an animal while searching for food. In consequence, the energy status of cells is never constant, but oscillating all the time. The coupling of AMP induction to the abundance of food could represent an ancient protection system, supporting organismal defense when the energy status is low. Nevertheless, starvation is not strictly IlS specific, but has an influence on different signalling pathways and cellular processes independent of dFOXO (Zinke et. al. 2002, Pletcher et. al. 2002, Bauer et. al. 2007). Another effort to target IlS more specifically was done by using SecinH3, which has already been shown to reproduce *steppke* mutant growth phenotypes in wild type animals (Fuss et. al. 2006). Feeding SecinH3 to wild type adult flies resulted in a likewise induction of AMP expression. This further strengthens that IlS activity is directly coupled to the expression of these immune effector genes and demonstrates that this mechanism is not restricted to *Drosophila* larvae, but also

used in adult flies. In contrast to larvae, adult flies are discontinuous feeders and organismal growth is already finished. Whereas in larvae IlS activity is predominantly used to control cellular and organsimal growth, in adult flies metabolic balance, reproduction (Flatt et. al. 2008a) and determination of the life-span are more tightly associated with IlS. Concerning this latter point, IlS and FOXO activity have been correlated with longevity in invertebrate (Hwangbo et. al. 2004, Giannakou et. al. 2007, Partridge 2008) and vertebrate (Bartke 2008, Papaconstantinou 2009) model organisms. Strikingly, gene expression studies in flies and mice revealed that immunity associated genes are significantly regulated in ageing animals (Pletcher et. al. 2002, Seroude et. al. 2002, Pletcher et. al. 2005), whereas genes associated with innate immunity are ramped up and those of adaptive immunity decline (DeVeale et. al. 2004). The expression of several AMPs is induced in ageing flies, which correlates well with a direct role of dFOXO in determining the life-span, since ectopic dFOXO expression resulted in both longevity (Hwangbo et. al. 2004, Giannakou et. al. 2004) and activation of AMP transcription (own data). The question whether AMP expression is directly dFOXO dependent has been investigated by a couple of biochemical and genetical methods. First, starvation as well as SecinH3 dependent upregulation of AMPs is gone in a *dfoxo* mutant background, using a transheterozygous *dfoxo* null allelic combination (Min et. al. 2008). This reveals that dFOXO is indispencible for IlS dependent AMP expression. Second, direct binding of dFOXO to an identified binding motif in the *drosomycin* promoter was shown biochemically by electromobility shift assays and third, usage of dFOXO/Forkhead binding motifs in the *drosomycin* promoter was shown by Luciferase assays in cell culture and *in-vivo*. Since the regulatory regions of most AMP genes in *Drosophila* contain dFOXO/Forkhead binding motifs, speculation about a general, probably age dependent regulation of these immune effector genes can be done. In contrast, it has been shown that chronic activation of Toll and IMD innate immune pathways lead to a reduction of live-span (Libert et. al. 2006), which indicates that either AMP expression levels have to be tightly controlled or activation of these NF-κB like pathways results in other processes beside AMP induction, which have a negative effect on life-span determination.

5.6 AMP expression by dFOXO and NF-κB like signalling

To exclude that dFOXO activation had an influence on Toll and IMD immunity pathways, some experiments were done in immune deficient larvae and adults. Double mutants for *relish* and *spätzle* have been shown to fail AMP expression in a NF-κB dependent manner, resulting in quick lethality after bacterial infection (De Gregorio et. al. 2002). For this purpose, *relish;spätzle* double mutant larvae and adults were subjected to starvation as well as SecinH3 feeding experiments. Upregulation of *drosomycin* in starved larvae and several other AMPs in SecinH3 treated adults indicate that a dFOXO dependent expression of AMP genes can be achieved independently of NF-κB like innate immune pathways. Nevertheless,

drosomycin expression in these larvae was weaker as compared to equally treated wild type animals. Moreover, using the short *drosomycin* promoter constructs Drs_287_WT, which contained dFOXO binding sites but lacked the NF-κB binding site, revealed that *luciferase* expression was likewise weaker as compared to constructs including the full regulatory region. This demonstrates that dFOXO alone is able to induce AMP expression, but argues for an interaction with other co-factors to provide full activation. So far, it is unclear whether these factors are NF-κB like proteins DIF or Relish, or any other transcription factor. One of these candidates could also be the Caudal protein, which has been shown to constitutively regulate *drosomycin* expression (Ryu et. al. 2004). The other way around, *dfoxo* mutant flies were analysed for survival and AMP induction after infection to see whether activation of Toll and IMD pathways depends on the presence of dFOXO. It was shown before that activation of NF-κB like pathways after infection is crucial and loss of one or both pathways results in reduced survival (Lemaitre et. al. 1996, Georgel et. al. 2001, De Gregorio et. al. 2002). Assays in *dfoxo* mutants revealed that both survival and AMP induction were largely comparable to wild type flies. This is further strengthened by another study, showing that *dfoxo* mutants are not hypersensitive to microbial infection (Dionne et. al. 2006). In fact, *dfoxo* mutants showed enhanced survival, but this could rely on specific host-pathogen interaction. Together, both studies indicate that Toll and IMD innate immune pathway activation is sufficient in case of a systemic infection, as done by pricking concentrated bacteria into the body cavity of adult flies. This strengthens a theory of dFOXO dependent AMP regulation in non-infected animals, for example as a mechanism to prevent infection when the animal is suffering from food and energy shortage or in context of ageing, when general fitness and physiological functions decline.

5.7 Tissue dependent AMP expression by dFOXO

An important aspect was to know in which tissues a dFOXO dependent regulation of AMP expression is used. Eight different classes of AMPs were described in *Drosophila* (Uvell et. al. 2007), being expressed in a highly variable pattern. In case of an infection, AMPs are produced either systemically by the fat body (Tzou et. al. 2002, Ferrandon et. al. 2007) or locally by barrier epithelia (Ferrandon et. al. 1998, Tzou et. al. 2000, Tingvall et. al. 2001, Ryu et. al. 2008). Analysis of isolated larval tissues after starvation revealed that AMPs were expressed in a dFOXO dependent manner in both, the fat body as well as epithelial tissues including epidermis, gut and trachea. Notably, an induced expression of nearly all AMPs was found in epithelial tissues, whereas a clear fat body derived expression was restricted to only three of these genes. This allows speculation about a broader range of AMPs being expressed in epithelial barrier tissues in a dFOXO dependent manner. Notably, expression levels of AMPs derived by dFOXO signalling are comparatively low as compared to those found by NF-κB dependent activation after infection. This raises the question about the importance of

such a mild mechanism of regulation, as AMP expression levels derived of NF-κB like signalling were up to 1000 fold stronger. In contrast, quick downregulation after an infection is essential since high AMP expression levels are detrimental to the host (Bischoff et. al. 2006). Furthermore, it is known from studies in barrier tissues in *Drosophila* and mammals that TLR signalling and activation of immune effector genes are downregulated to avoid chronic inflammation, which is associated with necrosis and cancer formation (Libert et. al. 2006, Abreu et. al. 2005). These tissues are permanently in contact with microorganisms and prolonged exposure to lipopolysaccharides or lipotechoic acid is known to result in tolerance and cross-tolerance to other pathogen-associated molecular patterns. Similarly, it has been shown in *Drosophila* that IMD signalling and the induction of NF-κB dependent immune effector gene expression in the gut epithelium is repressed by the intestinal homeobox gene *caudal*, thereby allowing and regulating symbiotic interactions of commensal bacteria with the intestinal epithelium (Ryu et. al. 2008). In this context, a dFOXO dependent regulation could ensure the sparse production of AMPs in barrier epithelia in healthy individuals, thereby maintaining and strengthening the defense barrier of these tissues, in particular when animals are suffering from energy shortage or stress (Fig. S9).

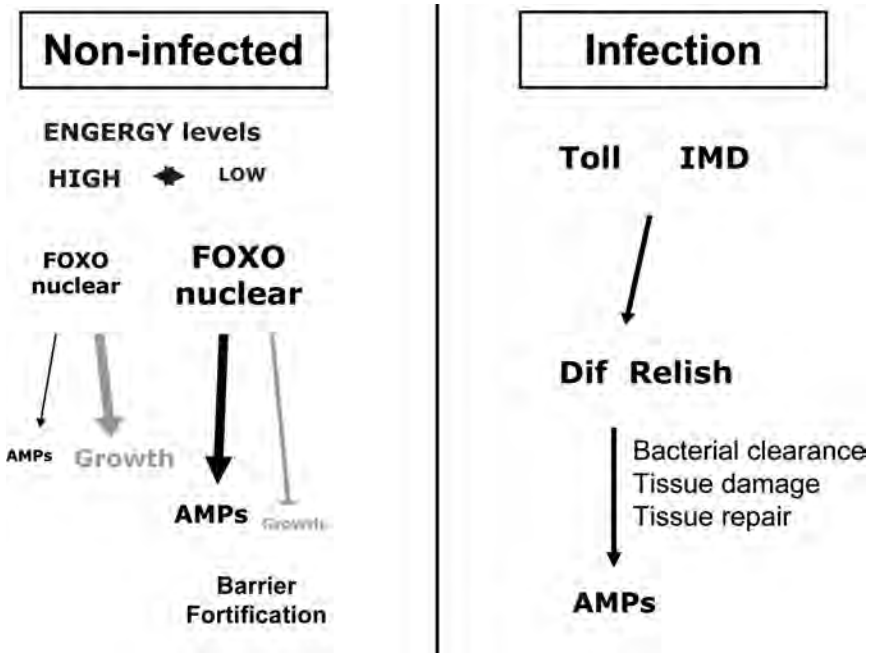

Fig. S9: Model of dFOXO dependent AMP expression and its role concerning regulation of organismal defense.

6 Summary of the results

This work uncovered a completely new mechanism of crossregulation between IlS and innate immunity at the level of dFOXO. In fact, this is the first description of a direct regulation of immune effector genes by IlS, a signalling pathway known to regulate growth, energy homeostasis and life-span (Hafen et. al. 2004). The nutrient dependent regulation of dFOXO directly couples energy homeostasis to organismal defense against pathogens (Lemaite et. al. 2007). In the first part of this work, a novel component of IlS was discovered, the *steppke* gene. Animals mutant for *steppke* showed phenotypes comparable to other well characterised IlS mutants like *chico*, the *Drosophila* homologue of vertebrate IRS proteins 1-4. Beside this, the *steppke* mutant phenotype was reproduced by using physiological conditions like starvation or specific inhibition of Steppke by the small molecule compound SecinH3 in wild type animals. Genetic rescue experiments using the GAL4/UAS system allowed to define the position of Steppke function in the IlS cascade, which is located at or closely downstream of the transmembrane Insulin Receptor. This function of Steppke is conserved in vertebrates, which was shown in an accompanying study of mammalian and murine Cytohesin proteins (Hafner et. al. 2006). Gene expression profiles of *steppke* mutants in *Drosophila* showed that IlS target genes, but surprisingly also genes involved in organismal defense against microorganisms, were misregulated. The regulation of antimicrobial peptide genes, small cationic proteins that function by damaging microbial cell membranes, thereby causing stasis or lysis of the target microorganism (Yeaman et. al. 2007), was further characterised. It turned out that transcriptional regulation of these genes is not restricted to NF-κB like immunity pathways, but also depending on IlS, which represents a novel link between metabolism and organismal defense. Again, it was shown that this mechanism is conserved in vertebrates by analysing IlS dependent expression of several *defensins* and *drosomycin-like-defensin* in human cell lines. A combination of genetic and biochemical experiments demonstrated that IlS dependent regulation of AMP genes is mediated by dFOXO, the main transactivator of IlS, which is conserved from worm to human. dFOXO has earlier been described in context of metabolic control, stress regulation, cell cycle control or ageing (Arden 2008). Using the *drosomycin* promoter region, it was shown that dFOXO directly binds to conserved motifs found in the regulatory regions of nearly all AMP genes. Moreover, direct regulation of AMP expression by dFOXO turned out to be independent of Toll and IMD pathways and to function predominantly under non-infected conditions in fat body and epithelial barrier tissues. These barrier epithelia are constantly exposed to omnipresent microorganisms and NF-κB like signalling is often reduced in these tissues to prevent necrosis, cancer formation and the induction of tolerance to pathogen-associated molecular patterns. Nevertheless, a dFOXO dependent mode of AMP expression probably allows modular adaptation of organsimal defense against microorganisms to environmental conditions without the severe side effects induced by activation of NF-κB like signalling pathways.

7 References

Abreu MT, Fukata M, Arditi M. TLR signaling in the gut in health and disease. *J Immunol. 2005 Apr 15;174(8):4453-60.*

Aggarwal K, Silverman N. Positive and negative regulation of the Drosophila immune response. *BMB Rep. 2008 Apr 30;41(4):267-77.*

Arden KC. FOXO animal models reveal a variety of diverse roles for FOXO transcription factors. *Oncogene. 2008 Apr 7;27(16):2345-50.*

Baker KD, Thummel CS. Diabetic larvae and obese flies-emerging studies of metabolism in Drosophila. *Cell Metab. 2007 Oct;6(4):257-66.*

Bartke A. Insulin and aging. *Cell Cycle. 2008 Nov 1;7(21):3338-43.*

Bauer M, Katzenberger JD, Hamm AC, Bonaus M, Zinke I, Jaekel J, Pankratz MJ. Purine and folate metabolism as a potential target of sex-specific nutrient allocation in Drosophila and its implication for lifespan-reproduction tradeoff. *Physiol Genomics. 2006 May 16;25(3):393-404.*

Belvin MP, Anderson KV. A conserved signaling pathway: the Drosophila toll-dorsal pathway. *Annu Rev Cell Dev Biol. 1996;12:393-416.*

Bernal A, Kimbrell DA. Drosophila Thor participates in host immune defense and connects a translational regulator with innate immunity. *Proc Natl Acad Sci U S A. 2000 May 23;97(11):6019-24.*

Birkenkamp KU, Coffer PJ. FOXO transcription factors as regulators of immune homeostasis: molecules to die for? *J Immunol. 2003 Aug 15;171(4):1623-9.*

Bischoff V, Vignal C, Duvic B, Boneca IG, Hoffmann JA, Royet J. Downregulation of the Drosophila immune response by peptidoglycan-recognition proteins SC1 and SC2. *PLoS Pathog. 2006 Feb;2(2):e14.*

Böhni R, Riesgo-Escovar J, Oldham S, Brogiolo W, Stocker H, Andruss BF, Beckingham K, Hafen E. Autonomous control of cell and organ size by CHICO, a Drosophila homolog of vertebrate IRS1-4. *Cell. 1999 Jun 25;97(7):865-75.*

Britton JS, Lockwood WK, Li L, Cohen SM, Edgar BA. Drosophila's insulin/PI3-kinase pathway coordinates cellular metabolism with nutritional conditions. *Dev Cell. 2002 Feb;2(2):239-49.*

Brogiolo W, Stocker H, Ikeya T, Rintelen F, Fernandez R, Hafen E. An evolutionarily conserved function of the Drosophila insulin receptor and insulin-like peptides in growth control. *Curr Biol. 2001 Feb 20;11(4):213-21.*

Broughton SJ, Piper MD, Ikeya T, Bass TM, Jacobson J, Driege Y, Martinez P, Hafen E, Withers DJ, Leevers SJ, Partridge L. Longer lifespan, altered metabolism, and stress resistance in Drosophila from ablation of cells making insulin-like ligands. *Proc Natl Acad Sci U S A. 2005 Feb 22;102(8):3105-10.*

Bulet P, Stöcklin R, Menin L. Anti-microbial peptides: from invertebrates to vertebrates. *Immunol Rev. 2004 Apr;198:169-84.*

Calnan DR, Brunet A. The FoxO code. *Oncogene. 2008 Apr 7;27(16):2276-88.*

Cantley LC. The phosphoinositide 3-kinase pathway. *Science. 2002 May 31;296(5573):1655-7.*

Chang YY, Juhász G, Goraksha-Hicks P, Arsham AM, Mallin DR, Muller LK, Neufeld TP. Nutrient-dependent regulation of autophagy through the target of rapamycin pathway. *Biochem Soc Trans. 2009 Feb;37(Pt 1):232-6.*

Cheadle JP, Reeve MP, Sampson JR, Kwiatkowski DJ. Molecular genetic advances in tuberous sclerosis. *Hum Genet. 2000 Aug;107(2):97-114.*

Chen C, Jack J, Garofalo RS. The Drosophila insulin receptor is required for normal growth. *Endocrinology. 1996 Mar;137(3):846-56.*

Cheng CL, Gao TQ, Wang Z, Li DD. Role of insulin/insulin-like growth factor 1 signaling pathway in longevity. *World J Gastroenterol. 2005 Apr 7;11(13):1891-5.*

Coffer PJ, Burgering BM. Forkhead-box transcription factors and their role in the immune system. *Nat Rev Immunol. 2004 Nov;4(11):889-99.*

De Gregorio E, Spellman PT, Rubin GM, Lemaitre B. Genome-wide analysis of the Drosophila immune response by using oligonucleotide microarrays. *Proc Natl Acad Sci U S A. 2001 Oct 23;98(22):12590-5.*

De Gregorio E, Spellman PT, Tzou P, Rubin GM, Lemaitre B. The Toll and Imd pathways are the major regulators of the immune response in Drosophila. *EMBO J. 2002 Jun 3;21(11):2568-79*

DeVeale B, Brummel T, Seroude L. Immunity and aging: the enemy within? *Aging Cell. 2004;3(4):195-208.*

Dionne MS, Pham LN, Shirasu-Hiza M, Schneider DS. Akt and FOXO dysregulation contribute to infection-induced wasting in Drosophila. *Curr Biol. 2006 Oct 24;16(20):1977-85.*

Engström Y, Kadalayil L, Sun SC, Samakovlis C, Hultmark D, Faye I. Kappa B-like motifs regulate the induction of immune genes in Drosophila. *J Mol Biol. 1993 Jul 20;232(2):327-33.*

Engström Y. Induction and regulation of antimicrobial peptides in Drosophila. *Dev Comp Immunol. 1999 Jun-Jul;23(4-5):345-58.*

Evans EA, Chen WC, Tan MW. The DAF-2 insulin-like signaling pathway independently regulates aging and immunity in C. elegans. *Aging Cell. 2008 Dec;7(6):879-93.*

Ferrandon D, Imler JL, Hetru C, Hoffmann JA. The Drosophila systemic immune response: sensing and signalling during bacterial and fungal infections. *Nat Rev Immunol. 2007 Nov;7(11):862-74.*

Ferrandon D, Jung AC, Criqui M, Lemaitre B, Uttenweiler-Joseph S, Michaut L, Reichhart J, Hoffmann JA. A drosomycin-GFP reporter transgene reveals a local immune response in Drosophila that is not dependent on the Toll pathway. *EMBO J. 1998 Aug 10;17(5):1217-27.*

Flatt T, Min KJ, D'Alterio C, Villa-Cuesta E, Cumbers J, Lehmann R, Jones DL, Tatar M. Drosophila germ-line modulation of insulin signaling and lifespan. *Proc Natl Acad Sci U S A. 2008a Apr 29;105(17):6368-73.*

Flatt T, Heyland A, Rus F, Porpiglia E, Sherlock C, Yamamoto R, Garbuzov A, Palli SR, Tatar M, Silverman N. Hormonal regulation of the humoral innate immune response in Drosophila melanogaster. *J Exp Biol, 211, 2712-24 (2008b).*

Furuyama T, Nakazawa T, Nakano I, Mori N. Identification of the differential distribution patterns of mRNAs and consensus binding sequences for mouse DAF-16 homologues. *Biochem J. 2000 Jul 15;349(Pt 2):629-34.*

Fuss B, Becker T, Zinke I, Hoch M. The cytohesin Steppke is essential for insulin signalling in Drosophila. *Nature. 2006 Dec 14;444(7121):945-8.*

Gao X, Neufeld TP, Pan D. Drosophila PTEN regulates cell growth and proliferation through PI3K-dependent and -independent pathways. *Dev Biol. 2000 May 15;221(2):404-18.*

Garofalo RS. Genetic analysis of insulin signaling in Drosophila. *Trends Endocrinol Metab. 2002 May-Jun;13(4):156-62.*

Garsin DA, Villanueva JM, Begun J, Kim DH, Sifri CD, Calderwood SB, Ruvkun G, Ausubel FM. Long-lived C. elegans daf-2 mutants are resistant to bacterial pathogens. *Science. 2003 Jun 20;300(5627):1921.*

Georgel P, Naitza S, Kappler C, Ferrandon D, Zachary D, Swimmer C, Kopczynski C, Duyk G, Reichhart JM, Hoffmann JA. Drosophila immune deficiency (IMD) is a death domain protein that activates antibacterial defense and can promote apoptosis. *Dev Cell. 2001 Oct;1(4):503-14.*

Giannakou ME, Goss M, Jünger MA, Hafen E, Leevers SJ, Partridge L. Long-lived Drosophila with overexpressed dFOXO in adult fat body. *Science. 2004 Jul 16;305(5682):361.*

Giannakou ME, Partridge L. Role of insulin-like signalling in Drosophila lifespan. Trends *Biochem Sci. 2007 Apr;32(4):180-8.*

Grewal SS, Evans JR, Edgar BA. Drosophila TIF-IA is required for ribosome synthesis and cell growth and is regulated by the TOR pathway. *J Cell Biol. 2007 Dec 17;179(6):1105-13.*

Grewal SS. Insulin/TOR signaling in growth and homeostasis: a view from the fly world. Int *J Biochem Cell Biol. 2009 May;41(5):1006-10.*

Gross DN, van den Heuvel AP, Birnbaum MJ. The role of FoxO in the regulation of metabolism. *Oncogene. 2008 Apr 7;27(16):2320-36.*

Hafen E. Cancer, type 2 diabetes, and ageing: news from flies and worms. *Swiss Med Wkly. 2004 Dec 18;134(49-50):711-9.*

Hafen E. Interplay between growth factor and nutrient signaling: lessons from Drosophila TOR. *Curr Top Microbiol Immunol. 2004b;279:153-67.*

Hafner M, Schmitz A, Grüne I, Srivatsan SG, Paul B, Kolanus W, Quast T, Kremmer E, Bauer I, Famulok M. Inhibition of cytohesins by SecinH3 leads to hepatic insulin resistance. *Nature. 2006 Dec 14;444(7121):941-4.*

Hall DJ, Grewal SS, de la Cruz AF, Edgar BA. Rheb-TOR signaling promotes protein synthesis, but not glucose or amino acid import, in Drosophila. *BMC Biol. 2007 Mar 19;5:10.*

Hashimoto C, Hudson KL, Anderson KV. The Toll gene of Drosophila, required for dorsal-ventral embryonic polarity, appears to encode a transmembrane protein. *Cell. 1988 Jan 29;52(2):269-79.*

Hedengren M, Asling B, Dushay MS, Ando I, Ekengren S, Wihlborg M, Hultmark D. Relish, a central factor in the control of humoral but not cellular immunity in Drosophila. *Mol Cell. 1999 Nov;4(5):827-37.*

Hennig KM, Colombani J, Neufeld TP. TOR coordinates bulk and targeted endocytosis in the Drosophila melanogaster fat body to regulate cell growth. *J Cell Biol. 2006 Jun 19;173(6):963-74.*

Hetru C, Troxler L, Hoffmann JA. Drosophila melanogaster antimicrobial defense. *J Infect Dis. 2003 Jun 15;187 Suppl 2:S327-34.*

Hoffmann JA, Reichhart JM. Drosophila innate immunity: an evolutionary perspective. *Nat Immunol. 2002 Feb;3(2):121-6.*

Horng T, Medzhitov R. Drosophila MyD88 is an adapter in the Toll signaling pathway. *Proc Natl Acad Sci U S A. 2001 Oct 23;98(22):12654-8.*

Hultmark D. Drosophila immunity: paths and patterns. *Curr Opin Immunol. 2003 Feb;15(1):12-9.*

Hwangbo DS, Gershman B, Tu MP, Palmer M, Tatar M. Drosophila dFOXO controls lifespan and regulates insulin signalling in brain and fat body. *Nature. 2004 Jun 3;429(6991):562-6.*

Ikeya T, Galic M, Belawat P, Nairz K, Hafen E. Nutrient-dependent expression of insulin-like peptides from neuroendocrine cells in the CNS contributes to growth regulation in Drosophila. *Curr Biol. 2002 Aug 6;12(15):1293-300.*

Ip YT, Reach M, Engstrom Y, Kadalayil L, Cai H, González-Crespo S, Tatei K, Levine M. Dif, a dorsal-related gene that mediates an immune response in Drosophila. *Cell. 1993 Nov 19;75(4):753-63.*

Irving P, Troxler L, Heuer TS, Belvin M, Kopczynski C, Reichhart JM, Hoffmann JA, Hetru C. A genome-wide analysis of immune responses in Drosophila. *Proc Natl Acad Sci U S A. 2001 Dec 18;98(26):15119-24.*

Jünger MA, Rintelen F, Stocker H, Wasserman JD, Végh M, Radimerski T, Greenberg ME, Hafen E. The Drosophila forkhead transcription factor FOXO mediates the reduction in cell number associated with reduced insulin signaling. *J Biol. 2003;2(3):20.*

Kaufmann E, Knöchel W. Five years on the wings of fork head. *Mech Dev. 1996 Jun;57(1):3-20.*

Kenyon C, Chang J, Gensch E, Rudner A, Tabtiang R. A C. elegans mutant thxuanat lives twice as long as wild type. *Nature. 1993 Dec 2;366(6454):461-4*

Kolanus W. Guanine nucleotide exchange factors of the cytohesin family and their roles in signal transduction. *Immunol Rev. 2007 Aug;218:102-13.*

Koyasu S. The role of PI3K in immune cells. *Nat Immunol. 2003 Apr;4(4):313-9.*

Kramer JM, Davidge JT, Lockyer JM, Staveley BE. Expression of Drosophila FOXO regulates growth and can phenocopy starvation. *BMC Dev Biol. 2003 Jul 5;3:5.*

Kramer JM, Slade JD, Staveley BE. foxo is required for resistance to amino acid starvation in Drosophila. *Genome. 2008 Aug;51(8):668-72.*

Leevers SJ, Weinkove D, MacDougall LK, Hafen E, Waterfield MD. The Drosophila phosphoinositide 3-kinase Dp110 promotes cell growth. *EMBO J. 1996 Dec 2;15(23):6584-94*

Lemaitre B, Hoffmann J. The host defense of Drosophila melanogaster. *Annu Rev Immunol. 2007;25:697-743.*

Lemaitre B, Kromer-Metzger E, Michaut L, Nicolas E, Meister M, Georgel P, Reichhart JM, Hoffmann JA. A recessive mutation, immune deficiency (imd), defines two distinct control pathways in the Drosophila host defense. *Proc Natl Acad Sci U S A. 1995 Oct 10;92(21):9465-9.*

Lemaitre B, Nicolas E, Michaut L, Reichhart JM, Hoffmann JA. The dorsoventral regulatory gene cassette spätzle/Toll/cactus controls the potent antifungal response in Drosophila adults. *Cell. 1996 Sep 20;86(6):973-83.*

Lemaitre B, Reichhart JM, Hoffmann JA. Drosophila host defense: differential induction of antimicrobial peptide genes after infection by various classes of microorganisms. *Proc Natl Acad Sci U S A. 1997 Dec 23;94(26):14614-9.*

Lemmon MA, Ferguson KM. Signal-dependent membrane targeting by pleckstrin homology (PH) domains. *Biochem J. 2000 Aug 15;350 Pt 1:1-18.*

LeMosy EK, Hong CC, Hashimoto C. Signal transduction by a protease cascade. *Trends Cell Biol. 1999 Mar;9(3):102-7.*

Letsou A, Alexander S, Orth K, Wasserman SA. Genetic and molecular characterization of tube, a Drosophila gene maternally required for embryonic dorsoventral polarity. *Proc Natl Acad Sci U S A. 1991 Feb;88(3):810-4.*

Leulier F, Rodriguez A, Khush RS, Abrams JM, Lemaitre B. The Drosophila caspase Dredd is required to resist gram-negative bacterial infection. *EMBO Rep. 2000 Oct;1(4):353-8.*

Levashina EA, Ohresser S, Lemaitre B, Imler JL. Two distinct pathways can control expression of the gene encoding the Drosophila antimicrobial peptide metchnikowin. *J Mol Biol. 1998 May 8;278(3):515-27.*

Liao XH, Majithia A, Huang X, Kimmel AR. Growth control via TOR kinase signaling, an intracellular sensor of amino acid and energy availability, with crosstalk potential to proline metabolism. *Amino Acids. 2008 Nov;35(4):761-70.*

Libert S, Chao Y, Chu X, Pletcher SD. Trade-offs between longevity and pathogen resistance in Drosophila melanogaster are mediated by NFkappaB signaling. *Aging Cell. 2006 Dec;5(6):533-43.*

Libert S, Chao Y, Zwiener J, Pletcher SD. Realized immune response is enhanced in long-lived puc and chico mutants but is unaffected by dietary restriction. *Mol Immunol. 2008 Feb;45(3):810-7.*

Lietzke SE, Bose S, Cronin T, Klarlund J, Chawla A, Czech MP, Lambright DG. Structural basis of 3-phosphoinositide recognition by pleckstrin homology domains. *Mol Cell. 2000 Aug;6(2):385-94.*

Ligoxygakis P, Pelte N, Hoffmann JA, Reichhart JM. Activation of Drosophila Toll during fungal infection by a blood serine protease. *Science. 2002 Jul 5;297(5578):114-6.*

Lin K, Dorman JB, Rodan A, Kenyon C. daf-16: An HNF-3/forkhead family member that can function to double the life-span of Caenorhabditis elegans. *Science. 1997 Nov 14;278(5341):1319-22.*

Lorberg A, Hall MN. TOR: the first 10 years. *Curr Top Microbiol Immunol. 2004;279:1-18.*

Martin TF. Phosphoinositide lipids as signaling molecules: common themes for signal transduction, cytoskeletal regulation, and membrane trafficking. *Annu Rev Cell Dev Biol. 1998;14:231-64.*

Michel T, Reichhart JM, Hoffmann JA, Royet J. Drosophila Toll is activated by Gram-positive bacteria through a circulating peptidoglycan recognition protein. *Nature. 2001 Dec 13;414(6865):756-9.*

Milán M, Campuzano S, García-Bellido A. Cell cycling and patterned cell proliferation in the Drosophila wing during metamorphosis. *Proc Natl Acad Sci U S A. 1996 Oct 15;93(21):11687-92*

Min KJ, Yamamoto R, Buch S, Pankratz M, Tatar M. Drosophila lifespan control by dietary restriction independent of insulin-like signaling. *Aging Cell. 2008 Mar;7(2):199-206.*

Miyata S, Begun J, Troemel ER, Ausubel FM. DAF-16-dependent suppression of immunity during reproduction in Caenorhabditis elegans. *Genetics. 2008 Feb;178(2):903-18.*

Montagne J, Stewart MJ, Stocker H, Hafen E, Kozma SC, Thomas G. Drosophila S6 kinase: a regulator of cell size. *Science. 1999 Sep 24;285(5436):2126-9.*

Murphy CT, McCarroll SA, Bargmann CI, Fraser A, Kamath RS, Ahringer J, Li H, Kenyon C. Genes that act downstream of DAF-16 to influence the lifespan of Caenorhabditis elegans. *Nature. 2003 Jul 17;424(6946):277-83.*

Onfelt Tingvall T, Roos E, Engström Y. The imd gene is required for local Cecropin expression in Drosophila barrier epithelia. *EMBO Rep. 2001 Mar;2(3):239-43.*

Pan D, Dong J, Zhang Y, Gao X. Tuberous sclerosis complex: from Drosophila to human disease. *Trends Cell Biol. 2004 Feb;14(2):78-85.*

Papaconstantinou J. Insulin/IGF-1 and ROS signaling pathway cross-talk in aging and longevity determination. *Mol Cell Endocrinol. 2009 Feb 5;299(1):89-100.*

Partridge L, Brüning JC. Forkhead transcription factors and ageing. *Oncogene. 2008 Apr 7;27(16):2351-63.*

Peng SL. Foxo in the immune system. *Oncogene. 2008 Apr 7;27(16):2337-44.*

Pletcher SD, Libert S, Skorupa D. Flies and their golden apples: the effect of dietary restriction on Drosophila aging and age-dependent gene expression. *Ageing Res Rev. 2005 Nov;4(4):451-80.*

Pletcher SD, Macdonald SJ, Marguerie R, Certa U, Stearns SC, Goldstein DB, Partridge L. Genome-wide transcript profiles in aging and calorically restricted Drosophila melanogaster. *Curr Biol. 2002 30;12(9):712-23.*

Puig O, Marr MT, Ruhf ML, Tjian R. Control of cell number by Drosophila FOXO: downstream and feedback regulation of the insulin receptor pathway. *Genes Dev. 2003 Aug 15;17(16):2006-20.*

Puig O, Tjian R. Transcriptional feedback control of insulin receptor by dFOXO/FOXO1. *Genes Dev. 2005 Oct 15;19(20):2435-46.*

Rulifson EJ, Kim SK, Nusse R. Ablation of insulin-producing neurons in flies: growth and diabetic phenotypes. *Science. 2002 May 10;296(5570):1118-20.*

Ryu JH, Kim SH, Lee HY, Bai JY, Nam YD, Bae JW, Lee DG, Shin SC, Ha EM, Lee WJ. Innate immune homeostasis by the homeobox gene caudal and commensal-gut mutualism in Drosophila. *Science. 2008 Feb 8;319(5864):777-82.*

Ryu JH, Nam KB, Oh CT, Nam HJ, Kim SH, Yoon JH, Seong JK, Yoo MA, Jang IH, Brey PT, Lee WJ. The homeobox gene Caudal regulates constitutive local expression of antimicrobial peptide genes in Drosophila epithelia. *Mol Cell Biol. 2004 Jan;24(1):172-85.*

Scanga SE, Ruel L, Binari RC, Snow B, Stambolic V, Bouchard D, Peters M, Calvieri B, Mak TW, Woodgett JR, Manoukian AS.The conserved PI3'K/PTEN/Akt signaling pathway regulates both cell size and survival in Drosophila. *Oncogene. 2000 Aug 17;19(35):3971-7.*

Scott RC, Juhász G, Neufeld TP. Direct induction of autophagy by Atg1 inhibits cell growth and induces apoptotic cell death. *Curr Biol. 2007 Jan 9;17(1):1-11.*

Scott RC, Schuldiner O, Neufeld TP. Role and regulation of starvation-induced autophagy in the Drosophila fat body. *Dev Cell. 2004 Aug;7(2):167-78.*

Selsted ME, Ouellette AJ. Mammalian defensins in the antimicrobial immune response. *Nat Immunol. 2005 Jun;6(6):551-7.*

Seroude L, Brummel T, Kapahi P, Benzer S. Spatio-temporal analysis of gene expression during aging in Drosophila melanogaster. *Aging Cell. 2002 Oct;1(1):47-56.*

Shelton CA, Wasserman SA. pelle encodes a protein kinase required to establish dorsoventral polarity in the Drosophila embryo. *Cell. 1993 Feb 26;72(4):515-25.*

Silverman N, Zhou R, Stöven S, Pandey N, Hultmark D, Maniatis T. A Drosophila IkappaB kinase complex required for Relish cleavage and antibacterial immunity. *Genes Dev. 2000 Oct 1;14(19):2461-71.*

Simon A, Kullberg BJ, Tripet B, Boerman OC, Zeeuwen P, van der Ven-Jongekrijg J, Verweij P, Schalkwijk J, Hodges R, van der Meer JW, Netea MG. Drosomycin-like defensin, a human homologue of Drosophila melanogaster drosomycin with antifungal activity. *Antimicrob Agents Chemother. 2008 Apr;52(4):1407-12.*

Skaug B, Jiang X, Chen ZJ. The role of ubiquitin in NF-kappaB regulatory pathways. *Annu Rev Biochem. 2009;78:769-96.*

Stocker H, Andjelkovic M, Oldham S, Laffargue M, Wymann MP, Hemmings BA, Hafen E. with lethal PIP3 levels: viability of flies lacking PTEN restored by a PH domain mutation in Akt/PKB. *Science. 2002 Mar 15;295(5562):2088-91.*

Teleman AA, Hietakangas V, Sayadian AC, Cohen SM. Nutritional control of protein biosynthetic capacity by insulin via Myc in Drosophila. *Cell Metab. 2008 Jan;7(1):21-32.*

Thompson KL, Decker SJ, Rosner MR. Identification of a novel receptor in Drosophila for both epidermal growth factor and insulin. *Proc Natl Acad Sci U S A. 1985 Dec;82(24):8443-7.*

Tzou P, Ohresser S, Ferrandon D, Capovilla M, Reichhart JM, Lemaitre B, Hoffmann JA, Imler JL. Tissue-specific inducible expression of antimicrobial peptide genes in Drosophila surface epithelia. *Immunity. 2000 Nov;13(5):737-48.*

Tzou P, Reichhart JM, Lemaitre B. Constitutive expression of a single antimicrobial peptide can restore wild-type resistance to infection in immunodeficient Drosophila mutants. *Proc Natl Acad Sci U S A. 2002 Feb 19;99(4):2152-7.*

Uvell H, Engström Y. A multilayered defense against infection: combinatorial control of insect immune genes. *Trends Genet. 2007 Jul;23(7):342-9.*

Verdu J, Buratovich MA, Wilder EL, Birnbaum MJ. Cell-autonomous regulation of cell and organ growth in Drosophila by Akt/PKB. *Nat Cell Biol. 1999 Dec;1(8):500-6.*

Weinkove D, Neufeld TP, Twardzik T, Waterfield MD, Leevers SJ. Regulation of imaginal disc cell size, cell number and organ size by Drosophila class I(A) phosphoinositide 3-kinase and its adaptor. *Curr Biol. 1999 Sep 23;9(18):1019-29.*

Xuan Z, Zhang MQ. From worm to human: bioinformatics approaches to identify FOXO target genes. *Mech Ageing Dev. 2005 Jan;126(1):209-15.*

Yeaman MR, Yount NY. Unifying themes in host defence effector polypeptides. *Nat Rev Microbiol. 2007 Sep;5(9):727-40.*

Zinke I, Schütz CS, Katzenberger JD, Bauer M, Pankratz MJ. Nutrient control of gene expression in Drosophila: microarray analysis of starvation and sugar-dependent response. *EMBO J. 2002 Nov 15;21(22):6162-73.*

8 List of figures